

Evolution of the Rodgers Creek–Maacama right-lateral fault system and associated basins east of the northward-migrating Mendocino Triple Junction, northern California

Robert J. McLaughlin¹, Andrei M. Sarna-Wojcicki¹, David L. Wagner², Robert J. Fleck¹, Victoria E. Langenheim¹, Robert C. Jachens¹, Kevin Clahan^{3*}, and James R. Allen⁴

¹U.S. Geological Survey, 345 Middlefield Road, Menlo Park, California 94025, USA

²California Geological Survey, 801 K Street, Sacramento, California 95814, USA

³California Geological Survey, 345 Middlefield Road, Menlo Park, California 94025, USA

⁴California State University East Bay, Hayward, California 94542, USA

ABSTRACT

The Rodgers Creek–Maacama fault system in the northern California Coast Ranges (United States) takes up substantial right-lateral motion within the wide transform boundary between the Pacific and North American plates, over a slab window that has opened northward beneath the Coast Ranges. The fault system evolved in several right steps and splays preceded and accompanied by extension, volcanism, and strike-slip basin development. Fault and basin geometries have changed with time, in places with younger basins and faults overprinting older structures. Along-strike and successional changes in fault and basin geometry at the southern end of the fault system probably are adjustments to frequent fault zone reorganizations in response to Mendocino Triple Junction migration and northward transit of a major releasing bend in the northern San Andreas fault.

The earliest Rodgers Creek fault zone displacement is interpreted to have occurred ca. 7 Ma along extensional basin-forming faults that splayed northwest from a west-northwest proto-Hayward fault zone, opening a transtensional basin west of Santa Rosa. After ca. 5 Ma, the early transtensional basin was compressed and extensional faults were reactivated as thrusts that uplifted the northeast side of the basin. After ca. 2.78 Ma, the Rodgers Creek fault zone again splayed from the earlier extensional and thrust faults to steeper dipping faults with more north-northwest orientations. In conjunction with the changes in orientation and slip mode, the

Rodgers Creek fault zone dextral slip rate increased from ~2–4 mm/yr 7–3 Ma, to 5–8 mm/yr after 3 Ma.

The Maacama fault zone is shown from several data sets to have initiated ca. 3.2 Ma and has slipped right-laterally at ~5–8 mm/yr since its initiation. The initial Maacama fault zone splayed northeastward from the south end of the Rodgers Creek fault zone, accompanied by the opening of several strike-slip basins, some of which were later uplifted and compressed during late-stage fault zone reorganization. The Santa Rosa pull-apart basin formed ca. 1 Ma, during the reorganization of the right stepover geometry of the Rodgers Creek–Maacama fault system, when the maturely evolved overlapping geometry of the northern Rodgers Creek and Maacama fault zones was overprinted by a less evolved, non-overlapping stepover geometry.

The Rodgers Creek–Maacama fault system has contributed at least 44–53 km of right-lateral displacement to the East Bay fault system south of San Pablo Bay since 7 Ma, at a minimum rate of 6.1–7.8 mm/yr.

GEOLOGIC SETTING OF THE RODGERS CREEK–MAACAMA FAULT SYSTEM

The transform boundary between the Pacific and North American plates in northern California (United States) is a wide zone that reflects eastward migration into the North American plate and lengthening since the late Tertiary (Fig. 1). East of the San Andreas fault (the western boundary of the transform margin) and south of the subducting Gorda–Juan de Fuca plate, this wide transform boundary is composed of mixed structural domains dominated in places by active extensional right-lateral faults associ-

ated with releasing bends and strike-slip basins. The Rodgers Creek–Maacama fault system is one such domain of extensional right-lateral faults and releasing bend basins, though the long-term history of faulting in the area appears to have included significant compression. Elsewhere, the transform boundary zone clearly includes mixed compressional and extensional right-lateral faulting. The Bartlett Springs fault zone west of the Sacramento Valley, for example (McLaughlin et al., 1990), is predominantly a steeply east dipping transpressional fault zone that includes right-stepped strike-slip basins (such as the Covelo and Lake Pillsbury basins) along its length. Clear Lake basin, another complex extensional strike-slip basin (Hearn et al., 1988), is bounded by northwest-trending faults that have pre-basin compressional strike-slip histories (Fig. 1).

The mixed histories of transtension and transpression associated with the wide transform boundary east of the San Andreas fault are the consequence of processes operating along the Pacific, Gorda–Juan de Fuca, and North American plate boundaries since the Late Miocene (ca. 10 Ma), and in some instances since much earlier in the Tertiary. These processes include northward-migrating slab window-related volcanism associated with migration of the Mendocino Triple Junction (Dickinson and Snyder, 1979; Fox et al., 1985; Stanley, 1987; McLaughlin et al., 1994, 1996; Graymer et al., 2002); large-scale block rotations and plate motions (Argus and Gordon, 2001; Wells and Simpson, 2001); and northward-migrating restraining and releasing bends in the northern San Andreas fault (Fox, 1976; Wakabayashi et al., 2004; Wilson et al., 2005). Other processes that may have indirectly influenced the long-term evolution of the transform boundary include partial coupling between

*Present address: Lettis Consultants Int., Inc., Walnut Creek, California 94596, USA.

Evolution of the Rodgers Creek–Maacama fault system

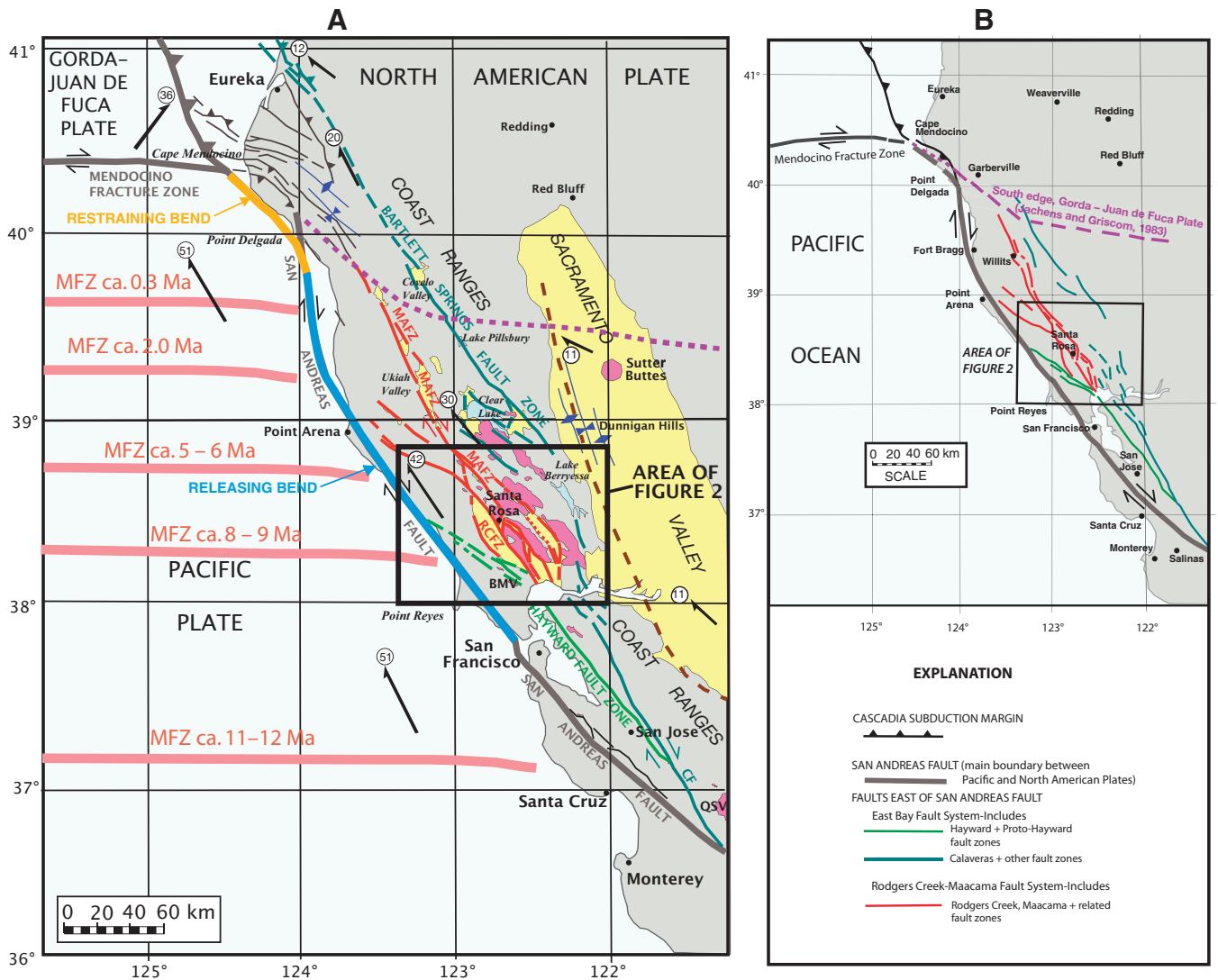


Figure 1. Maps showing the regional setting of the Rodgers Creek–Maacama fault system and the San Andreas fault in northern California. (A) The Maacama (MAFZ) and Rodgers Creek (RCFZ) fault zones and related faults (dark red) are compared to the San Andreas fault, former and present positions of the Mendocino Fracture Zone (MFZ; light red, offshore), and other structural features of northern California. Other faults east of the San Andreas fault that are part of the wide transform margin are collectively referred to as the East Bay fault system and include the Hayward and proto-Hayward fault zones (green) and the Calaveras (CF), Bartlett Springs, and several other faults (teal). Fold axes (dark blue) delineate features associated with compression along the northern and eastern sides of the Coast Ranges. Dashed brown line marks inferred location of the buried tip of an east-directed tectonic wedge system along the boundary between the Coast Ranges and Great Valley (Wentworth et al., 1984; Wentworth and Zoback, 1990). Dotted purple line shows the underthrust south edge of the Gorda–Juan de Fuca plate, based on gravity and aeromagnetic data (Jachens and Griscom, 1983). Late Cenozoic volcanic rocks are shown in pink; structural basins associated with strike-slip faulting and Sacramento Valley are shown in yellow. Motions of major fault blocks and plates relative to fixed North America, from global positioning system and paleomagnetic studies (Argus and Gordon, 2001; Wells and Simpson, 2001; U.S. Geological Survey, 2010), shown with thick black arrows; circled numbers denote rate (in mm/yr). Restraining bend segment of the northern San Andreas fault is shown in orange; releasing bend segment is in light blue. (B) Simplified map of color-coded faults in A, delineating the principal fault systems and zones referred to in this paper.

the North American and Gorda–Juan de Fuca plates and the reactivation of structural wedge-related thrust faults separating the Mesozoic basements of the Coast Ranges and northern Sacramento Valley (Berry, 1973; Wentworth *et al.*, 1984; Wentworth and Zoback, 1990; Jachens *et al.*, 1995).

However, details of how these processes have affected evolution of the transform boundary and associated basins east of the San Andreas fault are poorly known and data on long-term slip history and kinematic evolution of most of the eastern transform boundary zone faults are largely lacking north of San Francisco Bay, beyond paleoseismic investigations of Holocene faulting or geomorphologic studies (e.g., Prentice and Fenton, 2005; Hecker *et al.*, 2005; Lock *et al.*, 2006). The Rodgers Creek–Maacama fault system is well suited for detailed study of this long-term slip history because of its suggested continuity with the creeping Hayward fault zone south of San Pablo Bay, and because the fault system displaces thick sequences of Neogene volcanic and sedimentary layers that are readily datable and correlatable and useful in working out fault slip histories.

Based on the potential for constraining long-term slip rates, we have used framework geologic mapping, new $^{40}\text{Ar}/^{39}\text{Ar}$ dating, and tephrochronology to establish a detailed chronostratigraphy for interpreting the offset history of the Rodgers Creek–Maacama fault system. The timing of faulting and basin formation is determined from the sedimentologic and structural relations of interbedded sedimentary and volcanic units. Configurations of structural basins that we interpret to have formed during evolution of the Rodgers Creek–Maacama fault system are constrained from recent gravity and aeromagnetic investigations (Langenheim *et al.*, 2006, 2008, 2010; McPhee *et al.*, 2007). The amounts of offset and slip rates for the principal faults of the Rodgers Creek–Maacama fault system are determined from best estimates of the limits of distribution of the displaced volcanic and sedimentary sequences, including Mesozoic bedrock units. We compare the kinematics of fault zone and pull-apart basin evolution with laboratory models and determine the contribution of the Rodgers Creek–Maacama fault system to the total long-term slip budget of the Hayward fault zone and other faults of the East Bay fault system.

Geochronology and Tephrochronology Methods

Samples of Neogene volcanic rocks used to establish offsets and rates of slip across the Rodgers Creek–Maacama fault system (Table 1)

were analyzed by $^{40}\text{Ar}/^{39}\text{Ar}$ methodology, either by incremental-heating with a tantalum resistance furnace and molybdenum crucible, or by laser fusion analysis with a CO_2 laser. The $^{40}\text{Ar}/^{39}\text{Ar}$ analyses were done mainly in the Menlo Park Geochronology lab of the U.S. Geological Survey. One sample cited in Table 1 was dated by A. Deino at Berkeley Geochronology Center (Wagner *et al.*, 2011). (For details of dating methodology and mineral separation and sample processing procedures that apply to the samples of this study, see Sarna-Wojcicki *et al.*, 2011; Wagner *et al.*, 2011.)

Samples of volcanic ash used to make stratigraphic correlations (Table 2) were chemically analyzed by electron-microprobe analysis, energy- and wavelength-dispersive X-ray fluorescence, and instrumental neutron activation methods and compared to the compositions of other tephra units in a database of ~5500 analyses (Sarna-Wojcicki *et al.*, 2011). Correlations in Table 2 were established based on similarity coefficients to tephra units of known ages in the database. The tephra correlations in this study are partly reinforced by $^{40}\text{Ar}/^{39}\text{Ar}$ ages, but several local tephra layers are correlated primarily on the basis of their geochemical similarities and stratigraphic positions between well-dated widespread ash units in the region. The geochemical correlations are not only useful for age determinations, they also are useful in determining locations of the eruptive sources, especially for far-field volcanic eruptions. For a detailed discussion of the methodology used for tephra correlations in the northern San Francisco Bay region, see Sarna-Wojcicki *et al.* (2011, and references therein).

Fault Nomenclature

Figure 1B is a simplified representation of the hierarchy of fault nomenclature used in this paper. Our focus is on evolution of faulting east of the main boundary between the Pacific and North American plates (the San Andreas fault), recognizing that the plate boundary is broad and that relations between the San Andreas and the strike-slip faults to the east have changed with time due to northward migration of the main plate boundary. Here, we focus on two main fault systems east of the San Andreas fault: the East Bay and Rodgers Creek–Maacama fault systems, which are also considered to be linked by the Hayward and proto-Hayward fault zones of the East Bay fault system (Fig. 1B). Our study concentrates only on the part of the East Bay fault system that extends north of San Pablo Bay and west of Napa Valley. The Rodgers Creek–Maacama and East Bay fault systems include several other fault zones discussed in

the text and delineated in more detail in Figures 2 and 3 (and other figures). The Rodgers Creek–Maacama fault system includes both the Rodgers Creek and Maacama fault zones.

The proto-Hayward fault zone is largely transpressional and is located southwest of Sebastopol and Cotati; it predated initiation of the Rodgers Creek–Maacama fault system and contributed to long-term displacement of the Hayward and Calaveras faults (Figs. 1 and 2). The proto-Hayward fault zone, as used here, incorporates several local faults and fault zones, including the Tolay, Bloomfield, Petaluma Valley, and Burdell Mountain, discussed previously (e.g., Wagner *et al.*, 2005; Graymer *et al.*, 2002; McLaughlin *et al.*, 1996). Several recent studies suggest that beginning ca. 12 Ma, the composite proto-Hayward, Hayward, and Calaveras fault zones contributed to a cumulative offset of ~174 km across the southern Calaveras fault zone (Graymer *et al.*, 2002; McLaughlin *et al.*, 1996), though a somewhat larger total displacement has also been suggested (e.g., Wakabayashi, 1999). The amount of long-term displacement is inferred (1) from correlations of volcanic and sedimentary rocks at Burdell Mountain (BMV in Fig. 1) with the equivalent Miocene Quien Sabe Volcanics and underlying marine strata (QSV in Fig. 1) southeast of Hollister; (2) from distinctive offset Cretaceous rocks (McLaughlin *et al.*, 1996); and (3) from an offset northward-younging trend in ages of hydrothermal mineralization and volcanism across the proto-Hayward, Hayward, and Calaveras fault zones of the East Bay fault system (Graymer *et al.*, 2002; Obradovich *et al.*, 2000; McLaughlin *et al.*, 1996; Van Baalen, 1995).

The Rodgers Creek–Maacama fault system splays northeastward from the proto-Hayward fault zone, and the timing of this splaying is interpreted to represent initiation of the Rodgers Creek fault zone and abandonment of the proto-Hayward as the active extension of the East Bay fault system.

The southwestern side of the Rodgers Creek–Maacama fault system consists of the Rodgers Creek fault zone, which extends into San Pablo Bay, and steps southwest beneath the bay (Fig. 2) to emerge as the right-lateral Hayward fault in the eastern San Francisco Bay region west of Berkeley (Brown, 1970; Wright and Smith, 1992; Parsons *et al.*, 2003). North of Santa Rosa, the Rodgers Creek fault zone consists of the northern Rodgers Creek fault zone, which locally is referred to as the Healdsburg fault segment of the Rodgers Creek fault zone. The part of the Rodgers Creek fault zone extending south of Santa Rosa is here referred to as the southern Rodgers Creek fault zone.

Evolution of the Rodgers Creek–Maacama fault system

TABLE 1. ⁴⁰Ar/³⁹Ar AGE DATA FOR THE SONOMA, CLEAR LAKE, AND RELATED VOLCANICS

Locality	Field number	North latitude	West longitude	Rock type – material dated	Integrated age		Plateau age		Isochron age		Best estimate age		Converted age* (Ma)	
					(Ma)	MSWD	(Ma)	MSWD	(Ma)	Intercept†	(Ma)	MSWD		
1	995-24C	38.72567	122.89775	Andesite and dacite – groundmass	2.49 ± 0.12	6.0	2.5 ± 0.02	6.0	2.50 ± 0.09	292 ± 27	6.9	2.50 ± 0.02	6.0	2.53 ± 0.02
2	HRC-4A	38.50567	122.70250	Tuff – plagioclase	3.6 ± 0.18	1.13	3.12 ± 0.03	1.13	3.05 ± 0.11	307 ± 34	1.38	3.12 ± 0.03	1.13	3.16 ± 0.03
3	995-25A	38.57933	122.69986	Tuff – plagioclase	3.19 ± 0.16	0.40	3.186 ± 0.022	0.40	3.180 ± 0.022	293.7 ± 3.7	0.60	3.19 ± 0.02	0.40	3.23 ± 0.02
4	MRM 00-8	38.59808	122.67027	Vitric tuff – plagioclase	4.13 ± 0.15	none	none	none	4.61 ± 0.29	289 ± 49	4.6	3.19 ± 0.04	4.6	3.23 ± 0.04
5	995-25D	38.50447	122.73286	Basalt – groundmass	4.43 ± 0.22	none	none	none	4.61 ± 0.29	297 ± 24	6.1	4.61 ± 0.29	6.1	4.66 ± 0.05
6	MRM 1-97	38.48850	122.69483	Andesite – plagioclase	3.62 ± 0.88	none	none	none	5.00 ± 0.39	294.2 ± 1.5	1.68	5.0 ± 0.4	1.68	5.06 ± 0.41
7	995-24B	38.65047	122.84070	Basalt 1 – groundmass	5.33 ± 0.27	0.55	5.07 ± 0.03	0.55	5.04 ± 0.11	301.2 ± 4.2	0.68	5.07 ± 0.03	0.55	5.14 ± 0.03
8	995-24A	38.65647	122.83975	Basalt 2 – groundmass	5.29 ± 0.26	1.5	5.13 ± 0.04	1.5	5.09 ± 0.11	298 ± 13	1.52	5.09 ± 0.11	1.52	5.15 ± 0.11
9	995-25C	38.57242	122.70236	Basalt – groundmass	5.57 ± 0.28	none	none	none	5.01 ± 0.26	305 ± 12	2.2	5.01 ± 0.26	2.2	5.47 ± 0.20
10	MRM6-97 (HRC-5C)	38.40746	122.69791	Rhyolite or dacite – plagioclase	7.31 ± 0.37	0.29	7.26 ± 0.04	0.29	7.27 ± 0.06	292 ± 22	0.31	7.26 ± 0.04	0.29	7.35 ± 0.04
11	015-17B	38.54982	122.72000	Basalt – groundmass	4.63 ± 0.04	0.20	4.847 ± 0.029	0.20	4.81 ± 0.05	298.9 ± 7.8	0.016	4.85 ± 0.03	0.20	4.91 ± 0.03
12	015-17A	38.54982	122.72000	Welded, baked ash flow tuff – plagioclase	6.51 ± 0.04	none	none	none	5.02 ± 0.2	376 ± 150	7.8	5.02 ± 0.2	7.8	5.08 ± 0.02
13	015-18A	38.58157	122.64738	Ash flow tuff – plagioclase	2.85 ± 0.02	0.95	2.851 ± 0.012	0.95	2.869 ± 0.021	288.5 ± 8.7	0.95	2.85 ± 0.01	0.95	2.88 ± 0.02
14	MRM 3-01	38.70880	122.67138	Dacite – plagioclase	3.14 ± 0.02	1.00	3.15 ± 0.01	1.00	3.15 ± 0.02	295 ± 4	1.38	3.15 ± 0.01	1.00	3.19 ± 0.02
15	015-16A	38.73193	122.70645	Rhyolite – anorthoclase	2.20 ± 0.01	0.94	2.196 ± 0.007	0.94	2.200 ± 0.029	295.4 ± 5.6	1.6	2.20 ± 0.01	0.94	2.226 ± 0.01
16	015-171	38.69883	122.82942	Tuff – plagioclase	3.25 ± 0.02	0.60	3.214 ± 0.017	0.60	3.17 ± 0.04	307 ± 19	0.55	3.17 ± 0.04	0.55	3.21 ± 0.04
17	015-17E	38.58030	122.87795	Basalt – groundmass	4.81 ± 0.05	1.9	5.315 ± 0.036	1.9	5.60 ± 0.11	286.4 ± 6.3	1.4	5.32 ± 0.04	1.9	5.38 ± 0.04
18	015-18E	38.54837	122.49052	Obsidian	2.78 ± 0.02	0.52	2.779 ± 0.010	0.52	2.77 ± 0.02	307 ± 26	0.49	2.78 ± 0.01	0.52	2.813 ± 0.02
19	MRM 8-02	38.48450	122.72583	Andesite – groundmass	4.753 ± 0.037	2.2	4.532 ± 0.036	2.2	4.456 ± 0.116	297 ± 5	2.8	4.53 ± 0.04	2.2	4.58 ± 0.04
20	015-18G	38.53130	122.48910	Obsidian	2.5 ± 0.02	1.11	2.473 ± 0.017	1.11	1.6 ± 2.8	332 ± 120	1.9	2.47 ± 0.02	1.11	>2.50 ± 0.02
21	MRM 1-01	38.71169	122.68770	Blocky ash flow tuff – plagioclase	3.22 ± 0.02	1.8	3.222 ± 0.018	1.8	3.12 ± 0.11	334 ± 100	2.3	3.22 ± 0.02	1.8	3.26 ± 0.02
22	SPQ-A-256†	38.32034	122.73461	Well core A, Basalt – groundmass	7.87 ± 0.39	1.05	8.485 ± 0.047	1.05	8.51 ± 0.23	271 ± 55	1.70	8.49 ± 0.05	1.05	8.592 ± 0.051
23	SPQ-E-20-21†	38.32140	122.73500	Well core E, Tuff – plagioclase	8.29 ± 0.03	1.3	8.286 ± 0.014	1.3	8.308 ± 0.040	289.7 ± 7.4	0.72	8.29 ± 0.01	1.3	8.389 ± 0.01
24	Murphy#1-3787†	38.25957	122.56243	Well core, Andesite – plagioclase	9.03 ± 0.45	1.3	9.13 ± 0.06	1.3	9.27 ± 0.32	290.3 ± 6.6	4.6	9.13 ± 0.06	1.3	9.239 ± 0.061
25	Murphy#1-2492†	38.25957	122.56243	Well core, Andesite – plagioclase	8.87 ± 0.4	1.08	8.99 ± 0.06	1.08	9.05 ± 0.27	294.0 ± 3.1	3.1	8.99 ± 0.06	1.08	9.10 ± 0.06
26	MRM82-99 Run 1	38.44534	122.62030	Obsidian	4.509 ± 0.304	0.20	4.513 ± 0.054	0.20	4.513 ± 0.054	295 ± 18	1.6	4.513 ± 0.010	0.20	4.564 ± 0.01
26	MRM82-99 Run 2	38.44534	122.62030	Obsidian	4.542 ± 0.2	0.49	4.543 ± 0.011	0.49	4.552 ± 0.031	279 ± 61	0.24	4.543 ± 0.011	0.49	4.594 ± 0.01
27	047-13B Run 1	38.39097	122.67632	Rhyodacite – plagioclase	8.057 ± 0.02	1.6	7.941 ± 0.016	1.6	7.93 ± 0.08	298.1 ± 9.0	1.04	7.94 ± 0.02	1.6	8.04 ± 0.02
27	047-13B Run 2	38.39097	122.67632	Rhyodacite – plagioclase	8.077 ± 0.014	none	none	none	8.00 ± 0.06	300 ± 28	0.53	8.00 ± 0.06	0.53	8.08 ± 0.03
28	047-13C	38.45478	122.66211	Andesite – groundmass	4.195 ± 0.035	2.0	4.368 ± 0.025	2.0	4.37 ± 0.17	295 ± 13	9.4	4.37 ± 0.03	2.0	4.42 ± 0.03
29	047-14B Run 1	38.48188	122.64756	Porphyritic andesite – groundmass	4.77 ± 0.03	none	none	none	4.93 ± 0.17	290 ± 11	6.2	4.77 ± 0.03	NA	4.83 ± 0.03
29	047-14B Run 2	38.48188	122.64756	Porphyritic andesite – groundmass	4.63 ± 0.02	none	none	none	4.88 ± 0.33	288 ± 24	25	4.63 ± 0.02	NA	4.69 ± 0.02
30	047-14C	38.43635	122.61490	Andesite – plagioclase	4.69 ± 0.03	none	none	none	4.73 ± 0.28	298 ± 24	3.9	4.73 ± 0.28	3.9	4.76 ± 0.03
31	MRM2-04	38.61890	122.63653	Rhyolite – plagioclase	2.34 ± 0.02	2.8	3.127 ± 0.019	2.8	3.13 ± 0.09	269 ± 70	9.8	3.13 ± 0.02	2.8	3.16 ± 0.02
32	MRM 19-05	38.21162	122.48313	Vitric rhyodacite – plagioclase	7.749 ± 0.054	0.81	7.874 ± 0.018	0.81	7.884 ± 0.049	303 ± 26	0.45	7.75 ± 0.05	1.97	7.84 ± 0.05
33	MRM 16-05B	38.18575	122.45422	Vitric rhyodacite – plagioclase	7.833 ± 0.014	0.81	7.874 ± 0.018	0.81	7.884 ± 0.049	303 ± 26	0.45	7.87 ± 0.02	0.81	7.96 ± 0.02
34	RFBM7	38.13190	122.60450	Rhyolite – sanidine	11.07 ± 0.04	none	none	none	11.07 ± 0.04	no age spectrum or isochron	0.36	11.07 ± 0.04	1.2	11.20 ± 0.04
35	RFBM8	38.15280	122.60470	Andesite – groundmass	11.12 ± 0.09	0.27	10.99 ± 0.08	0.27	11.00 ± 0.38	295 ± 11	0.36	10.99 ± 0.08	0.27	11.122 ± 0.081
36†	PF-3 (MRM00-36)	38.29500	122.52610	Tuff – plagioclase	4.96 ± 0.06	none	none	none	4.96 ± 0.06	no age spectrum or isochron	10.9	4.8 ± 0.03	10.9	4.8 ± 0.03
37	MRM51-02	38.60592	122.66300	Andesite – groundmass	3.08 ± 0.02	none	none	none	3.06 ± 0.06	290 ± 38	10.9	3.06 ± 0.06	10.9	3.10 ± 0.06

Note: Keyed to localities in Figures 7 and 14. All uncertainties are reported at 1σ levels of confidence, except isochron intercepts, which are reported at 2σ. MSWD is mean square of weighted deviates. Except for

locality 36, ages for this study were determined in the U.S. Geological Survey ⁴⁰Ar/³⁹Ar dating laboratory in Menlo Park, California.

*For purposes of comparing ages run in the U.S. Geological Survey Menlo Park Geochronology Laboratory with those run in other labs, best-estimate ages have been recalculated to flux monitor values that produce an age of 28.02 Ma for the Fish Canyon tuff (FCT), a widely used and well dated lab standard.

†Age data for this locality were determined by A. Deino, Berkeley Geochronology Center. See also Wagner et al., 2011.

TABLE 2. TEPHROCHRONOLOGY OF THE SONOMA AND ASSOCIATED VOLCANICS OF THE RODGERS CREEK-MAACAMA FAULT SYSTEM

Map number	Field number	North latitude	West longitude	Tephra unit	Interpolated age (Ma)	Source of age and correlation data	Comments
1	MRM00-35	38.59075	122.68147	Franz Valley 2	2.85 ± 0.02	McLaughlin et al., 2004	
2	015-18B	38.58157	122.64738	Franz Valley 2	2.85 ± 0.02	McLaughlin et al., 2004	From 2 m below dated sample 015-18A (Table 1, location 13; Table 2, location 33)
3	015-18C and D	38.58132	122.64750	Franz Valley 2	2.85 ± 0.02	McLaughlin et al., 2004	From below 015-18B (Table 2, location 2)
4	MRM00-34	38.5925	122.68200	Franz Valley 1	>2.85, <3.34?	McLaughlin et al., 2004	
5	MRM87-99B	38.58118	122.67563	Franz Valley 3	undetermined	McLaughlin et al., 2004	Heterogeneous shard population
6	MRM57-99	38.60447	122.74042	Shilo Valley	undetermined	McLaughlin et al., 2004	Most like Franz Valley 3 unit
7	MRM77-99	38.52869	122.73661	Shilo Valley	undetermined	McLaughlin et al., 2004	Most like Franz Valley 3 unit
8	MRM13-97	38.5175	122.71150	Unnamed	<3.12 ± 0.03	McLaughlin et al., 2004	From above Riebli Road unit (Table 2, location 31)
9	MRM10-97	38.51467	122.71183	Unnamed	Mixed population, <3.12 ± 0.03	McLaughlin et al., 2004	Interbedded in gravel above dated Riebli Road unit (Table 1, location 2; Table 2, location 31). Mixed shard population includes a shards similar to Riebli Road unit.
10	MRM22-97	38.51133	122.70400	Unnamed	Mixed population, <3.12 ± 0.03	McLaughlin et al., 2004	Interbedded in gravels overlying Riebli Road unit; with shard populations contributed from Riebli Road, Petrified Forest and Roblar tufts
11	MRM96-01	38.61833	122.63850	Bidwell Creek	undetermined	McLaughlin et al., 2004	Most like Riebli Road (Table 1, location 31)
12	MRM51-99	38.61103	122.73964	Bidwell Creek	undetermined	McLaughlin et al., 2004	Most like Riebli Road (Table 1, location 31)
13	995-25B	38.57933	122.69986	Pepperwood Ranch	3.19 ± 0.02	McLaughlin et al., 2004	
14	MRM85-99A	38.56633	122.63892	Pepperwood Ranch	3.19 ± 0.02	McLaughlin et al., 2004	
15	MRM9-01B	38.56967	122.65450	Pepperwood Ranch?	3.19 ± 0.02 (?)	McLaughlin et al., 2004	From 7–8-m-thick section of multiple tufts at Lake Orth, Franz Valley area. Overlies Jordan Vineyards unit named for localities near Healdsburg (Table 2, locations 26, 83, 84; Figs. 7, 14)
16	MRM9-01C	38.56967	122.65450	Pepperwood Ranch?	3.19 ± 0.02 (?)	McLaughlin et al., 2004	
17	MRM85-99F	38.55824	122.64268	Petrified Forest	>3.19 ≤ 3.34	McLaughlin et al., 2004	
18	MRM85-99D	38.55711	122.63839	Petrified Forest	>3.19 ≤ 3.34	McLaughlin et al., 2004	
19	MRM78-99	38.52636	122.73228	Petrified Forest?	>3.19 ≤ 3.34(?)	McLaughlin et al., 2004	
20	MRM26-01	38.57383	122.65167	Devis Kitchen	>3.22 < 3.34	McLaughlin et al., 2004	
21	MRM00-26	38.56947	122.68464	Devis Kitchen	>3.22 < 3.34	McLaughlin et al., 2004	
22	MRM10-01	38.56892	122.65307	Devis Kitchen?	>3.22 < 3.34 (?)	McLaughlin et al., 2004	
23	MRM00-22	38.54758	122.65178	Putah	3.34	McLaughlin et al., 2004	
24	MRM00-30	38.57511	122.68392	Jordan Vineyards	>3.19 <5.04	McLaughlin et al., 2004	
25	MRM22-01	38.57333	122.65633	Jordan Vineyards?	>3.19 <5.04 (?)	McLaughlin et al., 2004	
26	MRM9-01A	38.56967	122.65450	Jordan Vineyards?	>3.19 <5.04 (?)	McLaughlin et al., 2004	From Lake Orth, Franz Valley area, where overlain by Pepperwood Ranch unit (Table 2, locations 15, 16; Figs. 7, 14)
27	015-17C	38.54982	122.72000	Lawlor	4.83	McLaughlin et al., 2004	
28	MRM28-99	38.54961	122.72122	Mark West Springs	>4.83 <5.0	McLaughlin et al., 2004	
29	MRM40-97	38.53256	122.72458	Mark West Springs	>4.83 <5.0	McLaughlin et al., 2004	
30	MRM61-01	38.54400	122.66400	Camp Neuman	undetermined	McLaughlin et al., 2004	Similar to Devils Kitchen (Table 2, location 21)
31	HRC-4A	38.50567	122.70250	Riebli Road	3.12 ± 0.03	McLaughlin et al., 2004	Dated locality (Table 1, location 2)
32	015-17A	38.54982	122.72000	Leslie Road	5.02 ± 0.20	McLaughlin et al., 2004	Dated locality (Table 1, location 12). From 2 m below dated basalt (Table 1, location 11) and 2 m above sample geochemically correlated with Lawlor tuff (Table 2, location 27).
33	015-18A	38.58157	122.64738	Franz Valley School Road, upper part	2.85 ± 0.02	McLaughlin et al., 2004	Dated locality; uppermost sampled part of Franz Valley tuff section (Table 1, location 3).
34	MRM6-97 (HRC-5C)	38.40746	122.69791	Zamaroni Quarry	7.26 ± 0.04	This paper; McLaughlin et al., 2008	From Zamaroni Quarry; rhyodacitic flow or neck
35	MRM10-03	38.4978	122.65400	Below Napa-Healdsburg	4.65 ± 0.03	This paper; McLaughlin et al., 2008	
36	MRM11-03	38.49745	122.65415	Calistoga Road 1	3.22 ± 0.02 (?)	This paper; McLaughlin et al., 2008	Similar to Putah tuff, but CaO is low
37	MRM11-03	38.49628	122.63087	Northeast Santa Rosa 1	undetermined	This paper; McLaughlin et al., 2008	No clear matches. Similarities to Pepperwood Ranch and Pinole tuff units.
38	MRM15-03	38.49395	122.65547	Calistoga Road 2	2.78–3.22 (?)	This paper; McLaughlin et al., 2005; 2008	Similar to Putah, Pepperwood Ranch and Franz Valley suite of tufts
39	MRM24-03	38.49252	122.64757	Calistoga Road 1	3.22 ± 0.02 (?)	McLaughlin et al., 2005, 2008	Similar to Putah Tuff, but CaO is low
40	MRM16-03	38.49247	122.65620	Putah	3.22 ± 0.02	McLaughlin et al., 2005, 2008	Good match to Putah Tuff
41	MRM12-02	38.4860	122.72900	Cloverleaf Ranch	≤3.12	This paper; McLaughlin et al., 2008	Similar to unnamed tuff above Riebli Road unit (Table 2, location 9)
42	MRM9-02	38.4860	122.72766	Lawlor	4.83	Sarna-Wojcicki, 1976; McLaughlin et al., 2004, 2005, 2008	Overlain? by basaltic andesite
43	MRM43-03	38.48168	122.64707	Lawlor	4.83	Sarna-Wojcicki, 1976; McLaughlin et al., 2004, 2005, 2008	Good match to Lawlor Tuff

(continued)

Evolution of the Rodgers Creek–Maacama fault system

TABLE 2. TEPHROCHRONOLOGY OF THE SONOMA AND ASSOCIATED VOLCANICS OF THE RODGERS CREEK–MAACAMA FAULT SYSTEM (continued)

Map number	Field number	North latitude	West longitude	Tephra unit	Interpolated age (Ma)	Source of age and correlation data	Comments
44	MRM29-03	38.48045	122.62735	Callistoga Road 1	3.22 ± 0.02 (?)	McLaughlin et al., 2004, 2005, 2008	Similar to Putah Tuff, but CaO is low
45	MRM45-03	38.47795	122.64095	Lawlor	4.83	Sarna-Wojcicki, 1976; McLaughlin et al., 2004, 2005, 2008	Good match to Lawlor Tuff
46	MRM40-03	38.47763	122.64358	Napa-Healdsburg	4.65	This paper; Sarna-Wojcicki, 1976; McLaughlin et al., 2005, 2008	
47	ASW-020102-C	38.4765	122.71996	Roblar	6.26 ± 0.03	Sarna-Wojcicki, 1976; McLaughlin et al., 2005, 2008	From along northeast side of southern Rodgers Creek fault zone
48	MRM33-03	38.476	122.62827	Northeast Santa Rosa 2	undetermined	This paper; McLaughlin et al., 2008	From southwest side of southern Rodgers Creek fault zone
49	MRM32-03	38.47593	122.62810	Goodyear Station	>4.67 < 4.83	This paper; McLaughlin et al., 2005, 2008	From northeast of Matanzas Creek reservoir in Bennett Valley
50	MRM68-04	38.42315	122.68035	Taylor Mountain 1	undetermined	This paper; McLaughlin et al., 2008	From Taylor Mountain, southwest of southern Rodgers Creek fault zone; Similar to Roblar Tuff
51	MRM25-04	38.41288	122.69162	Roblar	6.26 ± 0.03	Sarna-Wojcicki, 1976; McLaughlin et al., 2005, 2008	From Taylor Mountain, southwest of southern Rodgers Creek fault zone; good Roblar Tuff
52	MRM29-05	38.40658	122.64746	Mark West Springs	<-5.02 >4.8	McLaughlin et al., 2004, 2008	From northeast of Matanzas Creek reservoir.
53	MRM12-04	38.41505	122.59095	Roblar	6.26 ± 0.03	Sarna-Wojcicki, 1976; McLaughlin et al., 2008	From southwest side of southern Rodgers Creek fault zone; good match to Roblar Tuff
54	MRM31-05	38.40288	122.64661	Napa-Healdsburg	4.65	This paper; McLaughlin et al., 2008	From northeast of Matanzas Creek reservoir in Bennett Valley
55	MRM16-04	38.40083	122.67583	Taylor Mountain 2	-6.26–7.26	This paper; McLaughlin et al., 2008	From Taylor Mountain, southwest of southern Rodgers Creek fault zone; Similar to Roblar Tuff
56	MRM15A,B-04	38.40046	122.67798	Roblar	6.26 ± 0.03	Sarna-Wojcicki, 1976; McLaughlin et al., 2005, 2008	From Taylor Mountain, southwest of southern Rodgers Creek fault zone; good Roblar Tuff
57	MRM18-04A	38.39896	122.67205	Zamarroni Quarry?	~7.26 (?)	This paper; McLaughlin et al., 2005, 2008	Similar to Zamarroni Quarry unit; from southwest of southern Rodgers Creek fault zone.
58	MRM33-04	38.39858	122.65718	Mark West Springs	<-5.02 >4.83	This paper; McLaughlin et al., 2008	From northeast of southern Rodgers Creek fault zone, Taylor Mountain.
59	MRM36-04	38.39436	122.66755	Taylor Mountain 3	undetermined	This paper; McLaughlin et al., 2008	No clear matches. Similarities to Pepperwood Ranch and Pinole tuff units.
60	MRM20-04A,B	38.39392	122.67116	Unnamed, younger than Pinole	<5.2–5.4 (?)	This paper; McLaughlin et al., 2008	From southwest side of southern Rodgers Creek fault zone, mixed shard populations; similar to a tuff that overlies Pinole Tuff
61	MRM32-05	38.3891	122.65322	Guenza Road	≤3.12	This paper; McLaughlin et al., 2004, 2008	Mixed shard populations; similar to tuff that overlies Riebbi Road unit (Table 2, location 9)
62	MRM40-04	38.38928	122.65977	Pinole	5.2–5.4	This paper; McLaughlin et al., 2008	From southwest side of southern Rodgers Creek fault zone, Taylor Mountain area
63	MRM42-04	38.38863	122.66456	Zamarroni Quarry	7.26 ± 0.04	This paper; McLaughlin et al., 2008	From southwest side of southern Rodgers Creek fault zone, Taylor Mountain area
64	MRM49-04	38.38438	122.66243	Taylor Mountain 4	-6.26–7.26 (?)	This paper; McLaughlin et al., 2008	Similar to Roblar Tuff; high and low Fe shard populations; mapped as part of fault scarp breccia overlying rhyodacite of Cooks Peak
65	MRM50-04	38.38268	122.66855	Warrington Road breccia matrix	≥ 6.26(?)	This paper; McLaughlin et al., 2005, 2008	Mapped as part of fault scarp breccia overlying rhyodacite of Cooks Peak
66	MRM38-04	38.3825	122.65270	Zamarroni Quarry	7.26 ± 0.04	This paper; McLaughlin et al., 2005, 2008	From southwest of southern Rodgers Creek fault zone, Taylor Mountain
67	MRM35-03	38.47223	122.62253	Lawlor	4.83	This paper; McLaughlin et al., 2008	From quarry northwest of Los Alamos Road
68	ASW-020102-D	38.38671	122.59320	Mark West Springs	<-5.02 >4.83	This paper; McLaughlin et al., 2008	From along northeast side of Bennett Valley fault zone
69	015-17I 015-17E-H	38.69883	122.82942	Geysers Road section	3.17 ± 0.04	This paper; McLaughlin et al., 2005	From southwest side of Maacama fault zone. Dated locality (Table 1, location 16; Figs. 7, 14). Tephra section geochemically correlates with Putah Tuff and dated 3.2–3.4 Ma tuff section northeast of Maacama fault zone in Franz Valley (Fig. 14).
70	MRM 1-01	38.71169	122.68770	Putah	3.22 ± 0.02	This paper	Geochemical and age correlation with Putah Tuff
71	PF-3	38.2950	122.52610	Carriger Creek	4.96 ± 0.06	This paper; Wagner et al., 2011	Plagioclase dated by A. Deino, Berkeley Geochronology Center (Table 1, location 36).

(continued)

TABLE 2. TEPHROCHRONOLOGY OF THE SONOMA AND ASSOCIATED VOLCANICS OF THE RODGERS CREEK-MAACAMA FAULT SYSTEM (continued)

Map number	Field number	North latitude	West longitude	Tephra unit	Interpolated age (Ma)	Source of age and correlation data	Comments
72	MRM3-97 (HRC-3)	38.5008	122.69060	Bishop of Glass Mountain	1.2 - 0.8	This paper; McLaughlin et al., 2005	From ash layer in folded silt and gravel of northern Rincon Valley
73	MRM53-04	38.3695	122.65260	Unnamed	< 7.26 ± 0.04	This paper	From near base of gravel unit with abundant rounded Tertiary volcanic plus Mesozoic-sourced clasts. Overlies breccia of Warrington Road southwest of southern Rodgers Creek fault zone near Taylor Mountain.
74	MRM15-05	38.1820	122.45640	Unnamed	< 7.26 ± 0.04	This paper	Altered tuff horizon within unsorted fluvial gravel lense in coarse angular breccia unit of Sears Point area. Geochemistry somewhat similar (correlation index of .92) to Table 2, location 73 southwest of southern Rodgers Creek fault zone near Taylor Mountain.
75	MRM16-05A	38.1858	122.45420	Unnamed	≥ 6.26(?)	This paper	Obsidian pebbles from tuffaceous matrix of breccia unit in Sears Point area. Geochemistry similar to Table 2, location 65.
76	MRM16-05B	38.1858	122.45420	Sears Point breccia matrix	≥ 6.26 ≤ 7.26?	This paper	Overlain by andesite breccia and locally baked. Geochemistry similar to Roblar Tuff and tuff in Zamaroni Quarry of Taylor Mountain area southwest of southern Rodgers Creek fault zone
77	MRM17-05B	38.1818	122.45000	Unnamed, above Sears Point breccia	≥ 6.26 ≤ 7.26	This paper	From matrix of Sears Point area breccia similar to Roblar Tuff
78	MRM14-05A	38.1828	122.45690	Sears Point breccia matrix	≥ 6.26 ≤ 7.26?	This paper	Mixed shard populations; including one population similar to Riebli Road unit (Table 2, location 9)
79	DW-SPB-R-1	37.99241	122.30586	Roblar	6.26 ± 0.03	Wagner et al., 2011	Caps gravels that are underlain by 5.0-5.2 Ma basaltic andesite at Jordan Vineyards near Healdsburg (Table 1, locations 7, 8). Overlain by tuff correlative with 3.19 Ma Pepperwood Ranch unit in the Franz Valley area (Table 2, locations 26, 15, 16; Fig. 14).
80	MRM 10-97	38.51467	122.71183	Unnamed, above Riebli Road	≤ 3.12 ± 0.03	McLaughlin et al., 2004	Air fall and waterlain, from along Chalk Hill Road southeast of Healdsburg. Grading, crossbedding, rippled
81	MRM 55-02	38.51916	122.63683	Napa-Healdsburg	4.65	This paper	From along Chalk Hill Road southeast of Healdsburg
83	HRC-99-2	38.65632	122.84423	Jordan Vineyards	≥ 3.19 ≤ 5.04	This paper	Dark, lithic tuff beneath gravel veneer at top of Sugarloaf Peak, south of Gates Canyon. Tuff locally with serpentine inclusions.
84	HRC-99-1	38.65286	122.84675	Jordan Vineyards	≥ 3.19 ≤ 5.04	This paper	Grayish tan, siliceous, 3-4 m thick, intercalated with basaltic andesite and andesitic tuff
85	MRM 21-99	38.60389	122.77583	Napa-Healdsburg	4.65	This paper	From exposure along Cannon Road, interbedded in Petaluma Formation
86	MRM 45-02	38.57787	122.73960	Pepperwood Ranch	3.19 ± 0.02	This paper	From same unit dated by A. Deino, Berkeley Geochronology Center (Table 1, location 36; also Table 2, location 108)
87	MRM 26-99	38.56889	122.77278	Napa-Healdsburg	4.65	This paper	Correlates geochemically with dated tuff and rhyodacitic rocks of Zamaroni Quarry (Table 2, location 34; Table 1, location 10)
88	MRM 1-04	38.54125	122.63368	Putah	3.34	This paper	Mixed shard populations; no good matches, but includes population similar to Putah Tuff
89	MRM 64-02	38.53896	122.63058	Pepperwood Ranch	3.19 ± 0.02	This paper	Dark, lithic tuff beneath gravel veneer at top of Sugarloaf Peak, south of Gates Canyon. Tuff locally with serpentine inclusions.
90	MRM 21-02	38.50851	122.72466	Mark West Springs	>4.83 < -5.00	This paper	Grayish tan, siliceous, 3-4 m thick, intercalated with basaltic andesite and andesitic tuff
91	DW-SP-5	38.20219	122.53564	Roblar	6.26 ± 0.03	Wagner et al., 2011	From exposure along Cannon Road, interbedded in Petaluma Formation
92	DW-SP-7	38.17316	122.47327	Roblar	6.26 ± 0.03	Wagner et al., 2011	
93	DW-SP-8	38.15292	122.46031	Roblar	6.26 ± 0.03	Wagner et al., 2011	
94	DW-102GE	38.26315	122.50672	Ishi or Nomiaki	Ishi Tuff (2.5 Ma); Nomiaki Tuff (2.33 Ma)	Wagner et al., 2011	
95	DW-135GE	38.33974	122.52630	Carriger Creek	4.96 ± 0.06	Wagner et al., 2011	
96	DW-145b-GE	38.35202	122.55682	Unnamed	undetermined	Wagner et al., 2011	
97	DW-147-GE	38.37405	122.56102	Napa-Healdsburg	4.65	Wagner et al., 2011	
98	DW-150-GE	38.31782	122.60392	Zamaroni Quarry	7.26 ± 0.04	Wagner et al., 2011	
99	DW-137-GE	38.35795	122.52106	Putah-like	3.2-3.3?	Wagner et al., 2011	
100	DW-119-GE	38.32891	122.51394	Petrified Forest	≥ 3.19 ≤ 3.34	Wagner et al., 2011	
101	DW-36-GE	38.31687	122.54623	Pinole	5.2-5.4	Wagner et al., 2011	
102	DW-133-GE	38.30017	122.53742	Putah-like	3.2-3.3?	Wagner et al., 2011	
103	DW-159-GE	38.36849	122.56530	Napa-Healdsburg	4.65	Wagner et al., 2011	
105	DW-158-GE	38.36366	122.57257	Huichica	4.71	Wagner et al., 2011	
106	MP-P-2	38.36366	122.63551	Hardin Lane	>6.26 < 7.26	Wagner et al., 2011; Allen, 2003	Mapped originally as Roblar Tuff (Allen, 2003), but chemistry and stratigraphic relations now indicate unit is older than Roblar and younger than rhyodacitic rocks of Zamaroni Quarry (Table 2, location 34; Table 1, location 10).
107	JA080402A,B	38.31866	122.74807	Roblar	6.26 ± 0.03	Wagner et al., 2011; Allen, 2003	From type area of Roblar Tuff, southeast of town of Roblar, good geochemical match
108	MRM00-36B (PF-3)	38.295	122.52605	Carriger Creek	4.96 ± 0.06	This paper; Wagner et al., 2011	Locality of Carriger Creek tuff unit dated by Allen and Deino (Wagner et al., 2011; Table 1, location 36). Tuff is interbedded in lacustrine diatomite, lignitic mudstone and sandstone of Petaluma Formation. Geochemical signature is distinct.
109	MRM00-19	38.49944	122.85631	Roblar	6.26 ± 0.03	This paper	From fluvial gravel section of Petaluma Formation along north-trending fault north of Trenton

Note: Localities are keyed to Figures 7 and 14. Tephra names and inferred ages are based on geochemical correlations. Tephra data analysis and interpretation by A.M. Sarna-Wojcicki, E. Wan, and D. Wahi. All analytical work was done in the U.S. Geological Survey Tephrochronology Laboratory, Menlo Park, California.

Evolution of the Rodgers Creek–Maacama fault system

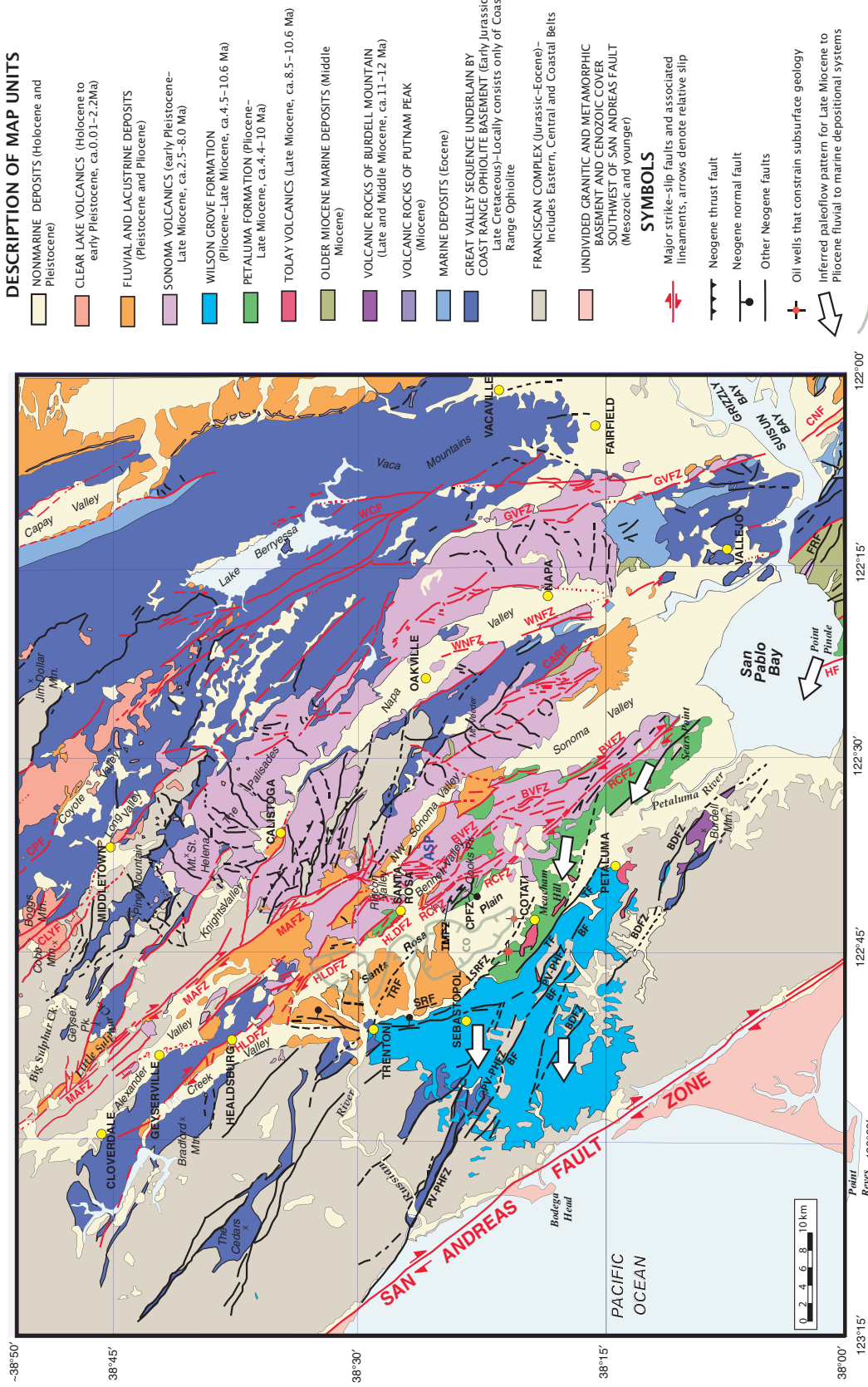


Figure 2. Geologic map of the study area (modified from Wagner and Bortugno, 1982) showing distribution of Miocene and younger sedimentary and volcanic rocks deposited during development of the Rodgers Creek–Maacama fault system. Tertiary rocks deposited prior to development of the San Andreas transform and northward passage of the Mendocino Triple Junction are also delineated. Mesozoic basement rocks west of the San Andreas fault are undivided, but east of the fault include the Coast Range Ophiolite, Great Valley Sequence and Mesozoic–Tertiary Franciscan Complex. Large white filled arrows show pattern of Miocene and Pliocene nonmarine to marine sediment transport. Basins (hachured) and bedrock ridge (not hachured) beneath the Santa Rosa Plain are shown with heavy gray line. Fault (F) and fault zone (FZ) abbreviations: BDFZ—Burdell Mountain; BF—Bloomfield; PV-PHFZ—Petaluma Valley–proto-Hayward; TF—Tolay; HF—Hayward; CNF—Concord; FRF—Franklin; GVFZ—Green Valley; CARF—Carneros; WNFZ—West Napa; CPEFZ—Cooks Peak; TMFZ—Taylor Mountain; RCFZ—Rodgers Creek; HLDZF—Healdsburg; BVFZ—Bennett Valley; LSRFZ—Laguna de Santa Rosa; SRF—Sanford Road; TRF—Trenton; MAFZ—Maacama; WCF—Wragg Canyon; CLYF—Collayomi; CPF—Childers Peak. ASP (blue) is Annadel State Park.

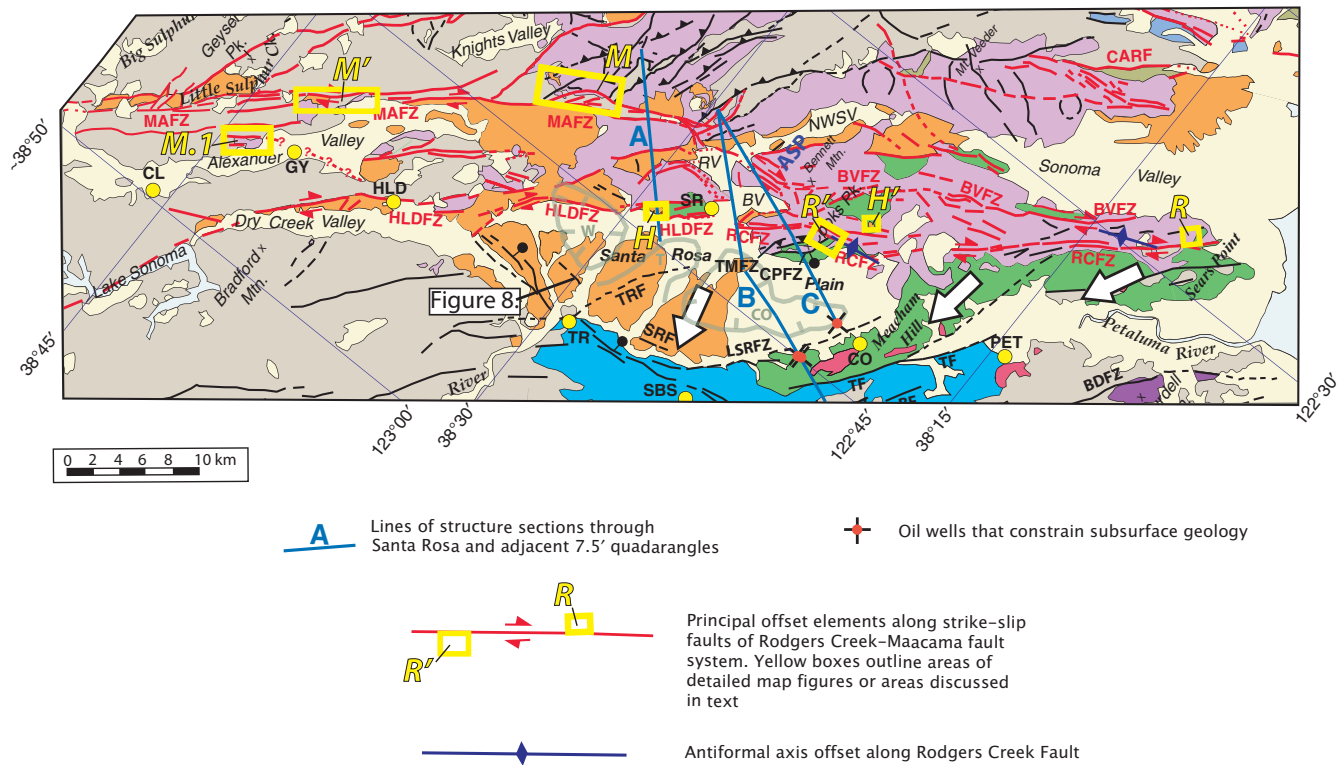


Figure 3. Strip map of the Rodgers Creek–Maacama fault system showing geologic features discussed in this paper that are offset across the Maacama fault zone (M–M' and M.1; see Fig. 14); the combined Healdsburg and Rodgers Creek fault zones (H–H'; see Figs. 9 and 12) and across the southern Rodgers Creek fault zone south of Santa Rosa (R–R'; see Figs. 7, 9, and 11). Offset segments of antiformal axis discussed in text are indicated in dark blue (see Fig. 11). Yellow boxes outline offset areas discussed in text and shown in more detail in Figures 9, 11, and 14. Lines of structure sections A, B, and C (Fig. 5) are shown with heavy blue lines. Geologic units, unit colors, symbols, and abbreviations are as in Figure 2, except that all Mesozoic rocks are here combined as one unit (brown). Additional abbreviations of geographic names include: CL—Cloverdale; GY—Geyserville; HLD—Healdsburg; SR—Santa Rosa; CO—Cotati; TR—Trenton; SBS—Sebastopol; PET—Petaluma; RV—Rincon Valley; NWSV—northwest Sonoma Valley; BV—Bennett Valley.

Collectively, the southern and northern Rodgers Creek fault zones step right, and also go through a complexly evolved releasing bend in transferring slip to the Maacama fault zone northeast of Santa Rosa (Wong and Bott, 1995; McLaughlin et al., 2005, 2006, 2008; McPhee et al., 2007; Langenheim et al., 2008). Multiple strands and segments composing the separate northern Rodgers Creek and Maacama fault zones form a right step in which the two fault zones are subparallel and overlap along strike for ~40 km between Santa Rosa and Geyserville. A non-overlapping right-releasing bend and pull-apart structure also links the Rodgers Creek and Maacama fault zones via the Bennett Valley fault zone in the Santa Rosa area. For the purpose of this paper, these right-stepped, overlapping, and bending links along with other segments and strands of the Rodgers Creek and Maacama fault zones define the Rodgers Creek–Maacama fault system (Figs. 1 and 2).

Tertiary and Mesozoic Basement Relations

The Rodgers Creek–Maacama fault system is underlain by a composite basement that includes Jurassic to Miocene accretionary rocks of the Franciscan Complex, Jurassic to early Tertiary forearc or marginal basin strata of the Great Valley Sequence, and Jurassic mafic igneous rocks of the Coast Range Ophiolite (Fig. 2). Beneath the Great Valley, the Coast Range Ophiolite is considered to be part of the crystalline basement of the Great Valley Sequence. In the area of this study, however, the ophiolite and lower part of the Great Valley Sequence are structurally attenuated and complexly interleaved with Mesozoic and Tertiary rocks of the Franciscan Complex as a consequence of tectonism that predated the Rodgers Creek–Maacama fault system (McLaughlin et al., 1988).

The distribution of distinctive arc-related rocks and igneous breccias in tectonostrati-

graphic terranes of the Coast Range Ophiolite west of Sacramento Valley suggests that the ophiolite has undergone at least 240–320 km of dextral translation subparallel to the northern California margin (McLaughlin et al., 1988). At least 66–146 km of this dextral translation is attributable to Miocene and older faulting that predated northward migration of the San Andreas transform to this latitude (McLaughlin et al., 1988, 1996).

Neogene Sedimentary Rocks

The Rodgers Creek–Maacama fault system is developed partly over remnants of a south-eastward extension of the Neogene Eel River forearc basin (Nilsen and Clarke, 1989) that existed in most of northern California prior to its disruption by strike-slip faulting. Evidence of a Neogene forearc basin predating 8–9 Ma in the study area, however, has largely been

Evolution of the Rodgers Creek–Maacama fault system

removed by uplift and erosion or is buried in basins, though minor forearc remnants are recognized locally (e.g., older Miocene marine strata of Figs. 2 and 3). The amount and timing of displacement and slip rates for the Rodgers Creek–Maacama fault system are mainly constrained by the stratigraphic relations of the post-forearc marine and nonmarine sedimentary units deposited during development of the faulting, enhanced by the age distribution of intercalated volcanic rocks (Figs. 2, 4, and 5).

Miocene to Pliocene Depositional System

From ca. 10 to 4 Ma, the northern San Francisco Bay region, San Pablo Bay, and the area east of the Hayward fault zone were the site of a nonmarine to marine sediment transport system that flowed westward across the northern part of the East Bay fault system and San Andreas fault to the northward-migrating Pacific plate.

North of San Pablo Bay, nonmarine deposits of this paleodepositional system are assigned to the Petaluma Formation, equivalent to parts of the Contra Costa Group south of San Pablo Bay (Graham et al., 1984; Linecki-Laporte and Andersen, 1988; Sarna-Wojcicki, 1992; Graymer et al., 2002; Allen, 2003; Wagner et al., 2005). These deposits are composed of fluvial gravels and sands exhibiting overall west-directed paleoflow, with local fresh-water diatomaceous (lacustrine) beds. Petaluma fluvial strata interfinger westward with brackish to estuarine deposits of mudstone and siltstone that may have encompassed the coastal outlet of a large river (Starratt et al., 2005; Allen, 2003). In the subsurface west of Santa Rosa, the Petaluma Formation interfingers with winnowed, bioclastic gravel and sandstone and siltstone of the marine Wilson Grove Formation, deposited in a shoreline to offshore open-ocean setting (Figs. 3, 4, 5B, and 5C; also see Sarna-Wojcicki, 1992; Graymer et al., 2002; Allen, 2003; Valin and McLaughlin, 2005; Wagner et al., 2005; Powell et al., 2006; Sweetkind et al., 2010). West of the Santa Rosa Plain (Figs. 2 and 3), Wilson Grove sediment was transported in submarine canyons across the San Andreas fault to the Pacific plate, where offset equivalents of these deposits are now found in the Delgada submarine fan southwest of the Mendocino Triple Junction (Drake et al., 1989; Sarna-Wojcicki, 1992).

Breccia of Warrington Road and Sears Point

A distinctive marker unit locally in the lower part of the Petaluma Formation, with an age between 7.3 and 6.7 Ma, consists predominantly of angular to rounded, unsorted volcanoclastic debris of rhyodacitic composition. The unit formed as a debris flow or talus

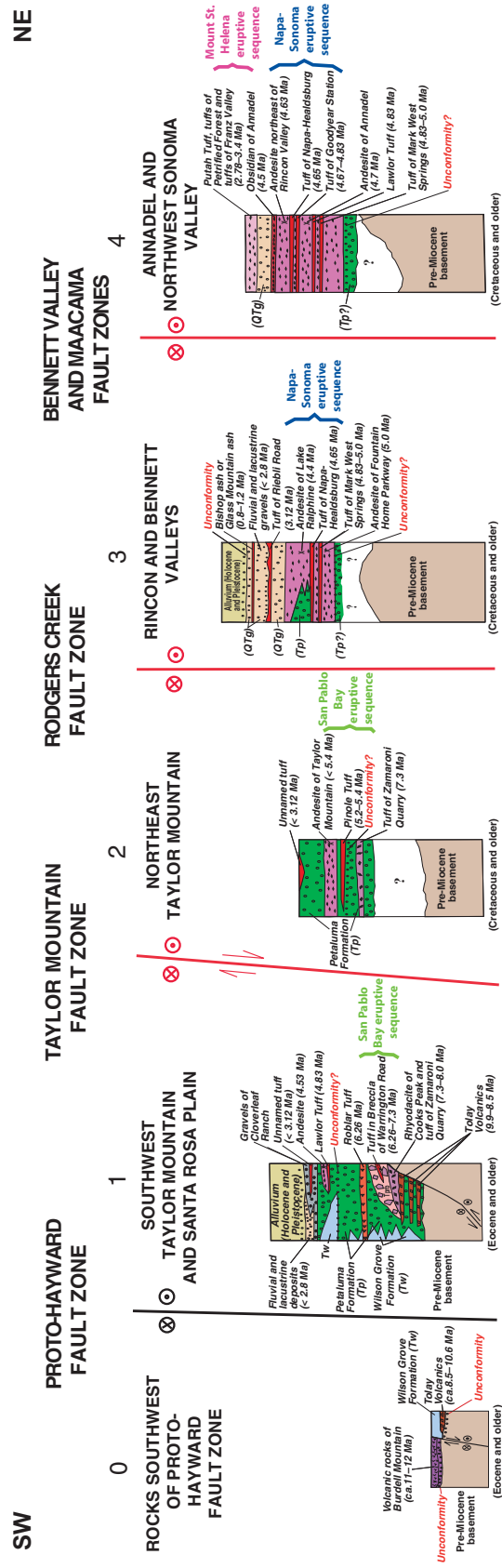
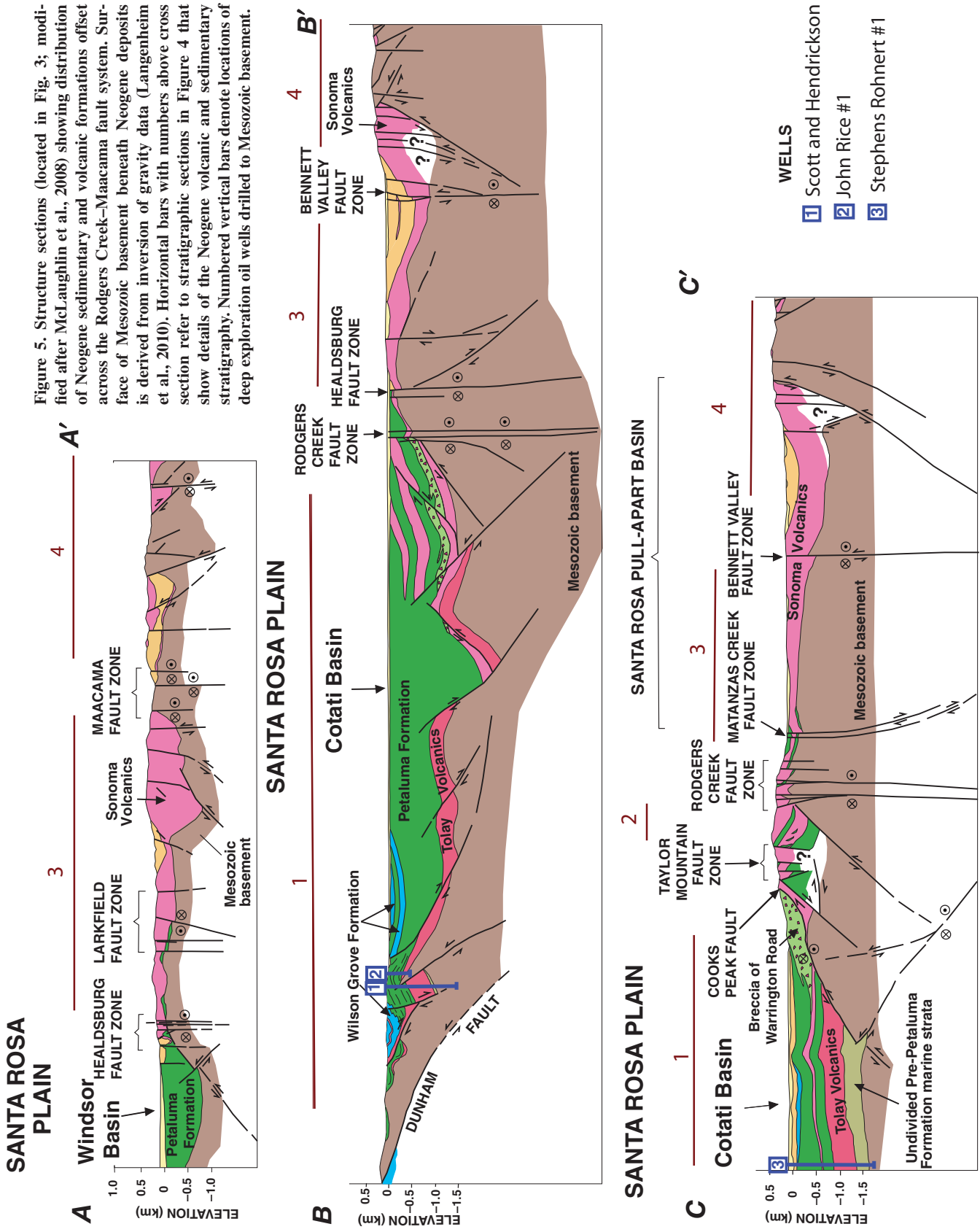


Figure 4. Generalized stratigraphic sections in fault blocks juxtaposed right-laterally across the Rodgers Creek–Maacama fault system. Stratigraphic sections are approximately keyed to areas along structure sections in Figure 5 by numbers above each stratigraphic section. Rocks southwest of the proto-Hayward fault zone (stratigraphic section 0) are not discussed in detail in this paper, but are shown to contrast age relations and stratigraphy of the northward-translated volcanic rocks of Burdell Mountain with volcanic rocks northeast of the proto-Hayward fault zone. SW—southwest; NE—northeast.

Figure 5. Structure sections (located in Fig. 3; modified after McLaughlin et al., 2008) showing distribution of Neogene sedimentary and volcanic formations offset across the Rodgers Creek–Maacama fault system. Surface of Mesozoic basement beneath Neogene deposits is derived from inversion of gravity data (Langenheim et al., 2010). Horizontal bars with numbers above cross section refer to stratigraphic sections in Figure 4 that show details of the Neogene volcanic and sedimentary stratigraphy. Numbered vertical bars denote locations of deep exploration oil wells drilled to Mesozoic basement.



Evolution of the Rodgers Creek–Maacama fault system

breccia deposit from underlying volcanic rocks prominently exposed at Cooks Peak along the southwest flank of Taylor Mountain near Santa Rosa (Figs. 3–7). Much of the angular rhyodacitic debris is slickensided and some of the rhyodacitic blocks are >3 m in diameter. The

locally cross-bedded breccia includes steep to moderately west-dipping lenses of nonvolcanic rounded fluvial gravel containing Franciscan Complex–derived clasts. The southeastern exposures of the breccia unit in the Taylor Mountain area terminate along strike at the southern Rod-

gers Creek fault zone (Figs. 3 [offset element R'] and 7). The breccia is exposed on the northeast side of the Rodgers Creek fault zone ~28 km to the southeast, in the Sears Point area (Fig. 3 [offset element R], 6A, 6B, and 7; see also Wagner et al., 2011).

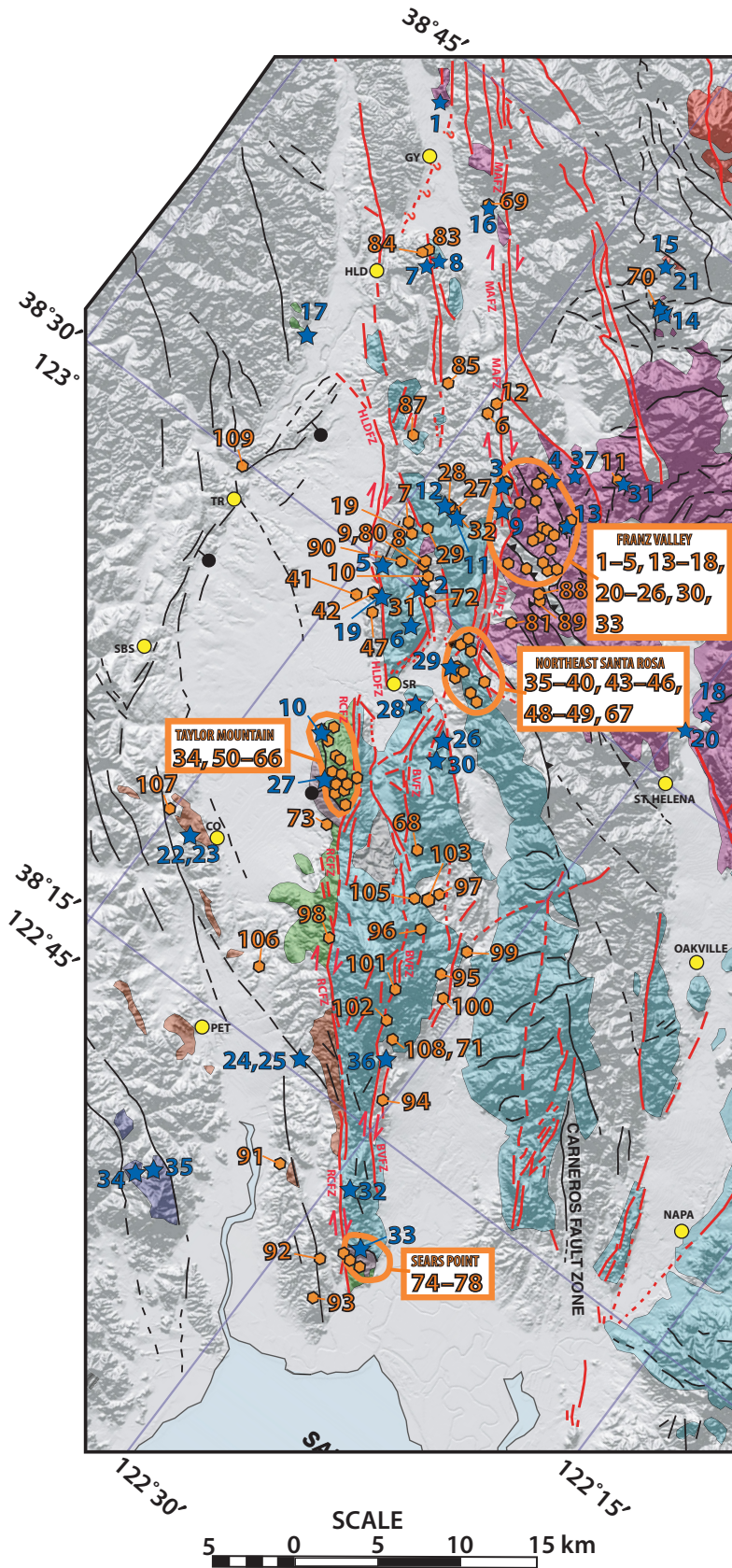
A. West of Rodgers Creek Fault Zone–



B. East of Rodgers Creek Fault Zone–



Figure 6. Photographs of uplifted fault scarp-related breccia of the Taylor Mountain and Donnell Ranch and Sears Point areas offset across the southern Rodgers Creek fault zone. (A) West of Rodgers Creek fault zone. Cross-bedded angular breccia in Petaluma Formation along Warrington Road southwest of Taylor Mountain, (Fig. 3, R'; Fig. 4, stratigraphic section 1; Fig. 5, cross-section C). Breccia was largely shed from fault scarps bounding underlying rhyolite and dacite of Cooks Peak. In left photo hand of person to left (west) rests on subround cobble of Franciscan sandstone. Coarse angular material is rhyodacitic debris, locally conspicuously slickensided. In right photo person points to rounded pebble-sized Franciscan clasts composing a minor (fluvial) component of breccia matrix. Left (west dipping) foreset beds are visible in both photos. (B) East of Rodgers Creek fault zone. Correlative fluvial deposits on the Donnell Ranch, east of Sears Point (Fig. 3, R). In photo on left, bedded gravelly fluvial deposits have a tuff-rich matrix; clasts include round to subround Tertiary volcanic clasts, and nonvolcanic Franciscan-derived clasts are in moderate abundance, in addition to angular rhyolite to dacite clasts identical to those in the breccia of Warrington Road. In right photo outcrops are composed dominantly of unsorted angular rhyolitic to dacitic debris, with bedding defined by vertical alternation of coarse and fine material. In both areas separated across the Rodgers Creek fault zone, isolated angular clasts in breccia reach dimensions >3 m.



EXPLANATION

CLEAR LAKE VOLCANICS

(.01–2.2Ma)

SONOMA VOLCANICS

- ERUPTIVE SEQUENCES

Mount St. Helena (2.5–3.4 Ma)

Napa-Sonoma Valley (~4.0–5.0 Ma)

San Pablo Bay (~5.2–8.0 Ma)
Breccias of Warrington Rd and Sears Pt (6.7–7.3 Ma)

TOLAY VOLCANICS

(~8.5–10.6 Ma)

VOLCANICS OF

BURDELL MOUNTAIN

(11.0 Ma)

★ 36 $^{40}\text{Ar}/^{39}\text{Ar}$ locality, number keyed to Table 1

○ 93 Tephra locality, number keyed to correlation data in Table 2

○ 1–10
Area of numerous closely spaced tephra samples, locality numbers keyed to Table 2.

Figure 7. Localities of $^{40}\text{Ar}/^{39}\text{Ar}$ ages and tephrochronologic analyses of volcanic rocks used in this study to establish offsets of eruptive sequences of Sonoma and related volcanics across the Rodgers Creek–Maacama fault system. The $^{40}\text{Ar}/^{39}\text{Ar}$ localities are shown by blue star symbols and numbers, keyed to map locality numbers in Table 1. Tephra localities are shown by orange polygon symbols and numbers, keyed to map locality numbers in Table 2. Irregular orange circles outline areas of tephra localities too closely spaced to show individually. Locality numbers in outlined areas (Franz Valley, northeast Santa Rosa, Taylor Mountain, and Sears Point) are shown in labeled boxes with leaders to specific map areas and are keyed to Table 2. Abbreviations for selected faults and place names are as in Figures 2 and 3.

Pliocene and Early Pleistocene Deposits

Pliocene and early Pleistocene fluvial and lacustrine sediments (Figs. 2, 4, and 5) unconformably overlie the Petaluma and Wilson Grove Formations. East of the northern Rodgers Creek fault zone, these deposits are compressed into northwest-trending open folds (Fig. 5, structure sections A and C). West of the northern Rodgers Creek fault zone, they are only mildly warped or undeformed, though water well and seismic data (Williams et al., 2008; Sweetkind et al., 2008) suggest that these strata are increasingly tilted and folded deeper in the subsurface.

Gravels of these deposits contain rare to common obsidian pebbles and generally are referred to as the Glen Ellen Formation, though regionally other names are locally applied. Geochemical fingerprinting of the obsidian pebbles (McLaughlin et al., 2004, 2005, 2008) shows their derivation is mainly from two widely separated obsidian sources of different age: one source area is 2.8 Ma flows and domes in the Napa and Franz Valleys (Figs. 7 and Table 1, location 18); the other source is 4.5 Ma flows in the Annadel area east of Santa Rosa (stratigraphic column 4 in Fig. 4; Table 1, location 26). The youngest folded deposits of the Glen Ellen Formation near Santa Rosa include a 0.8–1.2 Ma ash (stratigraphic section 3 in Fig. 4; location 72 in Table 2 and Fig. 7; see also Figs. 3 and 5), which correlates geochemically with the Bishop ash bed or the chemically similar younger set of the Glass Mountain ash beds from the Long Valley Caldera on the southeast side of the Sierra Nevada Mountains (McLaughlin et al., 2008; Sarna-Wojcicki et al., 2000, 2005; Metz and Mahood, 1991).

Obsidian clast provenance and paleoflow data show that paleodrainage for the Glen Ellen gravels was largely westward across the Rodgers Creek–Maacama fault system, into basins on the northern and southern parts of the Santa Rosa Plain (Sweetkind et al., 2008; see discussion of northern and southern Rodgers Creek fault zone displacement later in this paper). Though the timing and amount of strike-slip displacement of the Glen Ellen gravels along the Rodgers Creek fault zone seem to require it, the paleoflow and clast size distribution data show no clear indication that Glen Ellen deposition was concurrent with and controlled by strike-slip faulting. Perhaps the Rodgers Creek fault zone at that time was too diffuse and did not rupture to the surface often enough to create significant surface fault expression (e.g., basins, topographic barriers, and sediment transport channels) that would influence sedimentation patterns. In contrast, nearby studies (Nilsen and McLaughlin, 1985; McLaughlin and Nilsen,

1982) documented deposition concurrent with strike-slip faulting in basin gravels younger than 3 Ma uplifted along the Maacama fault zone.

Pleistocene and Holocene Deposits

Pleistocene deposits that overlie the deformed Pleistocene and older formations are generally flat lying and dissected, and may be mildly tilted locally, for example, as along the west side of the Santa Rosa Plain (Fig. 8). These deposits are broadly regarded as younger than the ca. 1.2–0.8 Ma tephra layer described near Santa Rosa.

Neogene Volcanic Rocks

Abundant volcanic rocks that range in age from ca. 12 to 1.2 Ma in our study area (Figs. 2, 4, and 5) provide the principal basis for dating faulting and related deformation. Analytical data for the $^{40}\text{Ar}/^{39}\text{Ar}$ ages determined for the Neogene volcanic units of this study are shown in Table 1. **Tephrochronologic correlations of numerous chemically analyzed volcanic ash samples used to constrain stratigraphic relations and complement the radiometric dates are in Table 2. The map distributions of the dated volcanics and correlated tephra layers are in Figure 7 (keyed to Tables 1 and 2).**

The volcanic rocks were largely erupted from volcanic centers east of, or dispersed along, the Rodgers Creek–Maacama and East Bay fault systems (Fig. 1), and are divided by age into different eruptive sequences intercalated with the sedimentary units described herein. As with the regional distribution of Neogene volcanics in all of the Coast Ranges, the ages of these volcanics generally young in a north-eastward direction, but the volcanics are also displaced right-laterally with associated enclosing and overlying sedimentary units by the Rodgers Creek–Maacama fault system. Volcanics that constrain displacements across the Rodgers Creek–Maacama fault system, from oldest to youngest and from southwest to northeast, include those of Burdell Mountain, and the Tolay, Sonoma, and Clear Lake Volcanics. A tephra layer correlated herein with the Bishop ash bed or younger set of the Glass Mountain ash beds, with a far-field eruptive source in south-eastern California, is recognized at one locality. Constraints imposed by the Neogene volcanic rocks on timing and amounts of displacement for specific faults of the stepover fault system are included in the discussion of faulting.

Tolay Volcanics and Volcanics of Burdell Mountain

The oldest volcanic fields in the progression of northward-younging volcanism (Fox et al., 1985; Graymer et al., 2002) are the volcanics

of Burdell Mountain and the Tolay Volcanics (Fig. 2), which are older than ca. 8 Ma and are southwest of the Rodgers Creek–Maacama fault system. These rocks have been displaced a minimum of many tens of kilometers from their in-place eruptive centers east of the Hayward and southern Calaveras faults. Details of these volcanic units and their displacements along faults predating the Rodgers Creek–Maacama fault system were discussed in detail elsewhere (McLaughlin et al., 1996; Graymer et al., 2002; Ford, 2003, 2007).

Sonoma Volcanics

The ca. 8.0–2.5 Ma Sonoma Volcanics (Weaver, 1949; Table 1) are intercalated in the middle and upper parts of the Petaluma Formation and in younger Pliocene deposits dispersed between faults of the Rodgers Creek–Maacama fault system (Figs. 4 and 5). The Sonoma Volcanics are informally divided into age groupings associated with spatially separated northward-younging volcanic centers. The younger volcanic sequences in places overlap the older volcanics and pre-Neogene rocks. In the direction of their younging pattern from south to north, these informal age groupings include the San Pablo Bay, Napa Valley, and Mount St. Helena eruptive sequences. Local details of the stratigraphy of these volcanic sequences that were used to constrain displacements and slip rates for faults of the Rodgers Creek–Maacama fault system, are included in the discussion of faulting.

RODGERS CREEK–MAACAMA FAULT SYSTEM

The Rodgers Creek–Maacama fault system consists of the Rodgers Creek and Maacama fault zones. The Rodgers Creek fault zone is divided into the northern Rodgers Creek fault zone north of the floodplain of Santa Rosa Creek (locally referred to as the Healdsburg fault segment) and the southern Rodgers Creek fault zone south of Santa Rosa Creek floodplain. In addition, the seismically active Bennett Valley fault zone, northeast and subparallel to the southern Rodgers Creek fault zone, partitions slip northeastward from the south end of the southern Rodgers Creek fault zone toward the Maacama fault zone. In the Santa Rosa area, this slip transfer is via the Spring Valley fault segment of the Bennett Valley fault zone that forms the eastern boundary of a prominent pull-apart basin beneath Santa Rosa and Rincon and Bennett Valleys (Figs. 3, 9, and 10). Significant transfer of slip between the Maacama and Rodgers Creek fault zones occurs across this pull-apart structure.

A

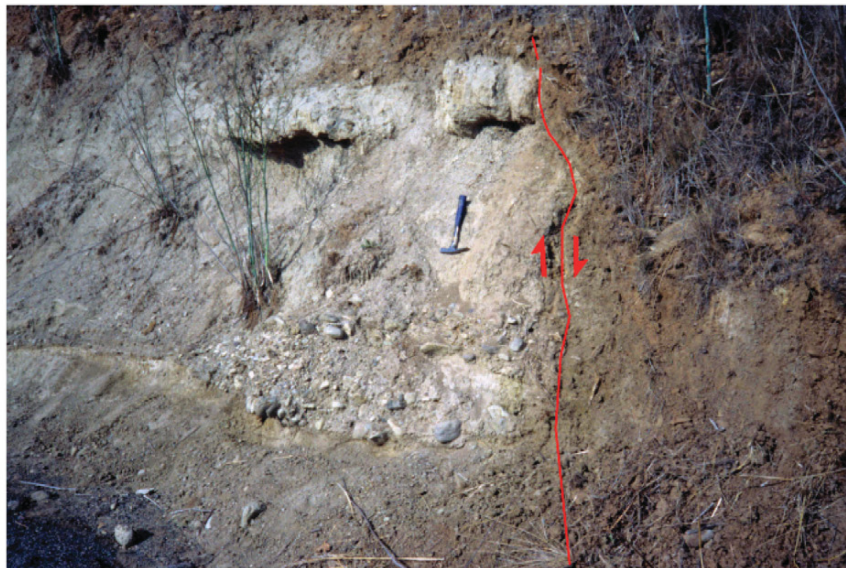


Figure 8. Photographs of normal faulting exposed on Laughlin Road along the west side of Windsor basin and the Santa Rosa Plain. See Figure 3 for map location. (A) View toward east from south side of Laughlin Road, at Pleistocene–late Pliocene fluvial gravels of the Glen Ellen Formation, unconformably capped by red-orange Pleistocene paleosol and flat-lying fluvial terrace gravel. The capping Pleistocene gravel forms the surface of Santa Rosa Plain. Road steps downward at east side of exposure at location of normal fault exposure shown in B and C. Mount St. Helena and uplands of stepover area east of Healdsburg segment of northern Rodgers Creek fault zone are visible in background. (B) View of stratigraphy and steep east-dipping normal fault, at east side of same roadcut as in A. Gently west-northwest-tilted fluvial gravel and tuffaceous sand and silt of Glen Ellen Formation on the west (left) side of the fault are capped unconformably by thin veneer of red-orange Pleistocene gravel. The Pleistocene gravel drapes across fault scarp and thickens on east side of tilted Glen Ellen block. (C) Close-up view of gravel channels truncated against west side of fault and of sheared red-orange clayey Pleistocene gravel draping fault scarp to east. Hammer for scale in B and C (handle is ~30 cm long).

B



C



Evolution of the Rodgers Creek–Maacama fault system

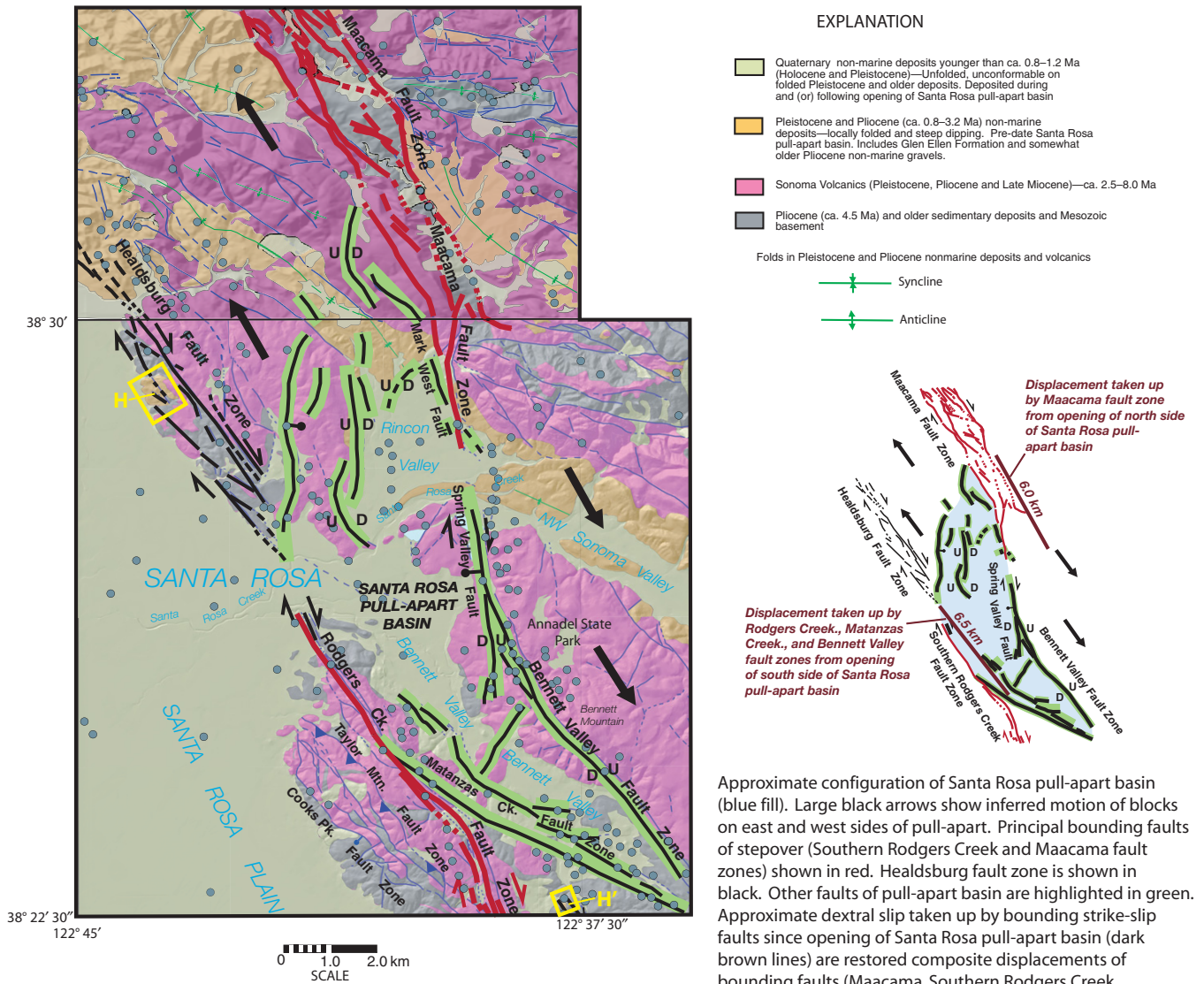


Figure 9. Map showing detail of link between Rodgers Creek and Maacama fault zones across Santa Rosa pull-apart basin (based on geologic maps of McLaughlin et al., 2003, 2008). Age of youngest folded Pleistocene–Pliocene deposits that underlie unfolded basin fill constrains timing of basin opening to ca. 0.8–1.2 Ma or later. The ~6.5-km-long southwest side of the pull-apart basin bounded by the southern Rodgers Creek, Matanzas Creek, and Bennett Valley fault zones presumably represents composite displacement since opening of the basin ca. 1 Ma. Similarly, an ~6.0-km-long length of the Maacama fault zone records slip since opening of northeast side of the basin. Dark gray filled circles are earthquake epicenters (Waldhauser and Schaff, 2008). Yellow boxes outline Glen Ellen gravels with Annadel-derived obsidian clasts that constrain offset across Southern Rodgers Creek and Healdsburg segments of Rodgers Creek fault zone (Fig. 3). D—downthrown; U—upthrown.

Rodgers Creek Fault Zone

As the principal southwestern bounding fault zone of the dextral right-stepped Rodgers Creek–Maacama fault system (Figs. 1–3), the Rodgers Creek fault zone represents the earliest and most complexly evolved part of the stepover system. The fault zone complex-

ity appears to result from at least four fault zone reorganizations that gave rise to separately named faults of different orientations and rates of right-lateral slip with time. Long-term slip rates for the Rodgers Creek fault zone have sequentially changed with fault zone geometries during these four reorganizations.

1. Early Basin-Bounding Extensional Faults

These faults bound concealed basins beneath the Santa Rosa Plain and are not mapped at the surface everywhere, but are inferred at depth from gravity data and from local normal faults draped by fault breccia (Figs. 3, 5, and 9). Basins buried beneath the Santa Rosa Plain are bounded on their east sides (Figs. 2, 3, and 5) by a

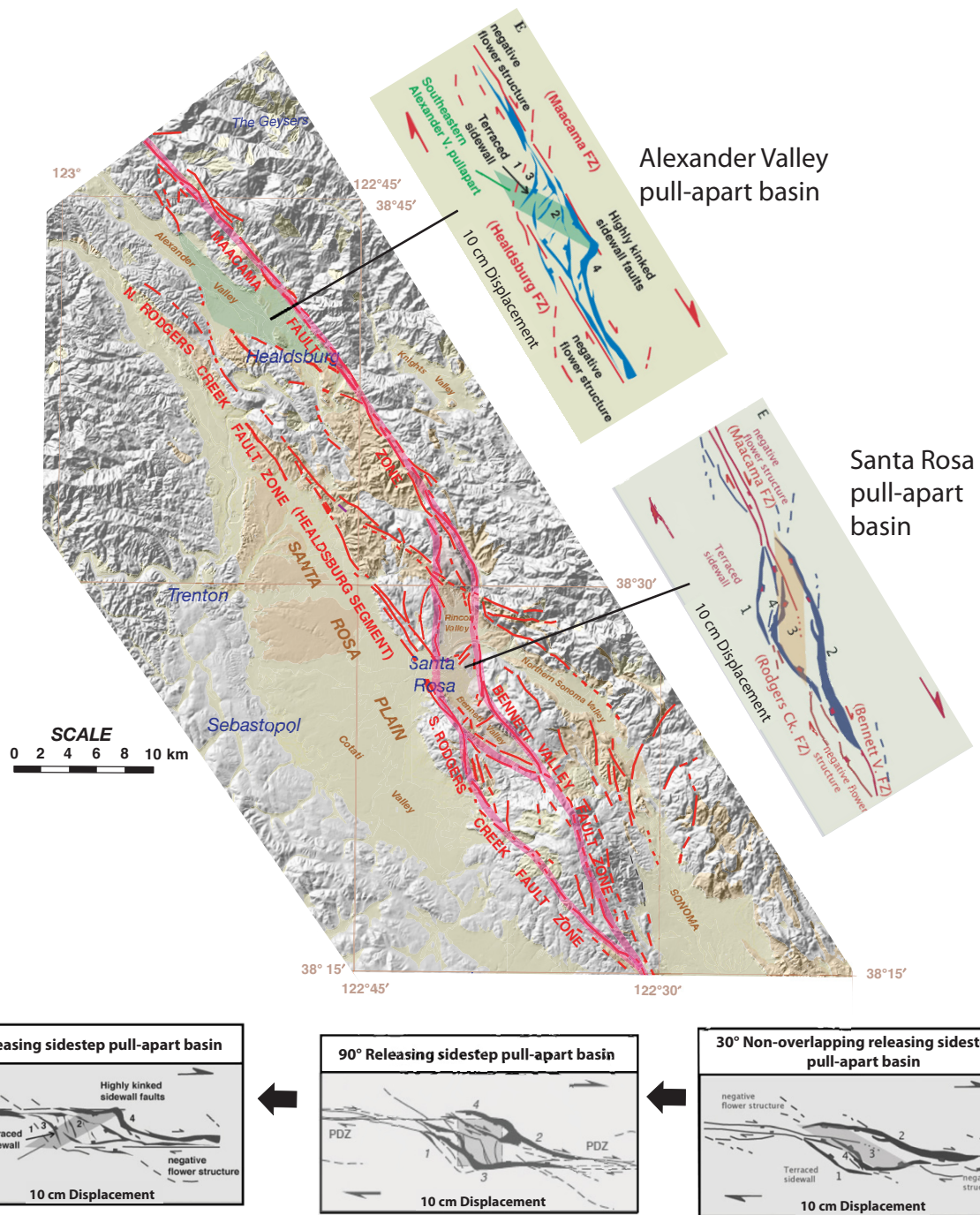


Figure 10. Map showing faults of the right-stepped Rodgers Creek–Maacama fault system compared with schematic drawings from laboratory models of pull-apart basin evolution (Dooley and McClay, 1997). In lower drawings pull-apart basin geometries are seen to evolve from right to left: from a basin oriented parallel to the $\sim 30^\circ$ non-overlapping step between principal basin-bounding strike-slip faults, to a basin that is roughly box shaped with principal basin-bounding faults at $\sim 90^\circ$ to each other, to a highly evolved basin geometry controlled by the amount of overlap (as much as 150° or more) of the principal bounding strike-slip faults. Based on these laboratory observations, the Rodgers Creek–Maacama fault system exhibits a highly evolved stepover predating ca. 1 Ma, marked by the large overlap along strike of the northern Rodgers Creek fault zone (Healdsburg segment) with the Maacama fault zone. The Rodgers Creek–Maacama fault system reorganized with opening of the Santa Rosa pull-apart basin after 1 Ma (faults involved with reorganization with heavy pink highlight), when the Santa Rosa pull-apart basin, having a 30° non-overlapping geometry opened, cutting across the maturely evolved, overlapped stepover geometry of the northern Rodgers Creek and Maacama fault zones. N—northern; S—southern; FZ—fault zone; V—valley; Ck.—Creek.

900–1400-m-high west-facing basement escarpment that is evident in gravity data (Langenheim et al., 2008, 2010; McPhee et al., 2007). This west-facing basement surface is inferred to be a west-side-down zone of normal faults bounding the Santa Rosa Plain, as shown in Figure 5 (section C–C'). The extensional character of these early faults is expressed at Cooks Peak south of Santa Rosa (Fig. 5), where a prominent 7.3–8.0 Ma rhyodacite unit (Table 1, locations 10, 27) is intruded along the Cooks Peak fault zone (mapped as a west-dipping normal fault by McLaughlin et al., 2008). The fault here is draped by the Breccia of Warrington Road and Sears Point (see discussion of stratigraphy of Neogene sedimentary rocks) composed of angular, coarse, blocky, slickensided debris (Fig. 6) derived from the rhyodacite of Cooks Peak with minor interbedded fluvial gravel of the lower Petaluma Formation (Fig. 5; see McLaughlin et al., 2008). Overlying Petaluma strata contain two tuffs that are dated as ca. 6.7 Ma (tuff of Lichau Creek; Wagner et al., 2011) and 6.3 Ma (the Roblar Tuff; see Table 2). Fault scarp breccias similar to the breccias of Warrington Road and Sears Point are particularly characteristic of extensional strike-slip basin margins, and are well documented in the Ridge Basin of southern California (Crowell and Link, 1982), the Hornelen Basin of Norway, and along the Maacama fault zone (the Little Sulfur Creek basins of Nilsen and McLaughlin, 1985). Although fault scarp breccia deposits conceivably can form in compressional settings, they are usually associated with faulted extensional strike-slip basin margins, consistent with the strike-slip setting of the breccias of Warrington Road and Sears Point. Breccias that might form along the scarps of thrust faults during basin inversion would probably not be exposed or preserved due to crustal shortening and structural burial. A thrust fault breccia, would be susceptible to entrainment in the fault zone and to being overridden by the hanging wall of the thrust. The breccia-draped extensional scarp along the Cooks Peak fault zone and its suggested westward connection with the escarpment beneath the Santa Rosa Plain is thus inferred to mark the opening of a large pull-apart basin between ca. 7.3 and 6.7 Ma (ca. 7.0 ± 0.3 Ma). The exposures of fault scarp breccias we correlate across the Rodgers Creek fault zone in the Taylor Mountain and Sears Point areas are now separated by a later stage of faulting along the southern Rodgers Creek fault zone.

Discontinuous normal faults are also mapped along the west side of the Santa Rosa Plain, including the Laguna de Santa Rosa fault, faulting uncovered in excavations near Sebastopol, and faulting seen in cuts along Laughlin Road

south of Sonoma County Airport (Figs. 2, 3, and 8). These faults displace early Pleistocene and older deposits and are inferred to be linked to the same extension as normal faults seen on the east side of the Santa Rosa Plain. They have been active in the Quaternary, but have relatively minor down-to-the-east displacements of less than a few meters, and are discontinuous at the surface. These faults are also weakly expressed in the subsurface based on gravity data, compared to the major subsurface basement escarpment bounding the east side of the Santa Rosa Plain (Langenheim et al., 2010; McPhee et al., 2007). Based on this structural relief we interpret normal fault displacement to have been focused along the east side of the plain and to reflect earliest slip on the Rodgers Creek fault zone. If this interpretation is correct, the age of the fault scarp breccias of Warrington Road and Sears Point constrains the timing of earliest slip on the Rodgers Creek fault zone to ca. 7.0 ± 0.3 Ma.

2. Northeast-Directed Transpressional Faulting

Northeast-directed imbricate thrust faults are mapped southwest of the southern Rodgers Creek fault zone south of Santa Rosa (McLaughlin et al., 2008), where they underlie Taylor Mountain and the Cooks Peak fault zone (Figs. 3, 5C, and 9). These poorly exposed thrust faults dip moderately southwest ($\sim 35^\circ$) and warp and imbricate the volcanic and sedimentary section. The thrusts generally place 7.3 Ma and older volcanics and Petaluma Formation strata on the southwest side of the Taylor Mountain fault zone, over 6.3 Ma and younger volcanics and strata to the northeast. The strike-slip-related, northeast-directed transpressional motion of these faults is interpreted to have uplifted and exposed the former normal fault–bounded margin of the basins beneath the Santa Rosa Plain. At the surface, the Taylor Mountain fault zone (Figs. 3 and 9) is mapped as dipping southwest beneath the earlier fault scarp breccia-draped extensional faults of the Cooks Peak fault zone. In the subsurface (Fig. 5, section C) this thrust faulting is interpreted to have reactivated faults of the west-facing extensional basement escarpment beneath the Santa Rosa Plain.

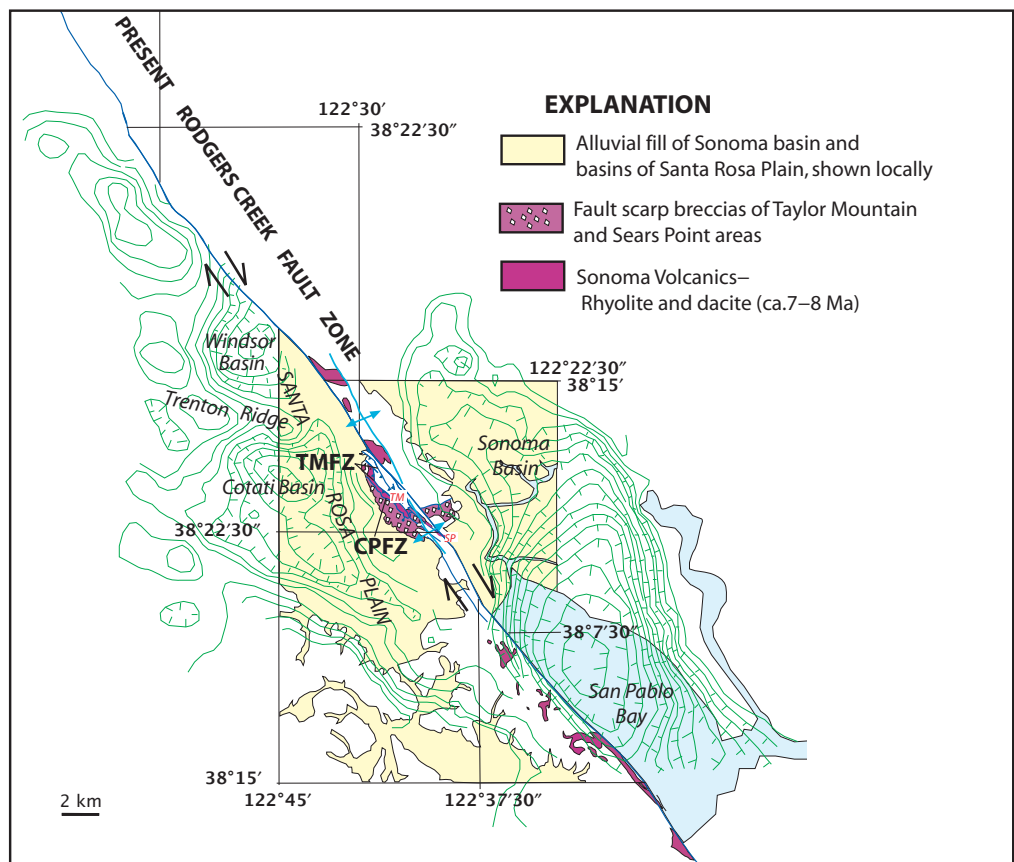
Structural repetition of ca. 5.4 Ma and older volcanic and sedimentary rocks by closely spaced faults of the Taylor Mountain fault zone is indicative that the transpressional faulting is ca. 5.4 Ma or younger (McLaughlin et al., 2008). We suggest a similar timing for the onset of transpression associated with blind thrusts beneath the Trenton Ridge structural high (Figs. 3, 5B, and 5C; McLaughlin et al., 2008; McPhee et al., 2007) that divides the Santa Rosa Plain into the Cotati and Windsor basins (Figs. 2 and

3). Well-log stratigraphy (Valin and McLaughlin, 2005; Powell et al., 2006; Sweetkind et al., 2010) and seismic reflection data (Williams et al., 2008; Sweetkind et al., 2008) show that growth of the Trenton Ridge began well before 3 Ma and that its uplift and erosion continued until ca. 1 Ma.

3. Quaternary Rodgers Creek Fault Zone

Transpressional deformation over Taylor Mountain, the east side of the Santa Rosa Plain, and beneath Trenton Ridge was followed by a shifting of slip to dominantly right-lateral, geomorphically youthful, steeply dipping faults of the southern Rodgers Creek fault zone. Southeast of Taylor Mountain and Santa Rosa, the transpressional Taylor Mountain fault zone (Figs. 2, 3, 5C, and 9) and basin-bounding extensional faults of the Cooks Peak fault zone splay northwest from a local north-northwest jog in the active southern Rodgers Creek fault zone. The youngest traces of the southern Rodgers Creek fault zone in that area are oriented $\sim 30^\circ$ clockwise from the trends of the Taylor Mountain and Cooks Peak fault zones (Figs. 2, 3, 7, and 9). The 7.3–8.0 Ma rhyodacitic volcanics of Cooks Peak and overlying fault scarp breccias of Warrington Road and Sears Point that are bounded by these splaying faults are truncated against the southern Rodgers Creek fault zone (McLaughlin et al., 2008; Figs. 2, 3, and 9). The recently active fault segments and the older transpressional and extensional fault segments, however, are colinear (Figs. 2 and 3) farther to the southeast. Restoration of the rhyodacitic volcanics and fault scarp breccia of the Cooks Peak–Taylor Mountain area across the southern Rodgers Creek fault zone to the Sears Point area, based on their truncation at the Southern Rodgers Creek fault zone, together with an antiformal axis that aligns after restoring offset of the volcanics and breccia (Figs. 3 and 11), suggests that $\sim 28 \pm 0.5$ km of right-lateral displacement is taken up by the combined Cooks Peak, Taylor Mountain, and more youthful southern Rodgers Creek fault zones. The 28 ± 0.5 km dextral displacement of the fault scarp breccia, rhyodacitic volcanics, and antiformal axis is inferred to have been taken up since ca. 7 Ma, first by transtensional slip along the Cooks Peak fault zone, followed by transpressional displacement along the Taylor Mountain fault zone, and most recently by steeply dipping active faults of the northern and southern Rodgers Creek fault zones. Relative amounts of the total strike slip partitioned to the Cooks Peak and Taylor Mountain fault zones is unknown, except that the extensional and compressional styles of these early faults imply that much pre-Quaternary displacement occurred as dip slip.

Figure 11. Restoration of 28 km of long-term offset on Rodgers Creek fault zone based on correlation of fault scarp breccias and antiformal axes (in turquoise) at Taylor Mountain (TM) and Sears Point (SP), which may indicate minimum displacement since ca. 7 Ma. Gravity contours (in green) show restored basin geometry that does not completely align the gravity lows (hachures) beneath the Santa Rosa Plain with those beneath San Pablo Bay and Sonoma Valley. Compression marked by structural highs such as Trenton Ridge and the high between Cotati and Sonoma basins is not removed for this reconstruction, accounting for some of the mismatch of gravity lows. Present position of San Pablo Bay on east side of Rodgers Creek fault zone is shown in light blue for reference. Latitude and longitude grid is displaced with restoration of respective blocks on either side of Rodgers Creek fault zone. Other abbreviations: TMFZ—Taylor Mountain fault zone; CPFZ—Cooks Peak fault zone.



4. Santa Rosa Pull-Apart Basin

The Santa Rosa pull-apart basin (McLaughlin et al., 2008; McPhee et al., 2007) is a structure that defines the most recent stage of Rodgers Creek–Maacama fault system reorganization. This pull-apart structure is a young, ~3-km-wide extensional depression between the Rodgers Creek and Maacama faults in the Santa Rosa area, filled with a thin cover of undeformed Quaternary sediments (Figs. 3, 5B, 5C, 9, 10, and 12). Faults bounding the east and west sides of this structure as well as the principal bounding faults of the Maacama and Rodgers Creek fault zones to the northeast and southwest are seismically active with prominent microseismicity (Fig. 9) extending to depths of ~10 km and with focal mechanisms indicating pure and oblique strike slip, with secondary components of extension or compression. The Santa Rosa area was severely shaken by two earthquakes (M5.6 and M5.7) in October 1969 that were located on the northern Rodgers Creek fault zone close to the western margin of the Santa

Rosa pull-apart basin (Wong and Bott, 1995; McPhee et al., 2007).

The geometry and timing of the opening of this pull-apart structure affected the long-term partitioning of slip between the Rodgers Creek and Maacama fault zones. Undeformed Quaternary sediments deposited in the north-oriented depression of the pull-apart basin unconformably overlie gravels and Sonoma Volcanics in northern Rincon Valley that are compressed into a northwest-trending synclinal trough. This relation is interpreted to indicate that the pull-apart depression postdates the folding and formed prior to and during deposition of the undeformed sediment fill. From the earlier section on Neogene stratigraphy, the upper part of the folded section includes the 0.8–1.2 Ma Bishop ash bed or an ash correlative with the younger set of the Glass Mountain ash beds, erupted from the Long Valley Caldera on the southeast side of the Sierra Nevada Mountains (McLaughlin et al., 2008; Sarna-Wojcicki et al., 2000, 2005; Metz and Mahood, 1991). This con-

strains opening of the pull-apart basin to after ca. 1.0 ± 0.2 Ma. The southwestern side of the Santa Rosa pull-apart basin is bounded partly by the southern Rodgers Creek fault zone and also by the Matanzas Creek fault zone, which splays southeast from the southern Rodgers Creek fault zone east of Taylor Mountain and merges with the Bennett Valley fault zone (Fig. 9). The approximate distance along the parallel trends of the Matanzas Creek and southern Rodgers Creek fault zones necessary to close the Santa Rosa pull-apart structure is $\sim 6.5 \pm 0.5$ km. We interpret this as the amount of dextral slip taken up by the Matanzas Creek and Bennett Valley fault zones during opening of the Santa Rosa pull-apart basin (Fig. 9).

Similarly, the northeast side of the Santa Rosa pull-apart basin is bounded for $\sim 6.0 \pm 0.5$ km (Fig. 9) by faults associated with the south end of the Maacama fault zone (including strands of the Maacama and Mark West fault zones). Like the south side of the pull-apart basin, this length of the Maacama fault zone that bounds the north

Evolution of the Rodgers Creek–Maacama fault system

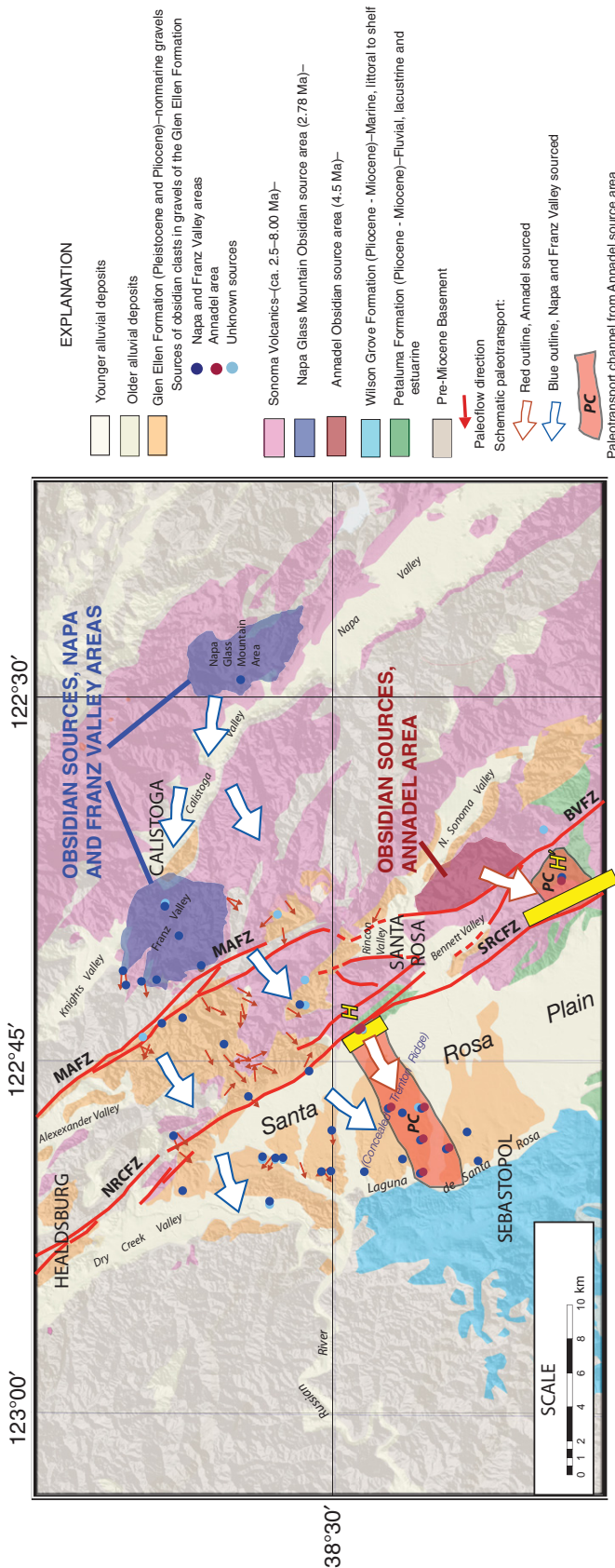


Figure 12. Fluvial transport patterns of different obsidian clast-bearing lithofacies of the Glen Ellen Formation that are offset by the combined northern (NRCFZ) and southern (SRCFZ) Rodgers Creek fault zones. One gravel lithofacies sourced from east of the Maacama fault zone (MAFZ) contains obsidian clasts (dark blue dots) from 2.78 Ma in-place Sonoma Volcanics in the Franz Valley and the Napa Glass Mountain areas. Another major source of Glen Ellen gravel obsidian clasts (dark red dots) are in-place 4.5 Ma vitric Sonoma rhyolites in the Annadel State Park area east of the southern Rodgers Creek and Bennett Valley (BVFZ) fault zones. The distribution of Annadel-derived clasts in gravels west of the NRCFZ and SRCFZ delineate a crude paleotransport channel (PC) ~2.5–3.0 km wide at its truncation on the southwest side of the NRCFZ (H; also Figs. 3 and 9). A remnant of the paleochannel is offset ~14.8 ± 6.0 km southeastward across the SRCFZ (H'; also Figs. 3 and 9). Yellow bar lengths indicate uncertainty to offset. See text for discussion of fault offset and Table 3.

side of the pull-apart basin is the approximate distance required to close the north side of the basin. As such, it is inferred to represent the approximate amount of dextral strike slip taken up by the Maacama fault zone during opening of the pull-apart basin. Thus, the Santa Rosa pull-apart basin represents a kinematic link between the Bennett Valley and Maacama fault zones that partly explains the partitioning of slip between the southern Rodgers Creek and Maacama fault zones across a prominent releasing bend or step initiated in the past 1 m.y. In the Santa Rosa area, however, the partitioning of slip between the Rodgers Creek fault zone and the Maacama fault zone since 1.0 Ma is accommodated on the Matanzas Creek and Bennett Valley fault zones rather than on the southern Rodgers Creek fault zone. The Bennett Valley fault zone converges with the southern Rodgers Creek fault zone only south of Sears Point, beneath Sonoma Valley or San Pablo Bay. The northern Rodgers Creek fault zone (Healdsburg fault segment), which is seismically active (Fig. 9) and displays evidence of Holocene surface displacement (Hecker and Kelsey, 2006; Crampton et al., 2004; Swan et al., 2003), is seemingly a continuation of the southern Rodgers Creek fault zone, apparently bypassing the Santa Rosa pull-apart structure. The northern and southern Rodgers Creek fault zones, north-trending faults bounding the west side of the Santa Rosa pull-apart basin, and the Matanzas Creek fault zone all merge or intersect each other beneath Santa Rosa Creek floodplain.

Northern Rodgers Creek Fault Zone (Healdsburg Fault Segment)

The Healdsburg fault segment is north of the Santa Rosa Creek floodplain (Figs. 2, 3, and 9). Gravity and aeromagnetic data suggest that the Healdsburg fault segment and southern Rodgers Creek fault zone are connected at shallow depth (Langenheim et al., 2008, 2010) and thus have overlapping histories and possibly similar long-term rates of slip. Surface geologic mapping (McLaughlin et al., 2008; Figs. 3 and 9) indicates that the fault connection occurs across a covered small right jog beneath the floodplain of Santa Rosa Creek.

Direct partitioning of slip from the Matanzas Creek fault zone to the northern Rodgers Creek fault zone (Healdsburg fault segment) is significantly diverted by faults associated with the eastern and western margins of the Santa Rosa pull-apart basin (e.g., the Spring Valley fault segment of the Bennett Valley fault zone; Fig. 9) link and clearly transfer slip between these faults and the Maacama fault zone, as indicated by seismicity. Other

seismicity and youthful fault geomorphology are dispersed along and between an overlap in the along-strike trends of the northern Rodgers Creek and Maacama fault zones northwest of Santa Rosa (Fig. 9). Faults that may accommodate the partitioning of slip to the northern Rodgers Creek fault zone include the likely link between the southern and northern Rodgers Creek fault zones beneath the Santa Rosa Creek floodplain; the Matanzas Creek fault and earlier extensional and transpressional faults that disrupt Neogene volcanic and sedimentary units north and south of the Santa Rosa Creek floodplain. Several faults mapped east of the northern and southern Rodgers Creek fault zones (McLaughlin *et al.*, 2004, 2008) exhibit strike slip, reverse slip, and normal slip, but their contributions to the Maacama or northern Rodgers Creek fault zones are largely unknown (McLaughlin *et al.*, 2002).

Displacement on the northern Rodgers Creek fault zone (Healdsburg fault segment) and its rate of slip north of Santa Rosa since 1 Ma are currently unconstrained by the bedrock geology. A longer term displacement history can be determined for the Healdsburg fault segment and southern Rodgers Creek fault zone between ca. 3 and 1 Ma, however, assuming that they were continuous prior to opening of the Santa Rosa pull-apart basin.

Correlative gravel remnants of the Glen Ellen Formation that now are separated right-laterally across the northern and southern Rodgers Creek fault zones are dated as younger than 2.8 ± 0.02 Ma from their contained obsidian clasts and a younger than 3.1 Ma basal tuff (Fig. 3, areas H and H'). The gravel remnants were therefore apparently right-laterally separated across the Rodgers Creek fault zone after ca. 3 Ma. The outcrop separation, however, does not provide a well-defined piercing blob for establishing fault displacement because the gravel remnant east of the Rodgers Creek fault zone is now isolated on a ridge top ~ 2 km from the main fault zone and because the original gravel distribution has been modified by dissection and erosion. However, the presence in the gravel of obsidian clasts derived from in-place sources in the Annadel State Park area to the northeast (location 26, Table 1) is distinct from other gravels of the Glen Ellen Formation east of the Rodgers Creek fault zone that contain only obsidian clasts sourced from the Napa and Franz Valley areas (locations 18, 20, Table 1). The correlative gravel remnant along the southwest side of the Rodgers Creek fault zone (Figs. 3 and 12, offset points H, H') is the northwesternmost area of known Annadel-sourced obsidian clasts southwest of the Rodgers Creek fault zone. The distribution of several other Glen Ellen gravel

localities containing Annadel-sourced obsidian clasts on the Santa Rosa Plain to the southwest, together with paleoflow data, constrains the aerial configuration of the fluvial system that transported these lithofacies from the Annadel area (McLaughlin *et al.*, 2005; Sweetkind *et al.*, 2008, 2010). The distribution of the Annadel lithofacies on the Santa Rosa Plain suggests that the fluvial transport system may have had a width of ~ 2.5 – 3.0 km where it crossed the Rodgers Creek fault zone (Fig. 12). Using this width to crudely constrain that of the Annadel-sourced fluvial system for our one locality east of the southern Rodgers Creek fault zone, and assuming that the gravel at this exposure was deposited in a 3-km-wide paleochannel, permits a crude restoration of dextral displacement. Based on this restoration (Fig. 12), we estimate that the Annadel-sourced gravel remnants are offset $\sim 14.8 \pm 6.0$ km across the northern and southern Rodgers Creek fault zones.

Rodgers Creek Fault Zone Slip Rates

Paleoseismology studies since the 1990s along the Rodgers Creek fault zone south of Santa Rosa provide a Holocene slip rate estimate for the southern part of the Rodgers Creek fault zone of 6.4–10.4 mm/yr, with an average rupture recurrence of 131–370 yr (Hecker *et al.*, 2005; Budding *et al.*, 1991). In addition, recent satellite-based permanent scatterer interferometric synthetic aperture radar (PS-InSAR) studies (Funning *et al.*, 2007) suggest that to the northwest and southeast of the Santa Rosa pull-apart basin, the Rodgers Creek fault zone is undergoing as much as 7.5 ± 2.6 mm/yr of shallow creep above a depth of 6 km.

Long-term slip rates for several time windows during evolution of the Rodgers Creek fault zone between ca. 7 and 0.8 Ma are inferred here, from displacement constraints on the several faults described here (Table 3). As the geometry and style of faulting associated with the Rodgers Creek fault zone evolved, the components of normal and reverse slip on early faulting stages appear to have increasingly been taken up by younger, steeper faults that accommodated larger components of right-lateral strike slip.

The 28 ± 0.5 km of total minimum offset estimated for the Rodgers Creek fault zone (Table 3) is partitioned between the combined active southern Rodgers Creek and northern Rodgers Creek fault zones, thrust faults that partitioned and uplifted the east side of the Santa Rosa Plain between ca. 5 and 3 Ma, and earlier extensional faults bounding the east side of Cotati basin (Fig. 13; Table 3). Approximately 13.2 ± 1.8 km of strike-slip displacement appears to have predated the later than $2.78 \pm$

0.02 Ma deposition of gravels offset along the combined southern and northern Rodgers Creek fault zones (Table 3). The unconstrained partitioning of this 13 km of slip could be taken up in part by the early transpressional faults (e.g., Taylor Mountain fault zone, active between 5 and 3 Ma) and extensional (probably trans-tensional) faults (e.g., Cooks Peak fault zone, active between ca. 5 and 7 Ma) that splay northwestward on Taylor Mountain from their junction (Figs. 3, 9, and 13) with the active southern Rodgers Creek fault zone.

The Santa Rosa pull-apart basin that initiated a well-delineated link of partitioned slip between the Bennett Valley and Maacama fault zones via the Spring Valley fault (Fig. 9) is not clearly linked to the Rodgers Creek fault zone at the surface. If the Matanzas Creek fault zone existed prior to ca. 2.8 Ma, unknown additional slip could have transferred between the northern Rodgers Creek and Bennett Valley fault zones via the Matanzas Creek fault zone. The northern Rodgers Creek fault zone (Healdsburg fault segment) may currently take up all southern Rodgers Creek fault zone slip, but complexities along the junction of the Rodgers Creek fault zone with the Santa Rosa pull-apart basin discussed here (Fig. 9) and lack of a recognized offset exclusively along the northern Rodgers Creek fault zone (Healdsburg fault segment) leads us to consider the northern Rodgers Creek fault zone slip rate since ca. 1.0 ± 0.2 Ma as unconstrained.

Based on these offset relations and an assumption that the earliest phase of extensional deformation for the Rodgers Creek fault zone included a component of dextral slip, the composite long-term slip rate of the Rodgers Creek fault zone since opening of the Cotati basin is 28 ± 0.5 km in 7.0 ± 0.3 m.y., or 4.1 ± 0.3 mm/yr (Table 3).

If the early phase of extensional deformation did not accommodate any of the long-term dextral displacement (a permissive but unproven interpretation), it can be argued that all strike slip on the fault zone has occurred since the initiation of transpression ca. 5 Ma. This latter interpretation would yield a higher composite long-term slip rate of ~ 5.6 mm/yr, which is similar to rates derived here for the more recent time windows of fault zone evolution and is compelling for that reason. Normal faults bounding the west side of the Santa Rosa Plain, however, have orientations slightly oblique to the direction of regional extension, suggesting a component of transtension during the early extensional basin phase of fault zone evolution that would contribute to and result in a lower composite long-term rate of strike slip. Both options for modeling early slip suggest that sig-

Evolution of the Rodgers Creek–Maacama fault system

TABLE 3. DISPLACEMENTS AND SLIP RATES OF FAULTS OF THE RODGERS CREEK–MAACAMA FAULT SYSTEM AND THEIR CONTRIBUTION TO LONG-TERM SLIP OF THE HAYWARD-CALAVERAS FAULT SYSTEM			
Fault zone	Timing of displacement (Ma)	Amount of dextral displacement (km)	Dextral slip rate (mm/yr)
Rodgers Creek fault zone*	7.0 ± 0.3 to 0	≥28 ± 0.5	4.1 ± 0.3
Pre-Santa Rosa pull-apart basin**	7.0 ± 0.3 to 1.8 ± 1.0	13.2 ± 1.8	2.8 ± 1.1
Northern and southern Rodgers Creek fault zones, post-Glen Ellen Formation***	2.78 ± 0.02 to 0	14.8 ± 6.0	5.3 ± 2.2
Bennett Valley and Matanzas Creek fault zones¹	1.0 ± 0.2 to 0	6.5 ± 0.5	6.8 ± 1.8
Maacama fault zone[§]			
	A 3.17 ± 0.04 to 0	17.5–24 (20.8 ± 3.3)	6.7 ± 1.2
	B 3.17 ± 0.04 to 0	21–22 (21.5 ± 0.5)	6.9 ± 0.4
	C 3.17 ± 0.04 to 0	12–26 (19 ± 7)	6.0 ± 2.3
Pre-Santa Rosa pull-apart basin slip ^{§§}	3.17 ± 0.04 to 1.0 ± 0.2	12.0–17.6 (14.8 ± 2.8)	7.0 ± 2.1
Slip since opening of Santa Rosa pull-apart basin	1.0 ± 0.2 to 0	6.0 ± 0.5	6.3 ± 1.8
Total slip partitioned to Hayward-Calaveras fault system^{§§§}	7.0 ± 0.3 to 0	44.4–52.5 (48.4 ± 1.4)	6.95 ± 0.85
<p>*Total cumulative displacement for the Rodgers Creek fault zone includes significant but unknown components of early normal slip (Cooks Peak fault zone) that occurred with inferred opening of a transtensional basin beneath Santa Rosa Plain 7.0 ± 0.3 Ma. Extensional faulting was followed by east-directed reverse faulting (Taylor Mountain fault zone) that uplifted the east side of Santa Rosa Plain and reactivated the normal faults as thrusts.</p> <p>**Displacement on northern and southern Rodgers Creek fault zones is based on total Rodgers Creek fault zone displacement less amount of displacement of Annadel-sourced gravels deposited after 2.80 Ma and before 0.8 Ma (between 2.78 ± 0.02 and 1.0 ± 0.2 Ma).</p> <p>***Displacement on northern and southern Rodgers Creek fault zones since 2.78 ± 0.02 Ma is based on offset constraints for Annadel-sourced gravel lithofacies of Glenn Ellen Formation.</p> <p>¹Quaternary fault displacement, interpreted as distance required to close south side of the Santa Rosa pull-apart basin depression along the Bennett Valley and Matanzas Creek fault zones. Displacement probably contributes to total slip of the Rodgers Creek fault zone south of Sears Point, and links with Quaternary Maacama fault zone displacement on north side of Santa Rosa pull-apart basin.</p> <p>[§]Total offset determinations for Maacama fault zone: (A) Timing of faulting and amount of displacement are determined from dated offset Sonoma Volcanics. Displacement includes 6.0 ± 0.5 km of slip from opening of the north side of Santa Rosa pull-apart basin. (B) Maximum amount of displacement determined from offset of Mesozoic Coast Range Ophiolite. Timing of faulting is assumed from displacement that is similar to that for offset Sonoma Volcanics (see A). (C) Maximum displacement inferred from magnetic anomalies correlated across Maacama fault zone. Timing of faulting is assumed similar to that for offset of Coast Range Ophiolite (see B).</p> <p>^{§§}Pre-Santa Rosa pull-apart basin slip displacement for Maacama fault zone is based on offset Sonoma Volcanics (see A) less slip since 1.0 ± 0.2 Ma.</p> <p>^{§§§}Maximum and minimum long-term displacements for the Maacama fault here are averages of summed maximum and minimum displacements of the Sonoma Volcanics, Coast Range Ophiolite, and offset magnetic anomalies (see notes A–C). Range in maximum slip attributed to the Rodgers Creek–Maacama fault system is therefore 28 ± 0.5 km added to the range of the averaged maximum and minimum long-term slip values (20.4 ± 3.6 km) for the Maacama fault zone.</p>			

nificant fault displacement during early stages in the evolution of the Rodgers Creek fault zone was translated into vertical slip, reducing the derived long-term rate of strike slip.

The composite long-term slip on the Rodgers Creek fault zone before 0.8–1.2 Ma is 13.2 ± 1.8 km in 5.2 ± 1.3 m.y., or 2.8 ± 1.1 mm/yr. Though not transferred to the Rodgers Creek fault zone north of Sears Point, displacement on the Bennett Valley and Matanzas Creek fault zones since the 1.0 ± 0.2 Ma opening of the Santa Rosa pull-apart basin appears to have been ~6.5 ± 0.5 km at a rate of ~6.8 ± 1.8 mm/yr. This slip rate is significantly higher than for the somewhat earlier faults of the Rodgers Creek fault zone in the Santa Rosa area.

The lithofacies of the Glen Ellen Formation containing obsidian pebbles derived both from

Annadel and sources in the Napa and Franz Valleys is offset 14.8 ± 6.0 km across the combined northern (Healdsburg fault segment) and southern Rodgers Creek fault zones, which are inferred to have been more continuous prior to formation of the Santa Rosa pull-apart basin. The displacement of these Glen Ellen Formation gravels yields a slip rate of 5.3 ± 2.2 mm/yr since 2.76–2.80 Ma, which is also higher than for the 3 Ma and older composite faulting on the northern and southern Rodgers Creek fault zones. The composite slip rate for the Rodgers Creek fault zone thus appears to have increased prior to ca. 3 Ma, close to when transpression along the Taylor Mountain fault zone largely ceased and slip splayed eastward onto a newly initiated, dominantly strike-slip Rodgers Creek fault zone (Fig. 13). Faults of the currently

active Rodgers Creek fault zone are subvertical in geometry and clearly accommodate dominant dextral strike slip (Wong and Bott, 1995), consistent with a comparatively higher observed rate of strike slip since 3 Ma.

Is All the Long-Term Rodgers Creek Fault Slip Accounted for?

If our proposed 7 Ma timing for initiation of slip on the Rodgers Creek fault zone is not valid, total slip on the Rodgers Creek fault zone could be significantly greater than 28 km, since no constraints on offset of units older than ca. 8 Ma are determined. Restoration of the offset breccia of Warrington Road to the breccias exposed near Sears Point is the minimum displacement needed to restore these rocks to

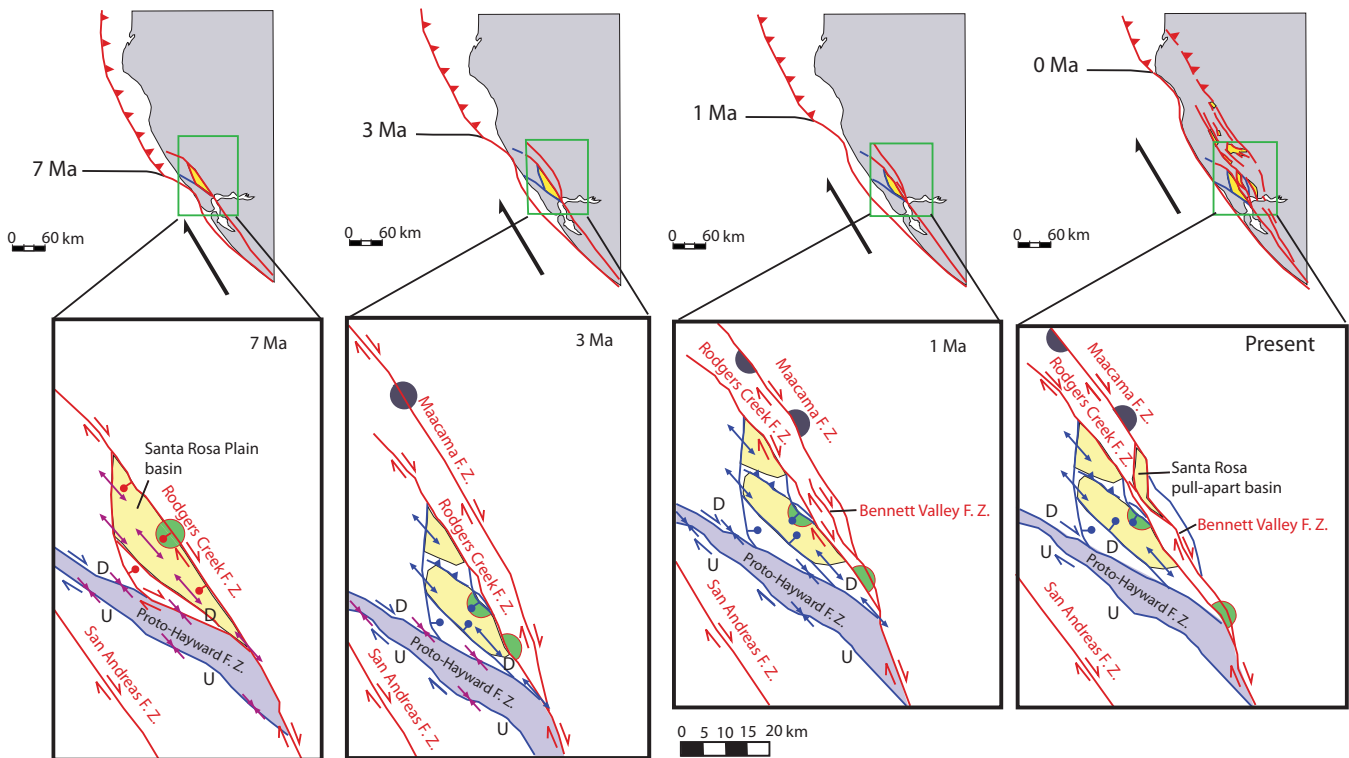


Figure 13. Schematic maps showing successive reorganizations of the Rodgers Creek–Maacama fault system with time in relation to adjacent northward migration of restraining and releasing bend geometries of the northern San Andreas fault zone in the wake of the Mendocino Triple Junction. F.Z.—fault zone; U—upthrown; D—downthrown. Time windows are shown beginning ca. 7 Ma, with formation of the buried transensional basin beneath Santa Rosa Plain. The fault system is seen to undergo successive reorganizations in response to the encroachment and passage of the releasing bend segment of the San Andreas fault zone between 7 Ma and the present. Continual northward lengthening of the transform margin imposes significant changes in fault geometry on the area east of the Mendocino Triple Junction because of the bending northern San Andreas fault geometry. In detail, the succession of compressional and extensional deformation in evolution of the Rodgers Creek–Maacama fault system appears to be a necessary response at the south end of the fault system to continual fault zone lengthening and reorganization at its northern end as the Mendocino Triple Junction propagates. Active faults for indicated time windows are shown in red; inactive faults in blue. Purple double-headed arrows indicate orientation of active extension (arrows point away from each other) or compression (arrows point toward each other). Double-headed blue arrows show inferred areas of formerly active transension or transpression. Green and dark gray circle symbols bisected by the Rodgers Creek and Maacama fault zones are arbitrary reference points illustrating offset across the Rodgers Creek (green circle) and Maacama (dark gray circle) fault zones, based on displacements established in this paper (Table 3).

their predisplacement location because the area southeast of Sears Point and Donnell Ranch is covered by alluvium and the San Francisco Bay margin. Although we have correlated the axes of antiformal features across the Rodgers Creek fault zone in addition to the offset fault scarp breccias (Figs. 3 and 11), this alignment is possibly fortuitous and the breccia of Warrington Road might restore farther south, to somewhere along the buried southern margins of Sonoma Valley or San Pablo Bay basins. The gravity expression of closure for Cotati and Windsor basins (Fig. 11; Table 3) suggests that an additional 24 km of slip along the Rodgers Creek fault would bring the northeast side of Windsor basin into alignment with the southwest side of

Sonoma and San Pablo Bay basins along the Rodgers Creek fault zone (Fig. 11). This would increase the maximum slip on the Rodgers Creek fault zone to ~52 km and raise the long-term slip rate to $\sim 7.7 \pm 0.6$ mm/yr, assuming the same timing of initiation of the faulting.

This larger displacement based on alignment of gravity-defined basin margins, however, implies that the Cotati and Windsor basins should include thick sections of the Coast Range Ophiolite overlain by Great Valley Sequence rocks as well as Tertiary strata that predate the Petaluma Formation, all of which occur in the Sonoma and San Pablo Bay basins (Wright and Smith, 1992). Significant sections of Great Valley Sequence and Coast Range Ophiolite are

exposed along the northwestern margins of the Santa Rosa Plain and project beneath the Windsor and Cotati basins. However, the deepest drilled wells, which are in Cotati basin (~1530–1820 m), bottomed in sedimentary rocks interpreted to be Franciscan Complex sandstone and argillite, with no intervening Coast Range Ophiolite or Great Valley Sequence. With the exception of oil having a Miocene Monterey Formation geochemical signature (Lillis et al., 2001), no actual pre-Petaluma Tertiary strata are known. An offset substantially greater than 28 km would also misalign the correlative fault scarp breccias of Warrington Road and Sears Point by 24 km along the Rodgers Creek fault zone, with no data from the intervening covered

area to corroborate their continuity. Without more information on the subsurface distribution of the fault scarp breccias of Warrington Road and Sears Point beneath Sonoma Valley, the larger displacement and greater slip rate are here considered highly speculative. The lower long-term displacement and slip rate proposed here are therefore favored, but viewed as a minimum.

Maacama Fault Zone

Displacement across the Maacama fault zone is estimated from several cross-fault correlations of distinctive units of the Sonoma Volcanics, Neogene gravels, and Mesozoic basement rocks. The most definitive estimate of long-term Neogene offset comes from the correlation of exposures of Sonoma Volcanics belonging to the Mount St. Helena eruptive sequence and associated distinctive fluvial strata (Fig. 7). The volcanics were vented from an area of flows, domes, intrusive vents, thick ash, and laharic breccia deposits that are exposed for ~11 km along the east side of the Maacama fault zone.

The northwesternmost and youngest outcrop areas of Sonoma Volcanics occur between the northern Rodgers Creek and Maacama fault zones (areas M.1 and M', Figs. 3 and 7). Together, these outcrop areas of Sonoma Volcanics constrain the maximum northwestward extent of Sonoma volcanism and seemingly also limit post-3.2 Ma offset across the Maacama fault zone.

The northwesternmost and youngest of these exposures are ~2 km southwest of the Maacama fault zone just northwest of Geyserville (M.1, Fig. 3). These dacitic volcanics are apparently the youngest of the Sonoma Volcanics, with a $^{40}\text{Ar}/^{39}\text{Ar}$ age of 2.5 ± 0.09 Ma (location 1, Table 1; Fig. 7). No Sonoma Volcanics of equivalent age (2.5 Ma) have been mapped on the northeast side of the Maacama fault zone, although they could be present in undated, stratigraphically high parts of the Mount St. Helena volcanic section. Alternatively, the 2.5 Ma dacitic rocks represent a small volcanic center that was not offset by the Maacama fault zone, that erupted separately from and slightly northwest of the Mount St. Helena eruptive sequence. Somewhat younger rhyolitic volcanics of Pine Mountain (location 15, Table 1; Fig. 7), dated at 2.2 ± 0.029 Ma, that occur east of the Maacama fault zone and northwest of Mount St. Helena, are considered part of the younger Clear Lake volcanic field, and this constrains the northwestern extent of Sonoma volcanism east of the Maacama fault zone.

A second area of youngest and most northwestward displaced exposures of Sonoma Vol-

canics is exposed to the southeast of the Geyserville volcanics for ~5 km along the southwest side of the Maacama fault zone (Figs. 7 and 14). These rocks are best exposed in the southeastern parts of these exposures, in roadcuts east of Alexander Valley (fault length M' in Figs. 3 and 14; also locations 16 and 69 in Fig. 7; Tables 1 and 2). At this locality, a west-dipping section of ash flow and air-fall tuff unconformably overlies basaltic andesite. The volcanics in turn overlie steeply dipping or folded Pliocene fluvial siltstone and pebble gravel composed of rounded to subrounded clasts derived entirely from mélangé of the Mesozoic Franciscan Central belt and the Coast Range Ophiolite. The gravels contain no clasts derived from Tertiary volcanics, distinguishing them from other 3.2 Ma and older gravel units of the region. The gravel, basaltic andesite, and tuff section abuts the southwest side of the Maacama fault zone along the Geysers–Healdsburg road. The tuff is dated by $^{40}\text{Ar}/^{39}\text{Ar}$ analysis of plagioclase at 3.17 ± 0.04 Ma (isochron age, location 15, Table 1; location 69, Table 2; Figs. 7 and 14). The lowermost tephra layers in the tuff section correlate geochemically with the Putah Tuff, dated elsewhere at 3.34–3.27 Ma and the uppermost ash-flow tuff of the section is correlated to tephra layers dated elsewhere at 3.25–3.19 Ma (McLaughlin et al., 2005, and this paper). Thus, the ash section was erupted in a relatively short time interval between ~3.3 and 3.2 Ma.

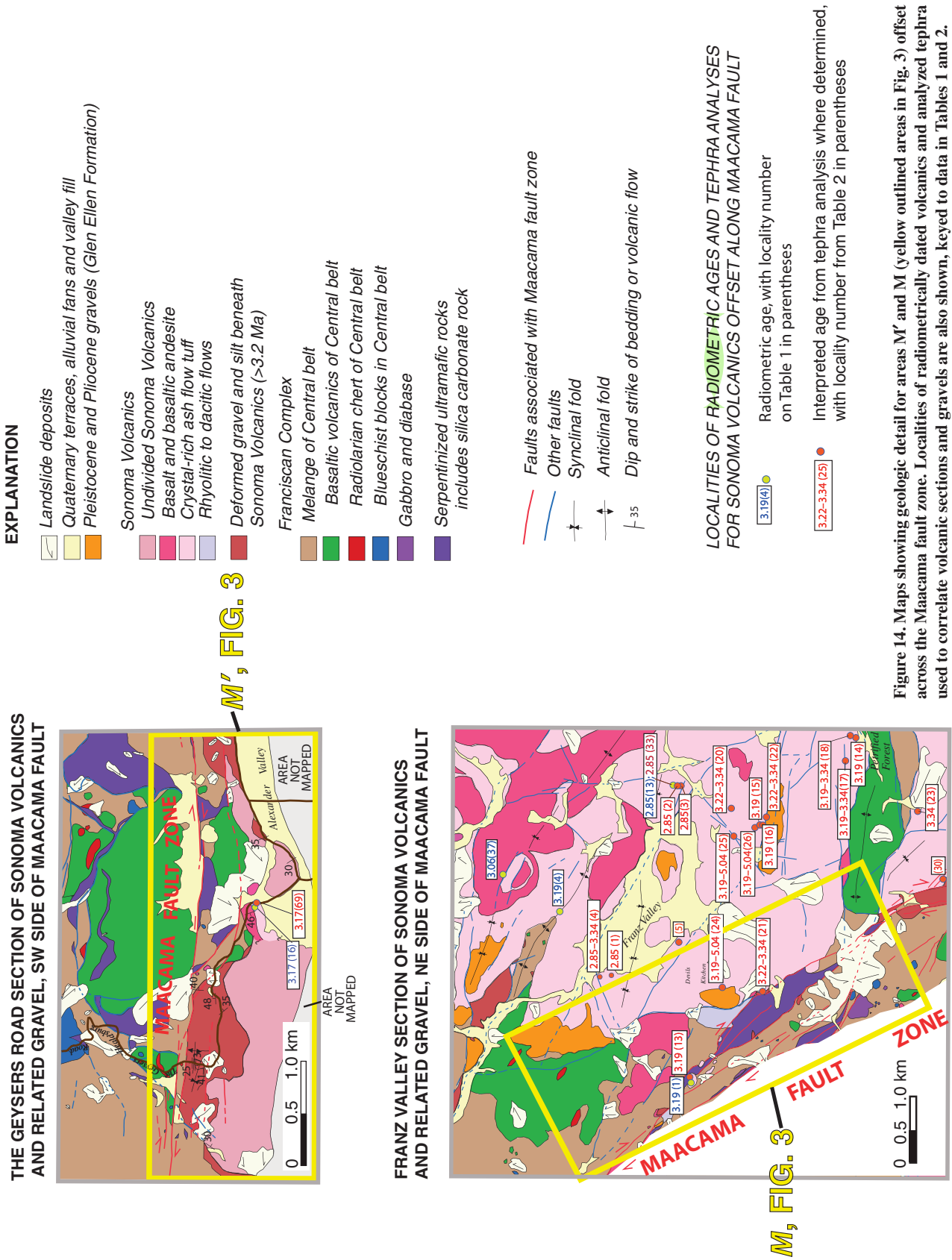
We correlate the part of the Mount St. Helena eruptive center abutting the Maacama fault zone for ~5–6 km along the southwest side of Franz Valley (fault length M in Figs. 3, and 14; McLaughlin et al., 2004) with the Geysers–Healdsburg road volcanics and gravels. Correlated tephra units and Ar/Ar ages in this area include the Putah Tuff (~3.3–3.2 Ma), the tuff of the Petrified Forest (~3.3–3.4 Ma), and a local tuff (tuff of the Pepperwood Ranch) dated at 3.19 Ma (See Tables 1 and 2 and Figure 7 for detailed age data and uncertainties). Locally, steeply dipping fluvial gravels with the same clast suite as the gravels along the Geysers–Healdsburg road unconformably underlie the volcanic section of Franz Valley. Basaltic andesite occurs sporadically and unconformably beneath the tuffs and gravels of Franz Valley and also higher in the tuff section. The proximal aspect and connection of the Franz Valley volcanic section to the Mount St. Helena eruptive center and its correspondence to the tuff and gravel section along the Geysers–Healdsburg road, suggests a displacement along the Maacama fault zone of between 17.5 and 24 km since ca. 3.2 Ma (Figs. 3, 7, and 14; Ar/Ar age location 3, Table 1; tephra locations 23 and 13–16, Table 2).

Basement Displaced across Maacama Fault Zone

A bedrock–offset relation corroborating Neogene displacement of the Sonoma Volcanics across the Maacama fault zone restores 21–22 km of displacement of the Coast Range Ophiolite from the vicinity of Hopland to the Geyser Peak area (Fig. 15; Table 3). This restoration aligns the northwest and southeast contacts of the Geyser Peak section of the Coast Range Ophiolite to the northeast, with northwest and southeast contacts of the ophiolite on the southwest side of the fault near Hopland (Fig. 15). The mapped extent of the Hopland ophiolite belt along the southwest side of the Maacama fault zone corresponds closely with the width of the Geyser Peak ophiolite section along the northeast side of the Maacama fault zone, providing an elongate 3 ± 0.5 km wide body that is offset 21.5 ± 0.5 km along the Maacama fault zone. The Hopland section, recognized in this report as part of the Coast Range Ophiolite, was previously only mapped in reconnaissance as a west-northwest–trending belt of serpentinite enclosed by mélangé of the Franciscan Complex (Irwin, 1960).

Reconnaissance of the Hopland area ophiolite section indicates that several aspects of its stratigraphy match that of the upper part of the Geyser Peak ophiolite section (Fig. 16). Criteria for this correlation include the presence of a gabbroic intrusive complex overlying serpentinitized peridotite, together overlain locally by a distinctive angular, coarse clastic breccia of mafic plutonic, volcanic, and volcanopelagic debris of Jurassic age shed from the underlying ophiolite. This clastic ophiolitic breccia is overlain in both the Hopland and Geyser Peak areas by turbiditic sandstone and argillite composed predominantly of mafic detritus (Fig. 16). The Geyser Peak and Hopland sections of the Coast Range Ophiolite are typical of a tectonostratigraphic terrane of the Coast Range Ophiolite and lower Great Valley Sequence referred to as the Elder Creek terrane (Blake et al., 1985; McLaughlin et al., 1988; Hopson et al., 2008) that is exposed along the western side of the Sacramento Valley.

Except for the Hopland section of the Elder Creek terrane, this distinctive stratigraphy, including ophiolitic breccia at the base of the Great Valley Sequence, is unknown west of the Maacama fault zone. A very different, well-studied terrane of the Coast Range Ophiolite plus Great Valley Sequence referred to as the Healdsburg terrane (Blake et al., 1984; Hopson et al., 1981, 2008) occurs 25–30 km south of the Hopland ophiolite and west of the Maacama and Healdsburg faults and Alexander and Dry Creek Valleys (Fig. 15). The Healdsburg terrane includes thick volcano-



Evolution of the Rodgers Creek–Maacama fault system

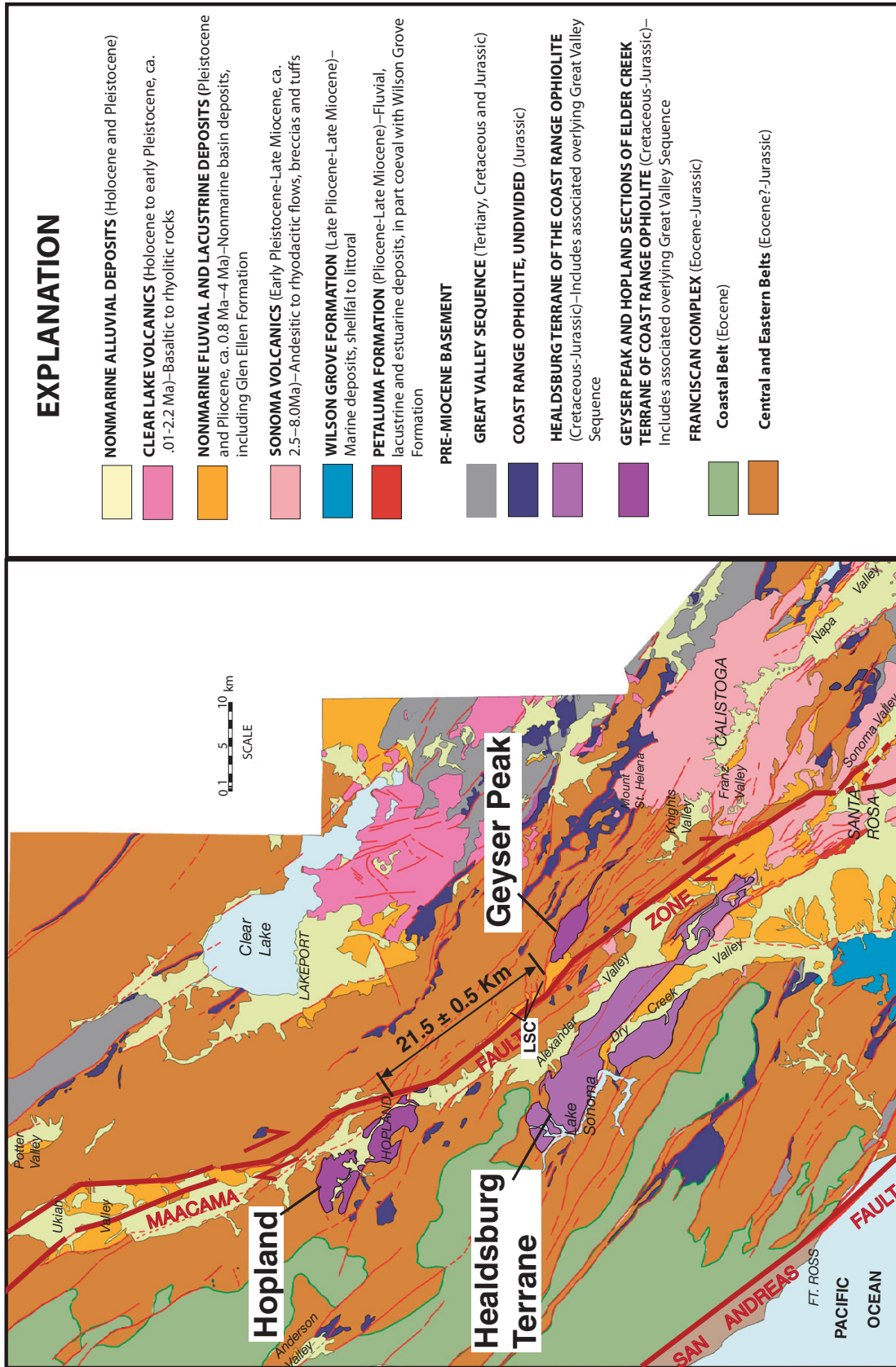
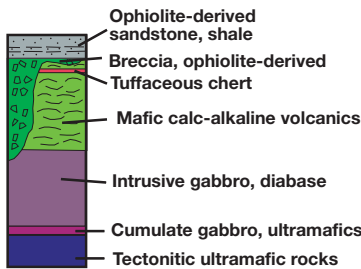
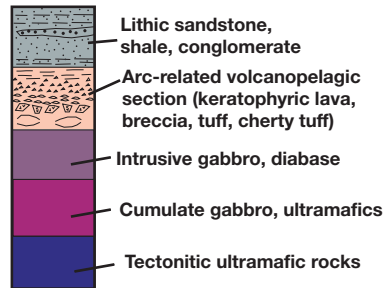


Figure 15. Regional geologic map showing locations of Elder Creek terrane sections of the Coast Range Ophiolite plus Great Valley Sequence offset along the Maacama fault zone. Also shown is location of the Healdsburg terrane, having a distinctively different ophiolite stratigraphy. See Figure 16 for comparative stratigraphic sections. LSC denotes location of Little Sulfur Creek strike-slip basins, which partially cover Geyser Peak ophiolite section along east side of Maacama fault zone.

A. GEYSER PEAK AND HOPLAND SECTIONS OF ELDER CREEK TERRANE OF COAST RANGE OPHIOLITE AND GREAT VALLEY SEQUENCE



B. HEALDSBURG TERRANE OF COAST RANGE OPHIOLITE AND GREAT VALLEY SEQUENCE



(schematic sections, not to scale)

Figure 16. (A) Schematic tectonostratigraphy for sections of the Elder Creek terrane at Geysler Peak and Hopland that are offset along the Maacama fault zone. (B) Generalized tectonostratigraphy of Healdsburg terrane on southwest side of Maacama fault zone south of Hopland, shown for comparison. (Sections are generalized from Blake et al., 1984; Hopson et al., 1981, 2008; McLaughlin et al., 1988.) See Figure 15 for map locations.

pelagic strata and keratophyric volcanic rocks in the ophiolite, overlain by Late Jurassic to Early Cretaceous non-ophiolite-derived conglomerate, sandstone, and shale (Fig. 16; Blake et al., 1984).

Magnetic Anomalies Displaced across Maacama Fault Zone

Fault offsets from aeromagnetic data are essentially based on the same criteria (ophiolitic or related mafic rocks) used to determine offset surface contacts of the correlated Geysler Peak and Hopland outliers of the Coast Range Ophiolite. Interpreted magnetic offsets, however, are based on the matching of similar maximum intensities and configurations of correlated magnetic (or nonmagnetic) bodies across the fault. Also, magnetic anomalies in general often reflect the geometry of a magnetic body at depth, and as such do not necessarily correspond with mapped surface contacts. In spite of these fundamental differences in how fault displacements are determined, the geologic and aeromagnetic data sets for the Maacama fault zone are complementary and provide similar independent long-term offset and slip rate estimates.

Separate basement offsets of 15 ± 3 km of a weakly magnetic mélangé unit in the Franciscan Complex and a 21 ± 5 km offset of parts of the Coast Range Ophiolite were obtained by matching magnetic anomalies across the Maacama fault zone (respectively, anomalies 1-1' and 2-2', Fig. 17). Offset anomaly 1-1' in Figure 17 corresponds to a mélangé unit of the Franciscan Complex along the Maacama fault zone, which at the surface contains entrained lenticular bod-

ies of serpentinite, gabbro, and greenstone. Offset anomaly 2-2' (Fig. 17) matches northwest and southeast limits of an anomaly associated with the Hopland ophiolite section where it abuts the southwest side of the Maacama fault zone, with the projected extent of an anomaly over the Geysler Peak ophiolite northeast of the fault zone. The Geysler Peak anomaly is separated from the main trace of the Maacama fault zone by fault strands bounding the strike-slip basins of Little Sulfur Creek (Fig. 15), and the fill of these basins obscures the magnetic expression of truncation of the Geysler Peak anomaly at the Maacama fault zone.

Maacama Fault Zone Offset and Slip Rates

Results of this study suggest that the Maacama fault zone has maintained a long-term average slip rate of -6.7 ± 1.2 mm/yr since ca. 3.17 ± 0.04 Ma, based on 17.5–24.0 km of offset of the Sonoma Volcanics. As discussed herein, the Maacama fault zone appears to have accommodated 6.0 ± 0.5 km of slip since 0.8–1.2 Ma, during Santa Rosa pull-apart basin opening. The average slip rate of 6.3 ± 1.8 mm/yr since 1.0 ± 0.2 Ma (Table 3) is generally comparable to the rate determined for the Maacama fault zone based on offset of the Sonoma Volcanics since 3.2 Ma. Geologic displacements of Jurassic ophiolitic basement across the Maacama fault zone favor a maximum displacement of -21.5 ± 0.5 km, which is about the same as the offset of the Sonoma Volcanics (20.9 ± 3.4 km). We therefore suggest an initiation time of ca. 3.17 ± 0.04 Ma for displacement along the Maacama

fault zone and a long-term slip rate based on the offset ophiolite sections of 6.9 ± 0.4 mm/yr.

Aeromagnetically determined fault displacements are in reasonably close agreement with the geologically determined displacements, given the uncertainties associated with the different approaches. Maximum displacements of 15 ± 3 and 21 ± 5 km for two separate offset magnetic anomaly sets, associated with the Franciscan Complex and the Coast Range Ophiolite, respectively, suggest a total long-term displacement of 19 ± 7 km for the Maacama fault zone, at a rate of 6.0 ± 2.3 mm/yr (Fig. 17; Table 3).

By comparison, geodetic and paleoseismic data along the Maacama fault zone north of Santa Rosa suggest that its slip rate in the Holocene has fluctuated between 6.5 and 14 mm/yr (Frey Mueller et al., 1999; Larsen et al., 2005; Sickler et al., 2005; Prentice and Fenton, 2005; Simpson, 2005). Local episodic creep that occurs along the fault both at the surface and at depth is poorly understood in the context of modern fault kinematics (Galehouse, 2002; Frey Mueller et al., 1999), and the role of creep in long-term evolution of the fault zone is largely unknown. For this reason, differences in long-term displacements and slip rates determined from the surface geology compared to near term rates from paleoseismic or geophysical data may reflect real differences in the kinematics of the Maacama fault zone over time both at the surface and at depth, and not merely uncertainties inherent in the comparison of results derived from geologic versus geophysical approaches. The data sets presented here suggest there is reasonably close agreement between geologic and potential field-derived displacement data for the Maacama fault zone.

CONTRIBUTION TO LONG-TERM HAYWARD-CALAVERAS FAULT SYSTEM

The total slip contributed to the Hayward fault zone by the Rodgers Creek fault zone amounts to at least 28 ± 0.5 km (Table 3). Based on averaged maximum and minimum displacements of all displacement criteria (Table 3), the Maacama fault zone separately contributes $\sim 20.4 \pm 3.6$ (16.8–24) km (Table 3) of displacement to the Hayward fault zone southeast of the Sears Point–Donnell Ranch area via the Bennett Valley fault zone (Figs. 11 and 13; Table 3). At least 44.4–52.5 (48.4 ± 1.4) km of slip is therefore contributed to the Hayward fault zone by the Rodgers Creek–Maacama stepover fault system south of the Sears Point–Donnell Ranch area.

Although antiformal axes appear to align after restoring displacement of a fault scarp

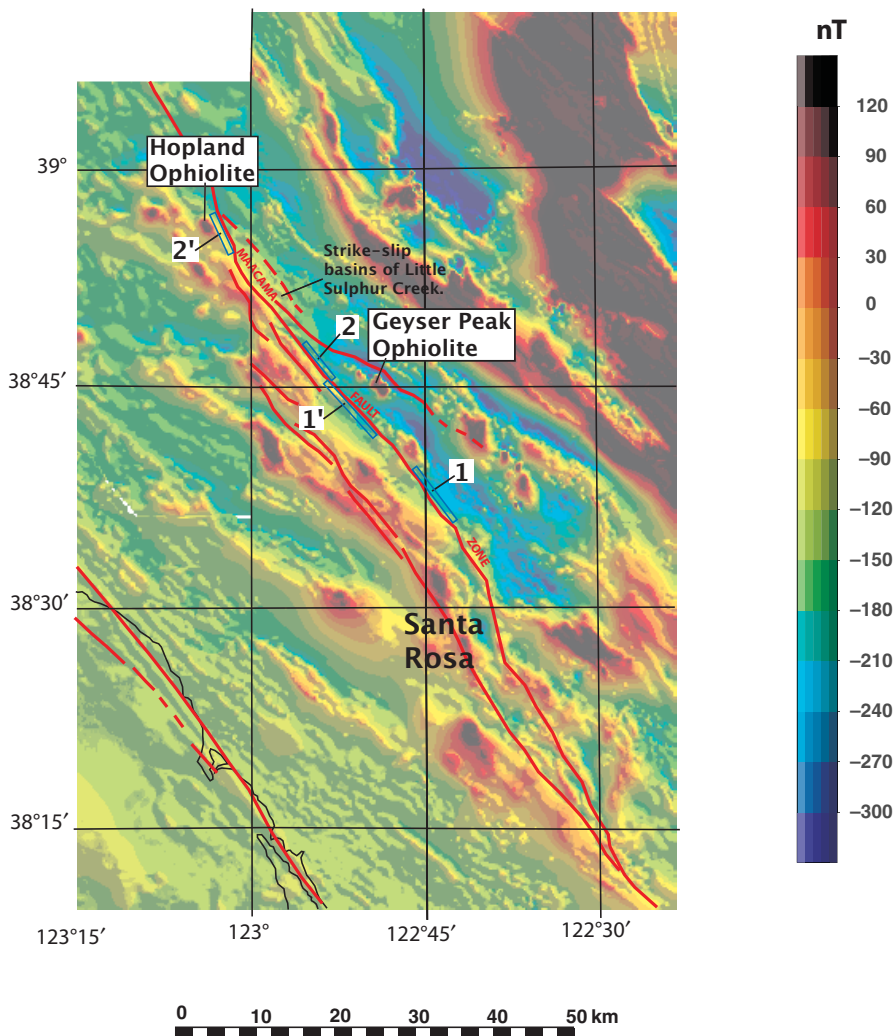


Figure 17. Aeromagnetic map delineating two sets of magnetic features offset across the Maacama fault zone. Magnetic intensity is shown in nanoteslas (nT), with increasingly higher magnetic intensity indicated by warmer colors ($nT \geq 0$) and lower magnetic intensity by cooler colors ($nT \leq 0$). Dark blue hollow bars delineate lengths of offset magnetic features along the Maacama fault zone, from which limits of uncertainty are derived. Magnetic feature 1–1', offset 15 ± 3 km, with a low to very low magnetic intensity, corresponds at the surface to mélangé of the Central Belt of the Franciscan Complex. Magnetic feature 2–2', offset 21 ± 5 km with a high to moderately low magnetic intensity, corresponds to the magnetic expression of the offset sections of the Coast Range Ophiolite at Geyser Peak (2) and Hopland (2'). Truncation of the Geyser Peak ophiolite along the northeast side of the Maacama fault zone is masked by gravels in Little Sulfur Creek strike-slip basins (Fig. 15). Projection of the ophiolite beneath these basins to the Maacama fault zone is based on subtle west-northwest-trending low-intensity lineaments. See text for additional discussion and Table 3.

breccia across the northern and southern Rodgers Creek fault zones, the correlation of the antiform axes is nonunique and their alignment could be fortuitous. The breccia exposures east of the Rodgers Creek fault in the Sears Point area also have an unknown distribution

beneath the alluvium of southern Sonoma Valley. It is not recognized at the surface south of San Pablo Bay or reported in the subsurface of San Pablo Bay (Wright and Smith, 1992). A conservative interpretation of this data set infers the 28 ± 0.5 km offset of the fault scarp

breccias to be a minimum displacement since 7.0 ± 0.3 Ma (Table 3).

As determined from different geologic criteria, long-term displacement has been 17.5–24 km and slip rates have been between 5.5 and 7.9 mm/yr on the Maacama fault since ca. 3.17 ± 0.04 Ma (Table 3). Displacement based on the matching of aeromagnetic anomalies across the Maacama fault zone yield a similar range of displacement (12–26 km) and a slip rate of 6.0 ± 2.3 mm/yr, if it is assumed that slip was initiated at 3.17 ± 0.04 Ma.

The total contribution of the Rodgers Creek–Maacama fault system to slip of the entire East Bay fault system south of San Pablo Bay since 7.0 ± 0.3 Ma appears to be at least 44.5–52.5 km, for a median long-term slip rate of 6.95 ± 0.85 mm/yr (6.1–7.8 mm/yr). Larger amounts of slip attributed to the East Bay fault system to the south are contributed from faults east of the Hayward fault and probably from poorly constrained pre-7 Ma slip on a proto-Hayward fault zone north of Burdell Mountain.

KINEMATICS OF THE FAULT SYSTEM

Although much of the northern Coast Ranges is now in compression (Fig. 1; Berry, 1973; Wentworth et al., 1984; Zoback and Argus, 1990; Argus and Gordon 2001) and the San Andreas fault is curved, with a restraining bend located at its northernmost end, the restraining bend is trailed to the south by a prominent releasing bend configuration (Fig. 1). Some studies (Stanley, 1987; Wilson et al., 2005) also suggest that this releasing and restraining bend configuration of the northern San Andreas fault has formed the Pacific–North American plate boundary since some time in the Miocene, and as such, its northward migration with the Mendocino Triple Junction should have influenced successive distributions of transtensional and transpressional structures for some distance east of the main plate boundary (the San Andreas fault). To a first order, this concept may be valid (that is, strike-slip-related basins become younger northward east of the San Andreas fault; Blake et al., 1978; McLaughlin and Nilsen, 1982; Nilsen and McLaughlin, 1985).

Numerous studies also point to the northward migration of a slab window beneath the Coast Ranges as having influenced the distribution of volcanism and related extension in the crust (Dickinson and Snyder, 1979; Lachenbruch and Sass, 1980; Fox et al., 1985; McLaughlin et al., 1996; Graymer et al., 2002). Thermal response of the crust to slab window migration may, in turn, have combined with the migrating releasing bend segment of the northern San Andreas fault (Fig. 1) to form the northward-younging

transtensional (strike slip) basins of the Rodgers Creek–Maacama fault system. Releasing bend-related extensional fault geometry is viewed here as a structural element, separate from the migrating slab window, that provided needed open conduits and pathways for upward migration of magma from asthenospheric depths and for volcanic venting coeval with, or younger than, the surface faulting.

The Rodgers Creek–Maacama fault system as characterized here has evolved in conjunction with lengthening of the San Andreas transform margin. The fault system evolved as a series of extensional right steps and northeastward clockwise splays beginning ca. 7.0 Ma, with the opening of basins beneath the Santa Rosa Plain. Several fault zone reorganizations between ca. 7 Ma and the present are inferred from the orientations, slip characteristics, and timing of different fault sets of the northern and southern Rodgers Creek fault zones. From these relations we infer a sequence of superposed fault zone reorganizations that began with extensional strike slip followed by transpression and uplift, in turn followed by pure strike slip, and most recently by younger than 1 Ma reoriented extensional strike-slip faulting (Figs. 2, 3, 9, and 13).

The right-stepped Maacama fault zone exhibits a younger overlapping history of at least two reorganizations beginning ca. 3.2 Ma, with eruption of the upper part of the Mount St. Helena eruptive sequence that was accompanied or closely followed northeast of Healdsburg by initiation of extensional strike-slip faults of the Maacama fault zone. These faults bound the basins of Little Sulfur Creek (Fig. 15) and their associated syntectonic sedimentary fills (McLaughlin and Nilsen 1982; Nilsen and McLaughlin, 1985). Deposition in these strike-slip basins along the Maacama fault zone was followed by transpression that uplifted, dissected, and compressed the basins. The recent north-northwest-trending, younger than 1 Ma extensional strike-slip faults that are associated with opening of the Santa Rosa pull-apart basin splay from the Matanzas Creek, Bennett Valley, and Rodgers Creek fault zones. Southeast of Santa Rosa, these north-northwest-trending faults overprint earlier, more northwest-oriented basin-bounding faults of the Maacama fault zone (Figs. 2, 3, 9, and 13).

The long releasing bend in the northern San Andreas fault zone is currently adjacent to and west-northwest of the Rodgers Creek–Maacama fault system, and thus may influence the extensional strike-slip setting of the Rodgers Creek–Maacama fault system relative to motion of the Pacific plate. However, the timing and sequence of reorganizations of the Rodgers Creek–Maacama fault system that we have observed do

not have a straightforward correspondence with the regional-scale patterns of compression and extension associated with bends in the northern San Andreas fault zone. The succession of extensional and compressional components of the Rodgers Creek–Maacama fault system with time instead appears to be a more complicated response to Mendocino Triple Junction migration. The reorganized fault geometries seen with the Rodgers Creek–Maacama fault zone actually may be initiated sequentially at the southern end of the fault system, as a separate but necessary response to continual lengthening and changing of fault geometry at the northern end of the fault system with triple junction migration. Local compressional structures also are shown in laboratory models to be integral parts of active pull-apart basin settings (e.g., pop-up structures described by Dooley and McClay, 1997) and thus may not always represent temporally separate transpression.

Other studies (Wells and Simpson, 2001; Williams *et al.*, 2006) suggest that faulting kinematics in the northern Coast Ranges east of the San Andreas fault are significantly influenced by basement fault block interactions north and south of the Mendocino Triple Junction (Fig. 1). Thrust faults of east-directed structural wedges formed during early Tertiary plate convergence that uplifted and unroofed the Mesozoic basement of the Coast Ranges are examples of preexisting block boundary structures that can be reactivated in later transpressional settings and influence locations and geometries of Quaternary blind thrusts (Unruh *et al.*, 2004, 2007; Wentworth *et al.*, 1984; Wentworth and Zoback, 1990). In contrast, recent seismic experiment results interpret the Maacama and other active strike-slip faults in the northern Coast Ranges to extend through the entire crust of the North American plate (Beaudoin *et al.*, 1998; Hole *et al.*, 1998, 2000; Henstock and Levander, 2003), raising questions of how the strike-slip faults of the Rodgers Creek–Maacama fault system might interact with reactivated wedge thrusts. The nature of Mesozoic terrane boundary faults in the upper to mid-crust and their unknown contribution to the kinematics of the Rodgers Creek–Maacama fault system are beyond the scope of this paper, but we note their demonstrated significance to the east along the boundary between the Sacramento Valley and northern Coast Ranges (Unruh *et al.*, 2004, 2007; Wentworth *et al.*, 1984; Wentworth and Zoback, 1990).

Comparison to Laboratory Models

Scaled-sandbox models of stepping strike-slip faults and derived pull-apart basins (Dooley and McClay, 1997) provide insight

into several features of the Rodgers Creek–Maacama stepover fault system. The modeling shows that northwest-trending principal bounding faults of an evolving dextral right-stepped fault system initially do not overlap along strike. Rhombic-shaped pull-apart basins that form with this geometry of non-overlapping strike-slip faults have bounding extensional faults with north-northwest orientations. These basins are referred to as 30° non-overlapping releasing sidestep pull-apart basins (Figs. 9 and 10). As the fault system evolves, the principal strike-slip faults bounding the right step area lengthen, to where their ends are at 90° to each other, resulting in a box-shaped basin geometry referred to as a 90° releasing sidestep pull-apart basin (Fig. 10). Additional lengthening of the principal bounding strike-slip faults results in a right-stepover region, the principal northeastern and southwestern bounding strike-slip faults of which overlap considerably along strike (e.g., the 150° releasing sidestep pull-apart basin of Fig. 10). This more highly evolved stage of stepover fault development possibly is analogous to some overlapping elements of the Maacama and northern Rodgers Creek fault zones north of Santa Rosa. These faults of the Rodgers Creek and Maacama fault zones exhibit much longer lengths of overlap and more complex histories, however, than those in the sandbox models (Fig. 10).

Comparison to the laboratory models suggests that progressive development of along-strike overlap in the principal bounding faults of the Rodgers Creek–Maacama stepover system has resulted in the local development of pull-apart basins of different geometries at different stages in the lengthening of these faults. The models also suggest that at least some compressional structures adjacent to the pull-aparts may be coeval pop-ups or flower structures (Dooley and McClay, 1997). In contrast to this progression from non-overlapping (immaturely evolved) to substantial overlapping (maturely evolved) geometry seen in sandbox models, an immature, 30° non-overlapping pull-apart basin geometry is associated with the recently developed Santa Rosa pull-apart basin. This geometry is apparently related to reorganization of fault orientations in the stepover, reverting to a less mature stage of stepover development that is superposed on the more evolved stepover geometry seen in the overlapping relation between the northern Rodgers Creek (Healdsburg fault segment) and Maacama fault zones (Figs. 2, 3, 10, and 13).

This pattern of fault zone reorientation may, to first order, account for abandonment of some older segments of the southern Maacama fault zone and further provide the rationale

Evolution of the Rodgers Creek–Maacama fault system

for an apparent southwestward migration of the southern Maacama fault zone toward the Rodgers Creek and Bennett Valley fault zones during the recent stepover fault system reorganization. Overlapping faults of the northern Rodgers Creek and Maacama fault zones that evolved between ca. 3 and 1 Ma were overprinted by the immature non-overlapping stepover geometry of the Santa Rosa pull-apart basin (Figs. 3, 9, 10, and 13) after ca. 1 Ma as the result of this reorganization, which as discussed herein may have been in response to fault zone lengthening at the northern end of the fault system closer to the Mendocino Triple Junction, rather than a direct response to the releasing bend geometry of the San Andreas fault zone to the northwest.

CONCLUSIONS

1. The Rodgers Creek fault zone was initiated between ca. 7.3 and 6.7 Ma, when faulting displayed northeastward from a west-northwest-oriented proto-Hayward fault zone, forming a new zone of faults having northwest orientations. We interpret a distinctive breccia that is derived from extensional fault scarps along the east side of Santa Rosa Plain to mark the normal fault-bounded (transtensional?) margin of basins beneath the Santa Rosa Plain and the time of initiation of the Rodgers Creek fault zone. Extensional displacement on the early Rodgers Creek fault zone was replaced after ca. 5.4 Ma by compression and associated east-directed thrusting that uplifted the east side of the Santa Rosa Plain. The thrusting and compression partitioned the initial strike-slip basin beneath the Santa Rosa Plain into the separate Windsor and Cotati basins.

2. Composite strike-slip fault displacement for the northern and southern Rodgers Creek fault zones since ca. 7.0 ± 0.3 Ma is $\geq 28 \pm 0.5$ km, based on right-lateral separation of the fault scarp breccia between the Sears Point and Santa Rosa areas. This displacement is viewed as a minimum, because the southeastward extent of fault scarp breccia beneath Sonoma basin east of the southern Rodgers Creek fault zone is unknown. The Rodgers Creek fault zone slipped right-laterally at a median rate of $\sim 2.8 \pm 1.1$ mm/yr from the Late Miocene to early Pleistocene, but the rate has increased to $\sim 5.3 \pm 2.2$ mm/yr since the earliest Pleistocene. Low early slip rates reflect significant dip-slip components of displacement prior to 2.78 ± 0.02 Ma. A part of the southern Rodgers Creek fault zone may be partitioning slip toward the Maacama fault zone via the Spring Valley fault and the Bennett Valley fault zone at depth. However, Holocene surface faulting and earthquake dis-

tribution north of Santa Rosa indicate that an unconstrained component of slip is still taken up by the Healdsburg fault segment of the northern Rodgers Creek fault zone along its 40-km-long map overlap with the Maacama fault zone.

3. Similar surface displacement of the Sonoma Volcanics (20.8 ± 3.3 km) and basement rocks of the Mesozoic Coast Range Ophiolite (21.5 ± 0.5 km) indicate that the Maacama fault zone north of Santa Rosa was initiated at or soon after 3.17 ± 0.04 Ma and it has maintained a long-term slip rate of ~ 5.5 – 7.9 mm/yr (median rate of 6.7 ± 1.2 mm/yr). Offset magnetic anomalies along the Maacama fault zone suggest a similar maximum displacement of 19 ± 7 km and median long-term rate of 6.0 ± 2.3 mm/yr. The slip rate since ca. 1.0 ± 0.2 Ma has been $\sim 6.3 \pm 1.8$ mm/yr.

4. The total contribution of the Rodgers Creek–Maacama fault system to slip of the East Bay fault system south of San Pablo Bay since 7.0 ± 0.3 Ma appears to be $>48.4 \pm 1.4$ km, for a median long-term slip rate of at least 6.95 ± 0.85 mm/yr. Larger slip attributed to the East Bay fault system to the south results from slip contributed from faults east of the Hayward fault and to poorly constrained pre-7 Ma slip on the proto-Hayward fault zone north of Burdell Mountain and southwest of the Rodgers Creek fault zone.

5. We infer, from comparison to analogous laboratory generated sandbox models (Dooley and McClay, 1997), that the most recently organized geometry of the Rodgers Creek–Maacama fault system is an immature stage of stepover fault zone development characterized by north-northwest-oriented pull-apart basins with principal bounding faults that do not overlap. The immature stepover geometry is superimposed on an older geometry with principal bounding strike-slip faults having a more west-northwest orientation that overlap for ~ 40 km along strike. Westward migration of the south end of the Maacama fault zone since the Pleistocene (ca. 1.2 Ma) may be the result of the superposition of these successive fault zone geometries. However, though the transtensional strike-slip basins of the Rodgers Creek–Maacama fault system have evolved within the realm of migrating major restraining and releasing bends of the northern San Andreas fault zone, the succession of the fault system reorganizations is not simply relatable to the migration of these bend geometries. Superimposed fault reorganizations with time at the southern end of the Rodgers Creek–Maacama fault system are probably a more direct kinematic response to the lengthening and reorganization of faulting at the northern end of the fault system, with northward migration of the Mendocino Triple Junction.

ACKNOWLEDGMENTS

An early version of this manuscript was reviewed by R.G. Stanley and J.J. Rytuba of the U.S. Geological Survey, who suggested numerous changes that were incorporated into the paper. Two anonymous reviewers for *Geosphere* provided extensive additional comments and suggestions for reorganizing and improving the manuscript, prompting rethinking, refinement, and clarification of some of our interpretations. We thank many colleagues at the U.S. Geological Survey, including Elmira Wan, David Wahl, Carl Wentworth, Russ Evarts, Russ Graymer, Carol Prentice, and David Schwartz, for providing data, insights, worthwhile discussions, and encouragement during this research over the past 12 years. McLaughlin is indebted to Tor Nilsen (deceased) for raising an awareness of strike-slip-related sedimentary basins and providing many insights into their recognition and unique sedimentologic and tectonic characteristics.

REFERENCES CITED

- Allen, J.R., 2003, Stratigraphy and tectonics of Neogene strata, northern San Francisco Bay area: [M.S. thesis]: San Jose, California, San Jose State University, 190 p.
- Argus, D.F., and Gordon, R.G., 2001, Present tectonic motion across the Coast Ranges and San Andreas fault system in California: *Geological Society of America Bulletin*, v. 113, p. 1580–1592, doi: 10.1130/0016-7606(2001)113<1580:PTMATC>2.0.CO;2.
- Beaudoin, B.C., Hole, J.A., Klemperer, S.L., and Trehu, A.M., 1998, Location of the southern edge of the Gordo slab and evidence for adjacent asthenospheric window: Results from seismic profiling and gravity: *Journal of Geophysical Research*, v. 103, no. B12, p. 30101–30115, doi: 10.1029/98JB02231.
- Berry, F.A.F., 1973, High fluid potentials in California coast ranges and their tectonic significance: *American Association of Petroleum Geologists Bulletin*, v. 57, p. 1219–1248.
- Blake, M.C., Jr., Campbell, R.H., Dibblee, T.W., Jr., Howell, D.G., Nilsen, T.H., Normark, W.R., Vedder, J.C., and Silver, E.A., 1978, Neogene basin formation in relation to plate-tectonic evolution of San Andreas fault system, California: *American Association of Petroleum Geologists Bulletin*, v. 62, p. 344–372.
- Blake, M.C., Jr., Howell, D.G., and Jayko, A.S., 1984, Tectonostratigraphic terranes of the San Francisco Bay region, in Blake, M.C., Jr., ed., *Franciscan geology of northern California*: Pacific Section, Society of Economic Paleontologists and Mineralogists Book 43, p. 5–22.
- Blake, M.C., Jr., Jayko, A.S., and McLaughlin, R.J., 1985, Tectonostratigraphic terranes of the northern Coast Ranges, California, in Howell, D.G., ed., *Tectonostratigraphic terranes of the Circum-Pacific region*: Houston, Texas, Circum-Pacific Council for Energy and Mineral Resources Earth Science Series Volume 1, p. 159–171.
- Brown, R.D., 1970, Faults that are historically active or that show evidence of geologically young surface displacement, San Francisco Bay region, a progress report: October 1970 (U.S. Department of the Interior and U.S. Department of Housing and Urban Development Basic Data Contribution 7): U.S. Geological Survey Open-File Map, scale 1:250,000.
- Budding, K.E., Schwartz, D.P., and Oppenheimer, D.H., 1991, Slip rate, earthquake recurrence, and seismicogenic potential of the Rodgers Creek fault zone, northern California: Initial results: *Geophysical Research Letters*, v. 18, p. 447–450, doi: 10.1029/91GL00465.
- Crampton, T., Abramson, W.H., Hanson, K., and Swan, F.H., 2004, Preliminary results of paleoseismic investigations of the northern Rodgers Creek–Healdsburg fault at Shiloh Ranch Regional Park, Sonoma County, California [abs.]: *Seismological Research Letters*, v. 74, no. 2, p. 238.
- Crowell, J.C., and Link, M.H., eds., 1982, *Geologic history of Ridge Basin, southern California*: Pacific Section,

- Society of Economic Paleontologists and Mineralogists, Special Publication 22, 304 p.
- Dickinson, W.R., and Snyder, W.S., 1979, Geometry of triple junctions related to San Andreas transform: *Journal of Geophysical Research*, v. 84, no. B2, p. 561–572, doi: 10.1029/JB084iB02p00561.
- Dooley, T., and McClay, K., 1997, Analog modeling of pull-apart basins: American Association of Petroleum Geologists Bulletin, v. 81, p. 1804–1826.
- Drake, D.E., Cacchione, D.A., Gardner, J.V., McCulloch, D.S., and Masson, D., 1989, Morphology and growth history of Delgada Fan: Implications for the Neogene evolution of Point Arena Basin and the Mendocino triple junction: *Journal of Geophysical Research*, v. 94, p. 3139–3158, doi: 10.1029/JB094iB03p03139.
- Ford, E.W., 2003, Mesozoic and Tertiary stratigraphy of the Burdell Mountain area and implications for slip along the East Bay fault system: Northern California Geological Society, 14 p.
- Ford, E.W., 2007, Geology of Burdell Mountain and implications for long-term slip along the East Bay fault system, California [M.S. thesis]: San Francisco, California, San Francisco State University, 96 p.
- Fox, K.F., Jr., 1976, Melanges in the Franciscan Complex, a product of triple-junction tectonics: *Geology*, v. 4, p. 737–740, doi: 10.1130/0091-7613(1976)4<737:MITFCA>2.0.CO;2.
- Fox, K.F., Jr., Fleck, R.J., Curtis, G.H., and Meyer, C.E., 1985, Implications of the northwestwardly younger age of the volcanic rocks of west-central California: *Geological Society of America Bulletin*, v. 96, p. 647–654, doi: 10.1130/0016-7606(1985)96<647:IOTNYA>2.0.CO;2.
- Frey Mueller, J.T., Murray, M.H., Segall, P., and Castillo, D., 1999, Kinematics of the Pacific–North America plate boundary zone, northern California: *Journal of Geophysical Research*, v. 104, p. 7419–7441, doi: 10.1029/1998JB900118.
- Funing, G.J., Burgmann, R., Feretti, A., Novali, F., and Fumagalli, A., 2007, Creep on the Rodgers Creek fault, northern San Francisco Bay area from a 10 year PS-InSAR dataset: *Geophysical Research Letters*, v. 34, L19306, doi: 10.1029/2007GL030836.
- Galehouse, J.S., 2002, Data from theodolite measurements of creep rates on San Francisco Bay region faults, California: 1979–2001: U.S. Geological Survey Open-File Report 02–225, 94 p., <http://geopubs.wr.usgs.gov/open-file/of02-225/>.
- Graham, S.A., McCloy, C., Hitzman, M., Ward, R., and Turner, R., 1984, Basin evolution during change from convergent to transform continental margin in central California: American Association of Petroleum Geologists Bulletin, v. 68, p. 233–249.
- Graymer, R.W., Sarna-Wojcicki, A.M., Walker, J.P., McLaughlin, R.J., and Fleck, R.J., 2002, Controls on timing and amount of right-lateral displacement on the East Bay fault system, San Francisco Bay region, California: *Geological Society of America Bulletin*, v. 114, p. 1471–1479, doi: 10.1130/0016-7606(2002)114<1471:COTAAO>2.0.CO;2.
- Hearn, B.C., Jr., McLaughlin, R.J., and Donnelly-Nolan, J.M., 1988, Tectonic framework of the Clear Lake basin, California, in Sims, J.D., ed., Late Quaternary climate, tectonism and sedimentation in Clear Lake, Northern California Coast Ranges: *Geological Society of America Special Paper* 214, p. 9–20.
- Hecker, S., and Kelsey, H., 2006, History and pre-history of earthquakes in wine and redwood country, Sonoma and Mendocino Counties, California, in Prentice, C.S., et al., eds., 1906 San Francisco earthquake centennial field guides: *Geological Society of America Field Guide* 7, p. 339–372.
- Hecker, S., Pantosti, D., Schwartz, D.P., Hamilton, J., Reidy, L.M., and Power, T.J., 2005, The most recent large earthquake on the Rodgers Creek fault, San Francisco Bay area: *Seismological Society of America Bulletin*, v. 95, p. 844–860, doi: 10.1785/0120040134.
- Henstock, T.J., and Levander, 2003, Structure and seismotectonics of the Mendocino Triple Junction, California: *Journal of Geophysical Research*, v. 108, no. B5, 2260, doi: 10.1029/2001JB000902.
- Hole, J.A., Beaudoin, B.C., and Henstock, T.J., 1998, Wide angle seismic constraints on the evolution of the deep San Andreas plate boundary by Mendocino triple junction migration: *Tectonics*, v. 17, p. 802–818, doi: 10.1029/98TC02261.
- Hole, J.A., Beaudoin, B.C., and Klemperer, S.L., 2000, Vertical extent of the newborn San Andreas at Mendocino triple junction: *Geology*, v. 28, p. 1111–1114, doi: 10.1130/0091-7613(2000)28<1111:VEOTNS>2.0.CO;2.
- Hopson, C.A., Mattinson, J.M., and Pessagno, E.A., Jr., 1981, Coast Range ophiolite, western California, in Ernst, W.G., ed., The geotectonic development of California: Rubey Volume 1: Englewood Cliffs, New Jersey, Prentice-Hall, p. 418–510.
- Hopson, C.A., Mattinson, J.M., Pessagno, E.A., and Luyendyk, 2008, California Coast Range ophiolite: Composite Middle and Late Jurassic oceanic lithosphere, in Wright, J.E., and Shervais, J.W., eds., Ophiolites, arcs, and batholiths: A tribute to Cliff Hopson: *Geological Society of America Special Paper* 438, p. 1–101, doi: 10.1130/2008.2438(01).
- Irwin, W.P., 1960, Geologic reconnaissance of the northern Coast Ranges and Klamath Mountains, California, with a summary of the mineral resources: California Division of Mines Bulletin 179, 80 p.
- Jachens, R.C., and Griscam, A., 1983, Three dimensional geometry of the Gordo plate beneath northern California: *Journal of Geophysical Research*, v. 88, p. 9375–9392, doi: 10.1029/JB088iB11p09375.
- Jachens, R.C., Griscam, A., and Roberts, C.W., 1995, Regional extent of Great Valley basement west of the Great Valley, California: Implications for extensive tectonic wedging in the California Coast Ranges: *Journal of Geophysical Research*, v. 100, no. B7, p. 12769–12790, doi: 10.1029/95JB00718.
- Lachenbruch, A.H., and Sass, J.H., 1980, Heat flow and energetics of the San Andreas fault zone: *Journal of Geophysical Research*, v. 85, no. B11, p. 6185–6222, doi: 10.1029/JB085iB11p06185.
- Langenheim, V.E., Roberts, C.W., McCabe, C.A., McPhee, D.K., Tilden, J.E., and Jachens, R.C., 2006, Preliminary isostatic gravity map of the Sonoma Volcanic Field and vicinity, Sonoma and Napa Counties, California: U.S. Geological Survey Open-File Report 2006–1056, scale 1:100,000, <http://pubs.usgs.gov/of/2006/1056/>.
- Langenheim, V.E., McLaughlin, R.J., McPhee, D.K., Roberts, C.W., and McCabe, C.A., 2008, Geophysical framework of the Santa Rosa 7.5' quadrangle, California, in McLaughlin, R.J., et al., eds., Geologic and geophysical framework of the Santa Rosa 7.5' quadrangle, Sonoma County, California: U.S. Geological Survey Open-File Report 2008–1009, p. 34–45, <http://pubs.usgs.gov/of/2008/1009/>.
- Langenheim, V.E., Graymer, R.W., Jachens, R.C., McLaughlin, R.J., Wagner, D.L., and Sweetkind, D.S., 2010, Geophysical framework of the northern San Francisco Bay region, California: *Geosphere*, v. 6, p. 594–620, doi: 10.1130/GES00510.1.
- Larsen, M., Prentice, C.S., Kelsey, H.M., Zachariasen, J., and Rotberg, G.L., 2005, Paleoseismic investigation of the Maacama fault at the Haehl Creek Site, Willits, California: *Geological Society of America Abstracts with Programs*, v. 37, no. 4, p. 68.
- Lillis, P.G., Magoon, L.B., Stanley, R.G., McLaughlin, R.J., and Warden, A., 2001, Characterization of northern California petroleum by stable carbon isotopes: U.S. Geological Survey Open-File Report 99–164, 19 p., <http://greenwood.cr.usgs.gov/energy/OF99-164>.
- Liniecki-Laporte, M., and Andersen, D.W., 1988, Possible new constraints on late Miocene depositional patterns in west-central California: *Geology*, v. 16, p. 216–220, doi: 10.1130/0091-7613(1988)016<0216:PNCOLM>2.3.CO;2.
- Lock, J., Kelsey, H., Furlong, K., and Woolace, A., 2006, Late Neogene and Quaternary landscape evolution of the northern California Coast Ranges: Evidence for Mendocino triple junction tectonics: *Geological Society of America Bulletin*, v. 118, p. 1232–1246, doi: 10.1130/B25885.1.
- McLaughlin, R.J., and Nilsen, T.H., 1982, Neogene non-marine sedimentation and tectonics in small pull-apart basins of the San Andreas fault system, Sonoma County, CA: *Sedimentology*, v. 29, p. 865–876, doi: 10.1111/j.1365-3091.1982.tb00089.x.
- McLaughlin, R.J., Blake, M.C., Jr., Griscam, A., Blome, C.D., and Murchey, B., 1988, Tectonics of formation, translation and dispersal of the Coast Range Ophiolite of California: *Tectonics*, v. 7, p. 1033–1056, doi: 10.1029/TC007i005p1033.
- McLaughlin, R.J., Sliter, W.V., Frederiksen, N.O., Harbert, W.P., and McCulloch, D.S., 1994, Plate motions recorded in tectonostratigraphic terranes of the Franciscan Complex and evolution of the Mendocino triple junction, northwestern California: U.S. Geological Survey Bulletin 1997, 60 p.
- McLaughlin, R.J., Ohlin, H.N., and Thormahlen, D.J., 1990, Geologic map and structure sections of the Little Indian Valley–Wilbur Springs geothermal area, northern Coast Ranges, California: U.S. Geological Survey Miscellaneous Investigations Map I-1706, scale 1:24,000.
- McLaughlin, R.J., Sliter, W.V., Sorg, D.H., Russell, P.C., and Sarna-Wojcicki, A.M., 1996, Large-scale right-slip displacement on the east San Francisco Bay region fault system—Implications for location of late Miocene to Pliocene Pacific plate boundary: *Tectonics*, v. 15, p. 1–18, doi: 10.1029/95TC02347.
- McLaughlin, R.J., Sarna-Wojcicki, A.M., Fleck, R.J., Graymer, R.W., and Wright, W.H., 2002, Kinematic and geochronologic evidence bearing on partitioning of dextral slip between the Rodgers Creek and Maacama faults, northern San Francisco Bay region, CA: *Geological Society of America Abstracts with Programs*, v. 34, no. 5, p. 99.
- McLaughlin, R.J., Sarna-Wojcicki, A.M., Fleck, R.J., Wright, T.H., Levin, V.R.G., and Valin, Z.C., 2004, Geology, tephrochronology, radiometric ages and cross sections of the Mark West Springs 7.5' Quadrangle, Sonoma and Napa Counties, California: U.S. Geological Survey Scientific Investigations Map 2858, 16 p., scale 1:24,000, <http://pubs.usgs.gov/sim/2004/2858/>.
- McLaughlin, R.J., Sarna-Wojcicki, A.M., Fleck, R.J., Langenheim, V.E., Jachens, R.C., and Deino, A., 2005, Framework geology and structure of the Sonoma Volcanics and associated sedimentary deposits of the right-stepped Rodgers Creek–Maacama fault system and concealed basins beneath Santa Rosa plain, in Stevens, C., and Cooper, J., eds., Late Neogene transition from transform to subduction margin east of the San Andreas fault in the wine country of the northern San Francisco Bay Area, California: Field trip guidebook and volume prepared for the joint meeting of the Cordilleran Section, GSA and Pacific Section, AAPG: Pacific Section, SEPM (Society for Sedimentary Geology) Book 98, p. 29–81.
- McLaughlin, R., Langenheim, V., Jachens, R., Sarna-Wojcicki, A., Fleck, R., Wagner, D., and Clahan, K., 2006, Geologic constraints on long-term displacements along the Rodgers Creek, Healdsburg and Maacama fault zones, northern California [abs.]: *Seismological Research Letters*, v. 77, no. 2, p. 201, doi:10.1785/gssrl.77.2.160.
- McLaughlin, R.J., Sarna-Wojcicki, A.M., Fleck, R.J., Langenheim, V.E., McCabe, C.A., and Wan, E., 2008, Geologic framework of the Santa Rosa 7.5' quadrangle, in McLaughlin, R.J., et al., eds., Geologic and geophysical framework of the Santa Rosa 7.5' quadrangle, Sonoma County, California: U.S. Geological Survey Open-File Report 2008–1009, p. 7–33, <http://pubs.usgs.gov/of/2008/1009/>.
- McPhee, D.K., Langenheim, V.E., Hartzell, S., McLaughlin, R.J., Aagaard, B.C., Jachens, R.J., and McCabe, C., 2007, Basin structure beneath the Santa Rosa plain, northern California: Implications for damage caused by the 1969 Santa Rosa and 1906 San Francisco earthquakes: *Seismological Society of America Bulletin*, v. 97, p. 1449–1457, doi: 10.1785/0120060269.
- Metz, J.M., and Mahood, G.A., 1991, Development of the Long Valley, California, magma chamber recorded in pre-caldera rhyolite lavas of Glass Mountain: Contributions to Mineralogy and Petrology, v. 106, p. 379–397, doi: 10.1007/BF00324565.
- Nilsen, T.H., and Clarke, S.H., 1989, Late Cenozoic basins of northern California: *Tectonics*, v. 8, p. 1137–1158, doi: 10.1029/TC008i006p1137.
- Nilsen, T.H., and McLaughlin, R.J., 1985, Comparison of tectonic framework and depositional patterns of

Evolution of the Rodgers Creek–Maacama fault system

- Hornelen strike-slip basin of Norway and the Ridge and Little Sulphur Creek strike-slip basins of California: Society of Economic Paleontologists and Mineralogists Special Publication 37, p. 79–103.
- Obrovich, J.D., Kunk, M.J., and Lanphere, M.A., 2000, Age and paragenesis of the unique mineral benitoite: Geological Society of America Abstracts with Programs, v. 32, no. 7, p. A-440.
- Parsons, T., Sliter, R., Geist, E.L., Jachens, R.C., Jaffe, B.E., Foxgrover, A., Hart, P.E., and McCarthy, J., 2003, Structure and mechanics of the Hayward–Rodgers Creek fault step-over, San Francisco Bay, California: Seismological Society of America Bulletin, v. 93, p. 2187–2200, doi: 10.1785/0120020228.
- Powell, C.L., II, McLaughlin, R.J., and Wan, E., 2006, Biostratigraphic and lithologic correlations of two Sonoma County Water Agency pilot wells with the type Wilson Grove Formation, Sonoma County, central California: U.S. Geological Survey Open-File Report 2006–1196, version 1.0, 37 p., <http://pubs.usgs.gov/of/2006/1196/>.
- Prentice, C.S., and Fenton, C., 2005, Paleoseismic evidence for Prehistoric earthquakes on the Northern Maacama fault, Willits, California: Geological Society of America Abstracts with Programs, v. 37, no. 4, p. 83.
- Sarna-Wojcicki, A.M., 1976, Correlation of late Cenozoic tuffs in the Central Coast Ranges of California by means of trace- and minor-element chemistry: U.S. Geological Survey Professional Paper 972, 30 p.
- Sarna-Wojcicki, A.M., 1992, Long-term displacement rates of the San Andreas fault system in northern California from the 6-Ma Roblar tuff [abs.], in Borchardt, G., et al., eds., Proceedings of the Second Conference on Earthquake Hazards in the Eastern San Francisco Bay Area: California Department of Conservation, Division of Mines and Geology Special Publication 113, p. 29–30.
- Sarna-Wojcicki, A.M., Pringle, M.S., and Wijbrans, J., 2000, New Ar-40/Ar-39 age of and sediment rate calibration for the Matuyama–Brunhes boundary: Journal of Geophysical Research, v. 105, p. 21,431–21,443, doi:10.1029/2000JB900901.
- Sarna-Wojcicki, A.M., and 10 others, 2005, Tephra layers of Blind Spring Valley and related upper Pliocene and Pleistocene tephra layers, California, Nevada, and Utah: isotopic ages, correlation, and magnetostratigraphy: U.S. Geological Survey Professional Paper 1701, 63 p.
- Sarna-Wojcicki, A.M., Deino, A.L., Fleck, R.J., McLaughlin, R.J., Wagner, D.L., Wan, E., Wahl, D., Hillhouse, J.W., and Perkins, M., 2011, Age, composition, and areal distribution of the Pliocene Lawlor Tuff, and three younger Pliocene tuffs, California and Nevada: Geosphere, v. 7, p. 599–628, doi: 10.1130/GES00609.1.
- Sickler, R.R., Prentice, C.S., and Dengler, L.A., 2005, Slip rate and age of the most recent event on the Central Maacama fault near Ukiah, Mendocino County, California: Geological Society of America Abstracts with Programs, v. 37, no. 4, p. 68.
- Simpson, G.D., 2005, Findings from fault hazard investigations along the Maacama fault for the proposed Willits hospital, Willits, California: Geological Society of America Abstracts with Programs, v. 37, no. 4, p. 83.
- Stanley, R.G., 1987, Implications of the northwestwardly younger age of the volcanic rocks of west-central California: Alternative interpretation: Geological Society of America Bulletin, v. 98, p. 612–614, doi: 10.1130/0016-7606(1987)98<612:IOTNYA>2.0.CO;2.
- Starratt, S.W., Allen, J.R., Powell, C.L., II, Peterson, D.E., Ruck, E., and Sarna-Wojcicki, A., 2005, New paleontological evidence supporting the Neogene transition from marine to non-marine conditions in Marin and Sonoma counties, California: Geological Society of America Abstracts with Programs, v. 37, no. 4, p. 69.
- Swan, F.H., Crampton, T., Abramson, H., and Hanson, K.L., 2003, Paleoseismic investigation of the Rodgers Creek/Healdsburg fault at Shiloh Regional Park, Sonoma County, California [abs.], in Ponce, D.A., et al., eds., Proceedings of the Hayward Fault Workshop, eastern San Francisco Bay area, California, September 19–20, 2003: U.S. Geological Survey Open-File Report 03–485, p. 25, <http://pubs.usgs.gov/of/2003/of03-485/>.
- Sweetkind, D.S., McLaughlin, R.J., Langenheim, V.E., Williams, R.A., Taylor, E.M., McPhee, D.K., Wahl, D.B., Sarna-Wojcicki, A.M., McKee, R.A., and Locke, K., 2008, Plio-Pleistocene evolution of concealed basins separated by a bedrock ridge West of the Rodgers Creek and Healdsburg Faults, northern California: Eos (Transactions, American Geophysical Union), v. 89, no. 53, abs. S11A-1718.
- Sweetkind, D.S., Taylor, E., McCabe, C., Langenheim, V.E., and McLaughlin, R.J., 2010, Three-dimensional geologic modeling of the Santa Rosa Plain, California: Geosphere, v. 6, p. 237–274, doi: 10.1130/GES00513.1.
- Unruh, J.R., O’Connell, D., and Block, L.V., 2004, Crustal structure of the ancestral northwestern California forearc region from seismic reflection imaging: Implications for convergent margin tectonics: Tectonophysics, v. 392, p. 219–240, doi: 10.1016/j.tecto.2004.04.018.
- Unruh, J.R., Dumitru, T.A., and Sawyer, T.L., 2007, Coupling of early Tertiary extension in the Great Valley forearc basin with blueschist exhumation in the underlying Franciscan accretionary wedge at Mount Diablo, California: Geological Society of America Bulletin, v. 119, p. 1347–1367, doi: 10.1130/B26057.1.
- U.S. Geological Survey, 2010, U.S. Geological Survey Earthquake Hazards Program crustal deformation monitoring, global positioning system observations, northern California and San Francisco Bay area: <http://earthquake.usgs.gov/monitoring/gps/SFBayArea/velocities>.
- Valin, Z.C., and McLaughlin, R.J., 2005, Locations and data for water wells of the Santa Rosa Valley, Sonoma County, California: U.S. Geological Survey Open File Report 2005–1318, 16 p., <http://pubs.usgs.gov/of/2005/1318/>.
- Van Baalen, M.R., II, 1995, The New Idria Serpentinite [Ph.D. thesis]: Cambridge, Massachusetts, Harvard University, 353 p.
- Wagner, D.L., and Bortugno, E.B., 1982, Geologic map of the Santa Rosa Quadrangle: California Division of Mines and Geology Regional Geologic Map Series 2A, scale 1:250,000.
- Wagner, D.L., Fleck, R.J., Sarna-Wojcicki, A.M., and Deino, A., 2005, Golden Gate to southern Sonoma County, Rodgers Creek fault, Burdell Mountain, Donnell Ranch, and Southern Sonoma Volcanics, in Stevens, C., and Cooper, J., eds., Late Neogene transition from transform to subduction margin east of the San Andreas fault in the wine country of the northern San Francisco Bay Area, California: Field trip guidebook and volume prepared for the joint meeting of the Cordilleran Section, GSA and Pacific Section, AAPG: Pacific Section, SEPM (Society for Sedimentary Geology) Book 98, p. 1–28.
- Wagner, D.L., Saucedo, G.J., Clahan, K.B., Fleck, R.J., Langenheim, V.E., McLaughlin, R.J., Sarna-Wojcicki, A.M., Allen, J.R., and Deino, A.L., 2011, Geology, geochronology, and paleogeography of the southern Sonoma volcanic field and adjacent areas, northern San Francisco Bay region, California: Geosphere, v. 7, p. 658–683, doi:10.1130/GES00626.1.
- Wakabayashi, J., 1999, Distribution of displacement on, and evolution of, a young transform fault system: The northern San Andreas fault system, California: Tectonics, v. 18, p. 1245–1274, doi: 10.1029/1999TC900049.
- Wakabayashi, J., Hengesh, J.V., and Sawyer, T.L., 2004, Four-dimensional transform fault processes: Progressive evolution of step-overs and bends: Tectonophysics, v. 392, p. 279–301, doi: 10.1016/j.tecto.2004.04.013.
- Waldhauser, F., and Schaff, D.P., 2008, Large-scale relocation using cross-correlation and double-difference methods: Journal of Geophysical Research, v. 113, B08311, doi: 10.1029/2007JB005479.
- Weaver, C.E., 1949, Geology of the Coast Ranges immediately north of the San Francisco Bay region, California: Geological Society of America Memoir 35, 242 p.
- Wells, R.E., and Simpson, R.W., 2001, Microplate motion of the Cascadia forearc and implications for subduction deformation: Earth, Planets and Space, v. 53, p. 275–283.
- Wentworth, C.M., and Zoback, M.D., 1990, Structure of the Coalinga region and thrust origin of the earthquake, in Rymer, M.J., and Ellsworth, W.L., eds., The Coalinga earthquake of May 2, 1983: U.S. Geological Survey Professional Paper 1487, p. 41–68.
- Wentworth, C.M., Blake, M.C., Jr., Jones, D.L., Walter, A.W., and Zoback, M.D., 1984, Tectonic wedging associated with emplacement of the Franciscan assemblage, California Coast Ranges, in Blake, M.C., Jr., ed., Franciscan geology of northern California: Pacific Section, Society of Economic Paleontologists and Mineralogists Book 43, p. 163–173.
- Williams, R.A., Langenheim, V.E., McLaughlin, R.J., Odum, J.K., Worley, D.M., Stephenson, W.J., Kent, R.L., McCullough, S.M., Knepprath, N.E., and Leslie, S.R., 2008, Seismic reflection profiles image the Rodgers Creek fault and Trenton Ridge beneath urban Santa Rosa, California: Seismological Research Letters, v. 79, no. 2, p. 317.
- Williams, T.B., Kelsey, H.M., and Freymueller, J.T., 2006, GPS-derived strain in northwestern California: Termination of the San Andreas fault system and convergence of the Sierra Nevada–Great Valley block contribute to southern Cascadia forearc contraction: Tectonophysics, v. 413, p. 171–184, doi: 10.1016/j.tecto.2005.10.047.
- Wilson, D.S., McCrory, P.A., and Stanley, R.G., 2005, Implications of volcanism in coastal California for the Neogene deformation history of western North America: Tectonics, v. 24, TC3008, doi: 10.1029/2003TC001621.
- Wong, I.G., and Bott, J.D.J., 1995, A new look back at the 1969 Santa Rosa, California, earthquakes: Seismological Society of America Bulletin, v. 85, p. 334–341.
- Wright, T.L., and Smith, N., 1992, Right step from the Hayward fault to the Rodgers Creek fault beneath San Pablo Bay, in Borchardt, G., et al., eds., Proceedings of the Second Conference on Earthquake Hazards in the Eastern San Francisco Bay Area: California Department of Conservation, Division of Mines and Geology Special Publication 113, p. 407–417.

MANUSCRIPT RECEIVED 3 MARCH 2011
 REVISED MANUSCRIPT RECEIVED 28 SEPTEMBER 2011
 MANUSCRIPT ACCEPTED 22 NOVEMBER 2011

Copyright of Geosphere is the property of Geological Society of America and its content may not be copied or emailed to multiple sites or posted to a listserv without the copyright holder's express written permission. However, users may print, download, or email articles for individual use.